THE PARTIAL CORRELATION FUNCTION IN THE IDENTIFICATION OF NON-LINEAR SYSTEMS

and

AN EYE POSITION TRANSDUCER.

T.M.W.WEEDON.

This thesis, being a report of research carried out under the direction of Professor J.L.Douce, B.Sc., M.Sc., Ph.D., D.Sc., F.I.E.E., C.E., is submitted to the University of Warwick for the degree of Doctor of Philosophy.

1970.

Abstract.

Section 1.

A correlation technique is developed which enables the identification of systems belonging to a restricted class of non-linear systems. The method is applicable to a system which may be represented as a single-valued, instantaneous, time-invariant non-linearity followed by linear dynamics. The characteristic of the non-linearity and the impulse response of the linear element are found simultaneously in a single experiment.

A class of pseudo-random test signals is studied, and results are derived for some situations in which the results are contaminated by noise.

Further work is required to extend the applicability of the technique, to compare its performance with other methods of identification, and to investigate alternative test signals.

Section 2.

A simple eye-position transducer is described, which measures eyeball rotation about two axes. Depending upon the characteristics of the subject's eye, and the operating conditions, an accuracy of as good as $\pm$ 5% may be obtained over a range of 12°.

The user wears a light-weight infra-red optical-electronic device on a spectacle frame. The transducer exploits the variation in infra-red reflectivity over the surface of the eyeball, and therefore varies in its performance from one subject to another. It may be used by some subjects in all lighting conditions except direct sunlight.

Further work is needed to eliminate the deficiencies of the device, but an investigation into television techniques, which are now feasible, should be made first.

Section 3.

The experimental determination of the region of asymptotic stability of a second order time invariant system may be considerably simplified by taking advantage of the nature of the trajectories which form the boundary of the region. These trajectories are found easily by reverse time simulation.

Further work is possible to investigate the extension of the method to higher order systems, but useful results seem unlikely.

Acknowledgment

I am grateful for the continuous help of my supervisor Professor J.L.Douce, and for the support of the Science Research Council. Also for the help and encouragement from my many friends, including those mentioned below, to all of whom I say 'Thank you'.

MR.B.D.ARMSTRONG.	MINISTRY OF AVIATION (R.A.E. BEDFORD)
MR.J.L.BAKER.	UNIVERSITY OF WARWICK (ELECTRONICS WORKSHOP)
MR.L.BULMER.	UNIVERSITY OF WARWICK (SCIENCE LIBRARIAN)
MR.J.K.CANNELL.	UNIVERSITY OF WARWICK
MR.J.DAVIES.	UNIVERSITY OF WARWICK (SCIENCE LIBRARIAN)
MR.K.R.GODFREY.	MINISTRY OF TECHNOLOGY (N.P.L.)
MR.P.H.HAMMOND.	MINISTRY OF TECHNOLOGY (N.P.L.)
DR.M.T.G.HUGHES.	UNIVERSITY OF WARWICK
MR.M.S.HUNT.	UNIVERSITY OF WARWICK
MR.R.L.HYDE.	BRITISH AIRCRAFT CORPORATION
MR.H.S.P.JONES.	UNIVERSITY OF WARWICK
MR.A.J.McINTYRE.	UNIVERSITY OF WARWICK (ENGINEERING WORKSHOPS)
DR.K.C.NG.	UNIVERSITY OF WARWICK
MR.P.C.PARKS.	UNIVERSITY OF WARWICK
PROF.J.G.THOMASON.	I.C.I.
MR.A.H.WHITEHEAD.	UNIVERSITY OF WARWICK (PHOTOGRAPHY DEPT.)

Timothy M.W. Weedon

INTRODUCTION.

This thesis is composed of three sections. The first describes work on the identification of a class of non-linear systems by a cross-correlation technique. The second describes an instrument for the measurement of eyeball position. The third consists of a paper published in 'Electronics Letters' on an experimental method of determining system stability.

Except where indicated, all of the work was carried out at the University of Warwick under the supervision of Professor J.L.Douce.

SECTION 1.

THE PARTIAL CORRELATION FUNCTION IN THE IDENTIFICATION OF NON-LINEAR SYSTEMS.

Chapter 1.

An engineer designing a controller for a given plant needs to know the characteristics of the plant, in terms of some relationship between its input and output, before he can achieve satisfactory performance from the system of plant and controller. The more stringent is the specification for system performance, the more detailed, and the more accurate must be his knowledge of the plant. By considering the nature of the plant he will be able to construct a theoretical model of the plant. Depending upon the extent of his initial knowledge, he will then need to carry out an experimental investigation to determine the suitability and parameters of his model. This is one example of the need to 'identify' a system; to find experimentally the relationship between its input and output.

If the plant is a linear system, it may be characterised by its frequency response, or by its impulse response. The two characterisations are equivalent, and each may be found from the other. Also, each may be related to the theoretical model in terms of a differential equation. This suggests two possible approaches to the identification of the plant. The first is to generate a sinusoidal input to the plant and measure the resulting gain and phase. By carrying out this procedure for all input frequencies the frequency response of the system is found. The second is to measure (as a time function) the output in response to an impulse input.

Unfortunately both methods have severe disadvantages. Sine wave testing is a very lengthy process, as the plant must be allowed to settle to a steady state after the application of each new frequency. Impulse testing must be carried out with very low input signal levels otherwise the plant may be driven outside its region of linear operation. Frequently economic considerationsdictate that the plant should remain in service while the identification is performed. This means that the normal input appears as a noise input to the system. It also means

that the test signal must be kept to a very low level to maintain satisfactory limits on the plant output. The signal to noise ratio may be very small therefore, and reasonable results may only be obtained by averaging over many observations.

Consequently, indirect methods have been developed to find the impulse response of a linear system. As the time derivative of a unit step is a unit impulse, for a linear system, the impulse response is the time derivative of the step response. Step response testing still gives a poor signal to noise ratio for the high frequency components. Better results are obtained using a correlation technique.

Impulse Testing by Cross-correlation.

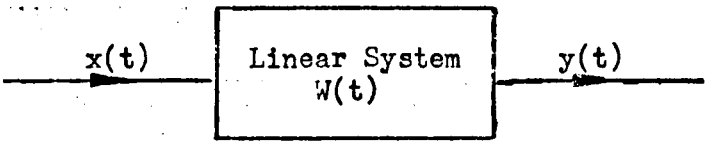

figure 1.1.1

In chapter (2) we define the cross-correlation function, a measure of the dependence of one signal upon the past values of another. We also define the auto-correlation function which is a measure of the dependence of a signal upon its own past value. It can be shown (see, for example, Douce [1] Chapter (6)) that the cross-correlation function of the input and output of a linear system is the convolution of the auto-correlation function of the input and the impulse response of the system. That is, for the system of figure (1)

$$\Phi_{xy}(\tau) = \int_{-\infty}^{\infty} W(\nu)\, \Phi_{xx}(\tau-\nu)\,d\nu \qquad 1.1.1$$

Where W(t) is the system impulse response

$\Phi_{xy}(\tau)$ is the cross-correlation function of x(t) and y(t)

A random signal has an auto-correlation function which is impulsive, because its current value is independent of all its past values. We can see from equation (1) that if x(t) is a random signal, then the cross-correlation function of the input and output is the impulse response of the system.

$$\Phi_{xy}(\tau) = W(\tau)$$

when $\Phi_{xx}(\tau) = \delta(\tau)$

We have therefore, an indirect method of finding the impulse response of the system, summarised in figure (2)

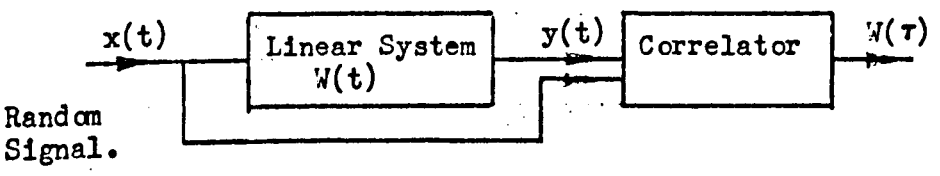

figure 1.1.2

The normal operating input of the plant may well be a random signal, and therefore suitable as the input test signal. As the auto-correlation function of a short length of a random signal is not necessarily impulsive, an experiment using the operating input must be very carefully designed, and the statistics of the input signal monitored over the time period of the experiment. This may be overcome by introducing a test signal which is deterministic and has statistics (notably its auto-correlation function) similar to that of a truly random signal. In section (3.2) we meet a class of deterministic signals which, in addition to having known statistics over a short sample, are quantised, allowing the correlator to be fairly simple.

Chapter 2.

In chapter (1) we saw how by correlation we could find the impulse response of a linear system. In this chapter we will define the partial correlation function and see how it may be used in the identification of a class of non-linear systems.

(2.1) Definitions of Partial Correlation Functions.

Consider two signals, each a function of time, x(t) and y(t) The cross-correlation function $\Phi_{xy}(\tau)$ is a measure of the dependence of the value of $y(t+\tau)$ upon the value of x(t). It is defined by the relationship

$$\Phi_{xy}(\tau) = \int_{-\infty}^{\infty}\int_{-\infty}^{\infty} X.Y.p(X,Y,\tau).dX.dY \qquad 2.1.1$$

where $p(X,Y,\tau)$ is the joint probability density function of x(t) and $y(t+\tau)$. That is,

$$P\left\{\begin{matrix} X \leqslant x(t) < (X + \delta X) \\ Y \leqslant y(t) < (Y + \delta Y)\end{matrix}\right\} = p(X,Y,\tau).\delta X.\delta Y$$

$\delta X, \delta Y \to 0$. ‡

We may rewrite equation (1)* as

$$\Phi_{xy}(\tau) = \int_{-\infty}^{\infty} X\left\{\int_{-\infty}^{\infty} Y.p(X,Y,\tau)\,dY\right\}dX$$

Let us now consider the term in curly brackets. This we will call the partial cross-correlation function, $\phi_{xy}(\tau,X)$. Clearly the partial cross correlation function is a function of the time shift τ, as was $\Phi_{xy}(\tau)$, and is in addition a function of the value of X for which it is evaluated, as a result of the dependence of $p(X,Y,\tau)$ on X.

We now define the partial cross-correlation function $\phi_{xy}(\tau,X)$ of x(t) and y(t) with respect to x(t) as

$$\phi_{xy}(\tau,X) = \int_{-\infty}^{\infty} Y.p(X,Y,\tau)\,dY \qquad 2.1.2$$

and it is clear from the definition that

$$\Phi_{xy}(\tau) = \int_{-\infty}^{\infty} X.\phi_{xy}(\tau,X)\,dX \qquad 2.1.3$$

---

‡ The symbol P {...} is used to mean "the probability that the statement in curly brackets is true".

* Equations are numbered starting from 1 in each section, with the section number as a prefix. Within the section the prefix is omitted. The same procedure is adopted for tables and figures.

Physically, $\phi_{xy}(\tau,X)$ is the expected value of y at a time τ after $x = X$. It is the function which West[2] calls the 'time dependent mean density function'. If x has a mean value that is zero, then $\phi_{xy}(\tau,x)$ becomes Nuttall's g-function.[3]

We will now define a component signal, $a(t,X)$, of $x(t)$ such that

$$a(t,X).\delta X = 1, \quad \begin{matrix} X \leqslant x(t) < X + \delta X \\ \delta X \to 0 \end{matrix}$$

$$= 0, \quad \text{otherwise} \qquad 2.1.4$$

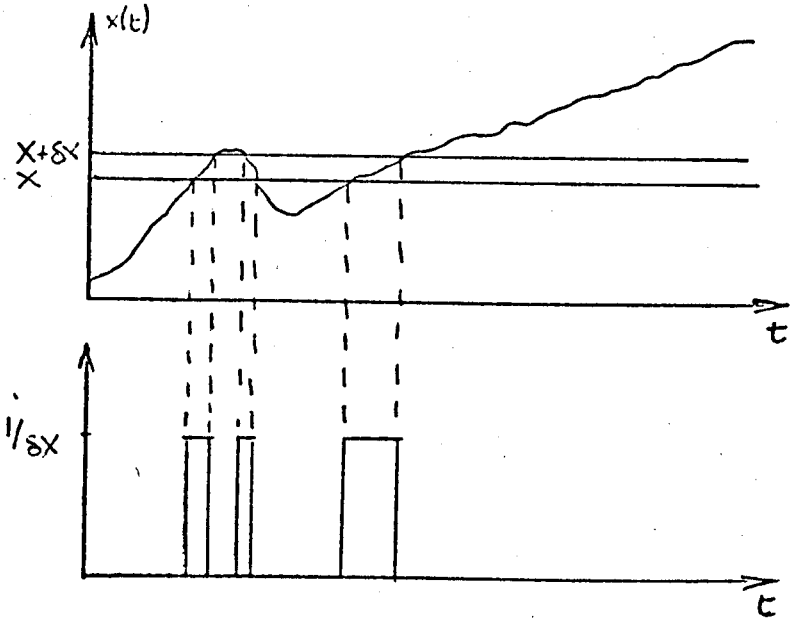

figure 2.1.1

from this definition we see that

$$x(t) = \int_{-\infty}^{\infty} X.\ a(t,X).dX \qquad 2.1.5$$

If $x(t)$ is an ergodic process, the probability that x lies between X and $(X + \delta X)$ is

$$\delta X.p_X(X) = \underset{T \to \infty}{\text{limit}} \frac{1}{2T} \int_{-T}^{T} \delta X.\ a(t,X).dt$$

and so $$p_X(X) = \underset{T \to \infty}{\text{limit}} \frac{1}{2T} \int_{-T}^{T} a(t,X)\, dt \qquad 2.1.6$$

where $p_X(X)$ is the probability density function of x,

$$P\{X \leqslant x < X + \delta X\} = \delta X.\ p_X(X)$$

now,

$$a(t,X_1).\ a(t+\tau,X_2).\ \delta X^2 = 1, \quad \begin{cases} X_1 \leqslant x(t) < X_1 + \delta X \\ X_2 \leqslant x(t+\tau) < X_2 + \delta X \end{cases}$$

$$= 0, \quad \text{otherwise}$$

so it follows that for an ergodic process

$$p_X(X_1,X_2,\tau).\delta X^2 = \underset{T\to\infty}{\text{limit}}\ \frac{1}{2T}\int_{-T}^{T} a(t,X_1).a(t+\tau,X_2)\,\delta X^2.\,dt$$

and

$$p_X(X_1,X_2,\tau) = \underset{T\to\infty}{\text{limit}}\ \frac{1}{2T}\int_{-T}^{T} a(t,X_1).\,a(t+\tau,X_2).\,dt \qquad 2.1.7$$

where $p_X(X_1,X_2,\tau)$ is the joint probability density of $x(t)$ and $x(t+\tau)$.

Let us now return, from our digression on component signals, to the correlation functions. If $x(t)$ and $y(t)$ are ergodic processes, then we may write their cross-correlation, $\Phi_{xy}(\tau)$ as

$$\Phi_{xy}(\tau) = \underset{T\to\infty}{\text{limit}}\ \frac{1}{2T}\int_{-T}^{T} x(t)y(t+\tau)dt \qquad 2.1.8$$

and by substituting equation (5) into this expression

$$\Phi_{xy}(\tau) = \underset{T\to\infty}{\text{limit}}\ \frac{1}{2T}\int_{-T}^{T}\int_{-\infty}^{\infty} X.a(t,X).y(t+\tau)dX.dt$$

$$= \int_{-\infty}^{\infty} X\left\{\underset{T\to\infty}{\text{limit}}\ \frac{1}{2T}\int_{-T}^{T} a(t,X).y(t+\tau)dt\right\}dX$$

clearly the term in curly brackets is the cross-correlation $\Phi_{ay}(\tau)$ between $a(t,X)$ and $y(t)$

$$\Phi_{xy}(\tau) = \int_{-\infty}^{\infty} X\ \Phi_{ay}(\tau)\ dX \qquad 2.1.9$$

Comparing equations (3) and (9) we see that

$$\phi_{xy}(\tau,X) = \Phi_{ay}(\tau)$$

where $\Phi_{ay}(\tau)$ is the cross-correlation function between $a(t,X)$ and $y(t)$

Hence, if $x(t)$ and $y(t)$ are ergodic,

$$\phi_{xy}(\tau,X) = \underset{T\to\infty}{\text{limit}}\ \frac{1}{2T}\int_{-T}^{T} a(t,X)y(t+\tau)dt \qquad 2.1.10$$

If we now replace y by x in all the previous expressions, we find the auto-correlation function, $\Phi_{xx}(\tau)$, and partial auto-correlation function, $\phi_{xx}(\tau,X)$, of the signal $x(t)$

$$\Phi_{xx}(\tau) = \int_{-\infty}^{\infty}\int_{-\infty}^{\infty} X_1.X_2.p(X_1,X_2,\tau).dX_1.dX_2 \qquad 2.1.11$$

$$\phi_{xx}(\tau,X) = \int_{-\infty}^{\infty} X_1.p(X,X_1,\tau).dX_1 \qquad 2.1.12$$

If x(t) is an ergodic process, then

$$\Phi_{xx}(\tau) = \lim_{T \to \infty} \frac{1}{2T} \int_{-T}^{T} x(t).x(t+\tau).dt \qquad 2.1.13$$

$$\phi_{xx}(\tau,X) = \lim_{T \to \infty} \frac{1}{2T} \int_{-T}^{T} a(t,X).x(t+\tau).dt \qquad 2.1.14$$

By substituting equation (5) into (13) and (14),

$$\Phi_{xx}(\tau) = \int_{-\infty}^{\infty} \int_{-\infty}^{\infty} X_1.X_2.\Phi_{a_1a_2}(\tau).dX_1.dX_2 \qquad 2.1.15$$

$$\phi_{xx}(\tau,X) = \int_{-\infty}^{\infty} X_1 \Phi_{aa_1}(\tau)\, dX_1 \qquad 2.1.16$$

where $\Phi_{aa_1}(\tau)$ is the cross-correlation between a(t,X) and $a(t,X_1)$

2.2

The Use of the Partial Correlation Function in the Identification of Non-Linear Systems.

The partial correlation function may be used in the identification of some non-linear systems. These are the systems which may be represented by figure (1), where a single-valued instantaneous non-linearity, defined for all inputs, is followed by a linear system.

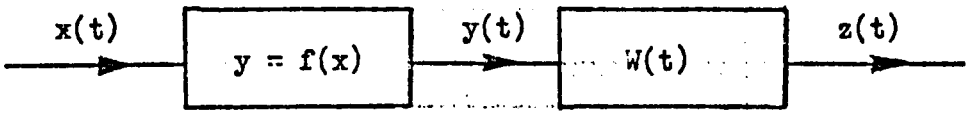

figure 2.2.1

In appendix (1), the partial cross-correlation function $\phi_{x3}(\tau,X)$ of x(t) and z(t) is found to be

$$\phi_{x3}(\tau,X) = \int_{\nu=0}^{\infty} W(\nu) \int_{X_1=-\infty}^{\infty} f(X_1)\ \Phi_{aa_1}(\tau-\nu).dX_1.d\nu \qquad 2.2.1$$

where $\Phi_{aa_1}(\tau)$ is the cross-correlation function of the components $a(t,X)$ and $a(t,X_1)$ of the input x(t)

If $\Phi_{aa_1}(\tau) = 0$, for all $X \neq X_1$, and all τ

then,

$$\phi_{x3}(\tau,X) = f(X) \int_{\nu=0}^{\infty} W(\nu).\Phi_{aa}(\tau-\nu)d\nu \qquad 2.2.2$$

where $\Phi_{aa}(\tau)$ is the autocorrelation function of $a(t,X)$, if, further, $\Phi_{aa}(\tau)$ has an impulsive form,

then,

$$\phi_{x3}(\tau,X) = f(X).W(\tau) \qquad 2.2.3$$

In practice there is a signal which has properties closely approximating those of x(t) above, and which we will discuss in chapter (3). Using this signal and a partial correlation process we can identify the dynamics of the linear system, and find the non-linearity f(X) to within a ~~arbitrary~~ scale factor.

2.3 Quantised Signals.

When the input signal $x(t)$ is quantised into, say, p levels $(X_0, X_1, \ldots X_{p-1})$, the component signal $a(t,X)$ of $x(t)$ must be zero when $X \neq X_i$, one of the p levels.

$$\left.\begin{aligned} \delta X.\ a(t,X) &= 1, \quad X = X_i = x(t) \\ &= 0, \quad \text{otherwise} \end{aligned}\right\} \qquad 2.3.1$$

We see that $a(t,X)$ is a unit impulse,

$$\left.\begin{aligned} a(t,X) &= \delta(X - X_i), \quad x(t) = X_i \\ &= 0, \quad \text{otherwise} \end{aligned}\right\} \qquad 2.3.2$$

It will be convenient when $x(t)$ is quantised to write

$$a(t,i) = \int_{X_i-\delta}^{X_i+\delta} a(t,X).dX \qquad 2.3.3$$

where $2\delta \ll (X_i - X_{i-1})$

$$\phi_{x3}(\tau,i) = \int_{X_i-\delta}^{X_i+\delta} \phi_{x3}(\tau,X).dX \qquad 2.3.4$$

from equation (2), we see that $a(t,X)$ is always zero outside the limits used in equations (3) and (4). We recall that

$$\phi_{x3}(\tau,X) = \int_{-\infty}^{\infty} Z.p(X,Z,\tau).dZ$$

which is zero outside the limits used in equations (3) and (4) since

$$p(X,Z,\tau) = 0, \qquad X \neq X_i \pm \delta$$

so in place of equations (2.1.5), (2.1.10) and (2.1.3), for a quantised signal

$$x(t) = \sum_{i=0}^{p-1} X_i.\ a(t,i) \qquad 2.3.5$$

$$\phi_{x3}(\tau,i) = \lim_{T \to \infty} \frac{1}{2T} \int_{-T}^{T} a(t,i).z(t+\tau)dt \qquad 2.3.6$$

(for $x(t)$ an ergodic process)

$$\Phi_{x3}(\tau) = \sum_{i=0}^{p-1} X_i.\ \phi_{x3}(\tau,i) \qquad 2.3.7$$

and equation (2.2.1) becomes

$$\phi_{x3}(\tau,i) = \int_{0}^{\infty} W(\nu) \sum_{j=0}^{p-1} f(X_j).\ \Phi_{a_i a_j}(\tau - \nu)d\nu \qquad 2.3.8$$

where $\Phi_{a_i a_j}(\tau)$ is the cross-correlation function of $a(t,i)$ and $a(t,j)$.

2.4 Periodic Input Signals.

Let us consider the partial cross-correlation function of two ergodic signals $x(t)$ and $z_1(t)$ with respect to $a(t)$. We found in section (2.1) that this may be written

$$\phi_{x31}(\tau,X) = \lim_{T \to \infty} \frac{1}{2T} \int_{-T}^{T} a(t,X).z_1(t+\tau).dt \qquad 2.4.1$$

where $a(t,X)$ is a component signal of $x(t)$

If $x(t)$ is periodic, with period T_c, then

$$x(t + NT_c) = x(t) \text{ for all integer } N \qquad 2.4.2$$

Let $z_1(t) = z(t) + n(t)$

where $z(t)$ is periodic, with period T_c, and $n(t)$ has no component with period T_c.

Since $z_1(t)$ is ergodic, and $z(t)$ is ergodic as a periodic signal is necessarily so, then $n(t)$ is ergodic

$$\phi_{x31}(\tau,X) = \lim_{T \to \infty} \frac{1}{2T} \int_{-T}^{T} a(t,X).z(t+\tau)dt + \lim_{T \to \infty} \frac{1}{2T} \int_{-T}^{T} a(t,X).n(t+\tau)dt \qquad 2.4.3$$

Now the first term in equation (3) is the average over all time of $a(t,X)$ and $z(t+\tau)$. Since both signals have period T_c, they will maintain the same phase relationship over all time, and so the average is the same as the average over one period.

$$\lim_{T \to \infty} \frac{1}{2T} \int_{-T}^{T} a(t,X).z(t+\tau).dt = \frac{1}{T_c} \int_{0}^{T_c} a(t,X).z(t+\tau).dt$$

As $n(t)$ has no component with period T_c, the second term in equation (3) is just the product of the expected values of $a(t,X)$ and $n(t)$

$$\lim_{T \to \infty} \frac{1}{2T} \int_{-T}^{T} a(t,X).n(t+\tau)dt = E\{a(t,X)\}.E\{n(t)\}$$

so,

$$\phi_{x31}(\tau,X) = \frac{1}{T_c} \int_{0}^{T_c} a(t,X).z(t+\tau)dt + E\{a(t,X)\}.E\{n(t)\} \qquad 2.4.4$$

A special case is when $n(t)$ has zero mean value, equation (4) then becomes

$$\phi_{x31}(\tau,X) = \frac{1}{T_c} \int_{0}^{T_c} a(t,X).z(t+\tau)dt \qquad 2.4.5$$

In particular, equation (5) holds if n(t) = 0, for instance if x(t) and z(t) are the input and output of a noise free system.

If n(t) has zero mean value, the cross-correlation function $\Phi_{x3_1}(\tau)$ is given by

$$\Phi_{x3_1}(\tau) = \frac{1}{T_c}\int_0^{T_c} x(t).z(t+\tau)dt \qquad 2.4.6$$

It is important to observe that it is $z(t + \tau)$ that appears under the integral sign in equations (5) and (6), and not $z_1(t + \tau)$. Errors occur in estimates, of $\phi_{x3_1}(\tau,X)$ or of $\Phi_{x3_1}(\tau)$, based on correlation performed with z_1 for a finite integration time, since in general even when $E\{n(t)\} = 0$,

$$\int_0^{T_c} x(t).n(t+\tau).dt \neq 0$$

This is taken into account in appendix (6) where the variance of such an estimate is found.

In chapter (4) we will study the identification of the system of figure (1), in which the output z(t) is contaminated by noise n(t).

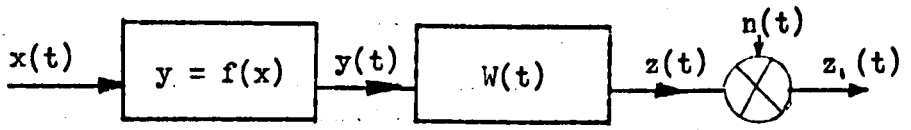

figure 2.4.1

We see from equation (5) that if n(t) has zero mean,

$$\phi_{x3_1}(\tau,X) = \phi_{x3}(\tau,X)$$

This suggests that we could use an experimental estimate of $\phi_{x3_1}(\tau,X)$ as an estimate of $\phi_{x3}(\tau,X)$

2.5 Periodic, Quantised Input Signals.

We will be dealing later with quantised signals which are periodic. For this case, the results of both sections (2.3) and (2.4) are applicable, and we will summarize them here in a combined form, for future use

$$x(t) = \sum_{i=0}^{p-1} X_i . a(t,i) \qquad 2.5.1$$

where $a(t,i) = 1 \quad , \qquad x(t) = X_i$

$= 0 \quad , \qquad$ otherwise

$$x(t) = x(t + NT_c) \qquad 2.5.2$$

where T_c is the period of $x(t)$ and N is any integer

$$\phi_{x3i}(\tau,i) = \frac{1}{T_c} \int_0^{T_c} a(t,i).z(t + \tau).dt \qquad 2.5.3$$

where $z_i(t) = z(t) + n(t)$

$n(t)$ has zero mean, and is uncorrelated with $x(t)$

$$\Phi_{x3i}(\tau) = \sum_{i=0}^{p-1} X_i . \phi_{x3_i}(\tau,i) \qquad 2.5.4$$

Also, it is obvious from equation (2) that

$$a(t,i) = a(t + NT_c,i)$$

If $W(\nu) = 0$ for $\nu \geq T_c$, then equation (2.3.8) becomes

$$\phi_{x3}(\tau,i) = \int_0^{T_c} W(\nu) \sum_{j=0}^{p-1} f_j . \Phi a_i a_j(\tau - \nu)d\nu \qquad 2.5.5$$

which is the partial cross-correlation function of the input and output of the system in figure (2.2.1), with respect to a quantised, periodic input signal $x(t)$

Chapter (3):

3.1 Realisation of a Test Signal for Indentification.

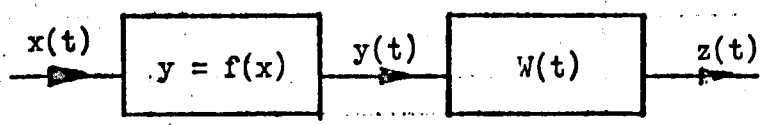

figure (3.1.1)

In section (2.4) we found that we could identify the system shown in figure (1) using the partial correlation function, provided we could find a test signal x(t) with certain special properties. Ideally these would be

(a) $\Phi_{a_i a_j}(\tau) = 0$ for all $X_j \neq X_i$

(b) $\Phi_{a_i a_j}(\tau) = \Phi_i . \delta(\tau)$ for all i

(c) x(t) periodic with period T_c, so that the identification may be carried out with a finite integration time

In this chapter we will define a class of signals which has properties closely approximating to those above, and we will investigate its use in the identification of the system in figure (1)

3.2 The p - level m - sequence.

A random number sequence is a sequence of numbers in which each element is independent of all previous elements. We may consider a particular random signal which is generated from such a random sequence, in the following way. A generator produces an output which may change only at the instants when regularly spaced clock pulses are received by the generator. The output after the arrival of a clock pulse is independent of the output before the pulse arrived. Let us find the autocorrelation function $\Phi_{rr}(\tau)$ of the output $\mathbf{r}(t)$, when the clock period is λ.

$$\Phi_{rr}(i\lambda) = E\{r(t).r(t - i\lambda)\} \quad \text{for all integer } i$$
$$= E\{r(t)\}\, E\{r(t - i\lambda)\} \quad \text{for all } i \neq 0$$
$$= E^2\{r(t)\} \quad \text{for all } i \neq 0$$
$$\Phi_{rr}(0) = E\{r^2(t)\}$$

In appendix (7) it is shown that the autocorrelation function of a clocked signal changes linearly between $\tau = i\lambda$ and $\tau = (i + 1)\lambda$ for all i, so we have the correlation function shown in figure (1) The feature at the time origin is defined in appendix (5) as a 'spike', and approximates to an impulse of strength $(E\{r^2(t)\} - E^2\{r(t)\}).\lambda$

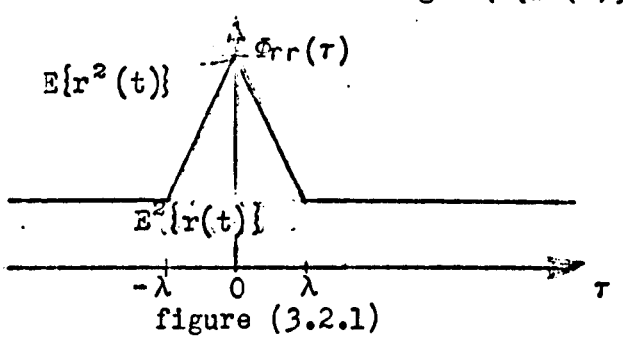

figure (3.2.1)

A pseudo-random sequence is a periodic number sequence which has statistical properties approximating to those of a random number sequence. In particular, the autocorrelation function of a pseudo-random sequence is similar to that of the random sequence.

Clearly, as the pseudo-random sequence is periodic, its auto-correlation function must be periodic and so the best approximation that could be obtained is shown in figure (2) where T_c is the period of the sequence, and x(t) is a pseudo-random sequence.

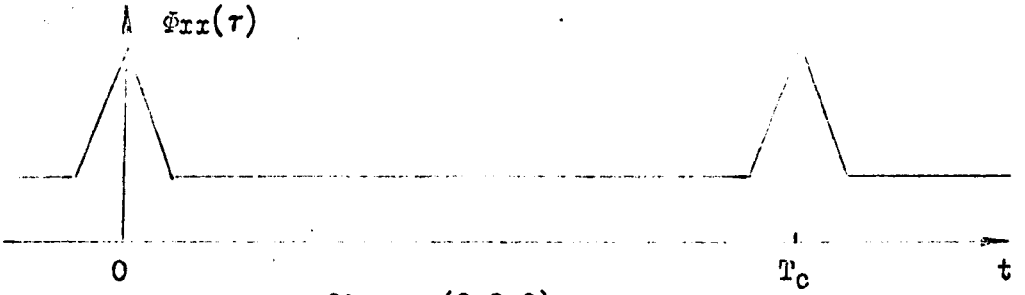

figure (3.2.2)

In practice it may also have other spikes of various heights in each period. Of course, if the signal is physically realisable these spikes cannot be of magnitude greater than the one at the time origin.

Now consider a register of n stages, each of which has p stable states. Upon receipt of a (regularly spaced) clock pulse, each stage adopts the state of the previous stage before the clock pulse. Such a register is called a p-level n-stage shift register, and is represented in figure (3)

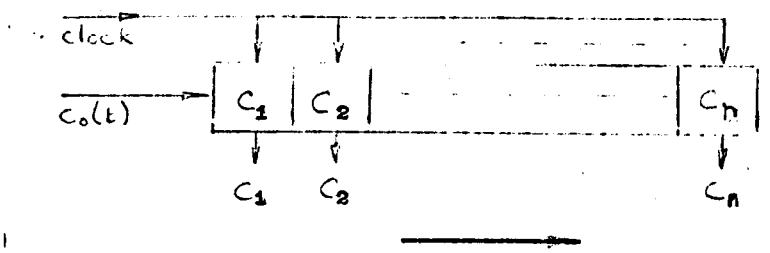

figure (3.2.3)

$c_i(t)$ is the state of (and output from) the ith stage at time t. We may write

$$c_i(t) = c_{i-1}(t - \lambda) \qquad i = 1, 2, \ldots n$$

where λ is the period between clock pulses.

If the input to the shift register, $c_0(t)$, is formed by modulo p operations upon the outputs $c_1(t) \ldots c_n(t)$, we have a feedback shift register as represented in figure (4)

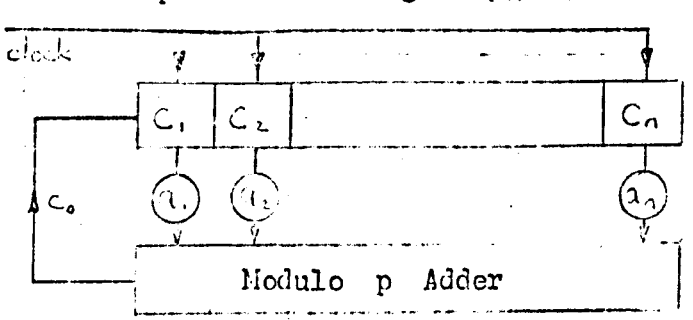

figure (3.2.4)

We can describe the operation of this device by the equation

$$c_0 = \langle a_1 c_1 + a_2 c_2 + \ldots\ldots a_n c_n \rangle_p \qquad 3.2.1$$

Where the symbol $\langle \ldots\ldots \rangle_p$ is used to mean that the operations between the brackets $\langle$ and $\rangle$ are all performed modulo p.

If p is a prime, we may choose a_1, a_2 .....a_n such that $c_0(t)$ is a periodic sequence of $(p^n - 1)$ elements, in the course of which every n-tuple $(c_1, c_2 \ldots c_n)$ occurs once, except the null n-tuple (0, 0, 0 ... 0) and this never occurs. Such a sequence is a 'maximal-length pseudo random p-level sequence', and we will refer to it as a p-level m-sequence.

The p-level m-sequence has (p-1) equally spaced spikes in each period of its autocorrelation function. If the levels X_0, $X_1 \ldots X_{p-1}$ of the output of the shift register are chosen symmetrically about zero, then the mean value of the sequence is zero and the auto-correlation function is zero, between the (p-1) spikes in each period. Some of the spikes may have zero amplitude, for example if (p=4N+1, N integer) then the spikes at delays of one quarter and three quarters of a period are of zero amplitude.

Figure (5) is an example of the autocorrelation function of a p-level m-sequence. In this case p = 3, so there are just two spikes in each period of the autocorrelation function.

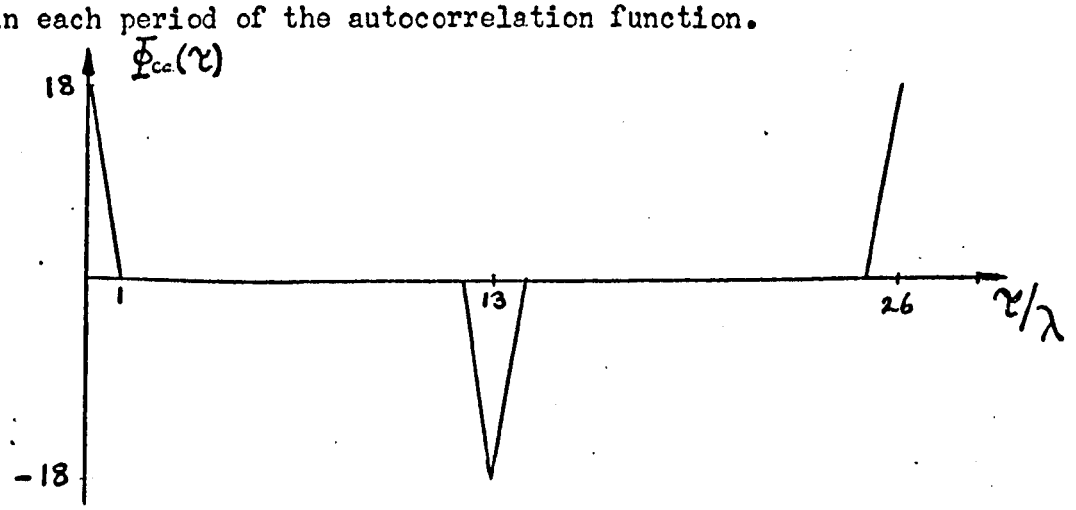

Autocorrelation function of a 3-level m-sequence of length $[(3^3 - 1) = 26]$ clock periods.

figure (3.2.5)

In appendix (2) the cross-correlation functions of the components of the p-level m-sequence are found. The results are shown in figure (6) for the general case.

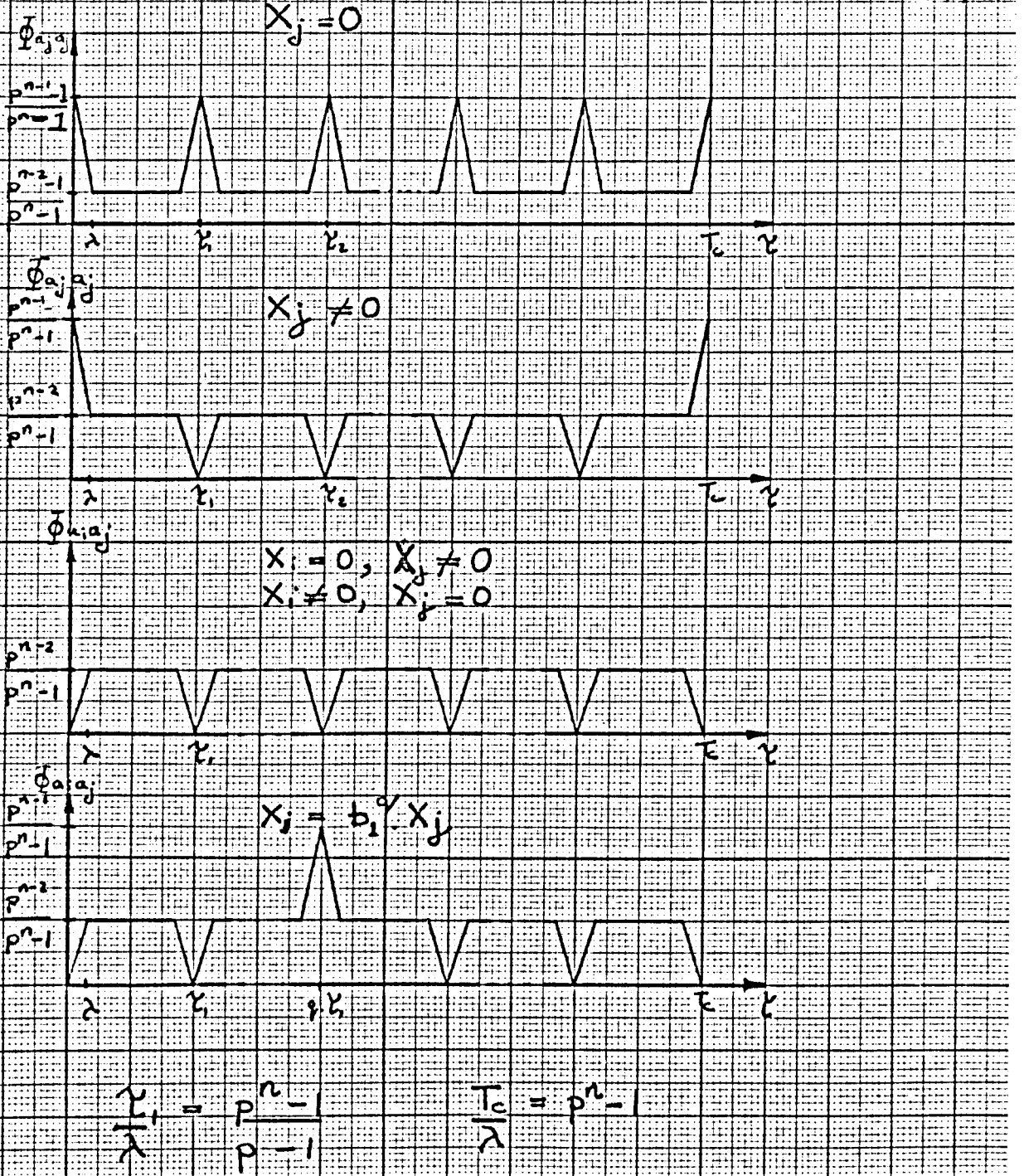

$$\frac{\tau_1}{\lambda} = p\frac{p^{n-1}}{p-1} \qquad \frac{T_c}{\lambda} = p^n - 1$$

FIGURE 3·2·6

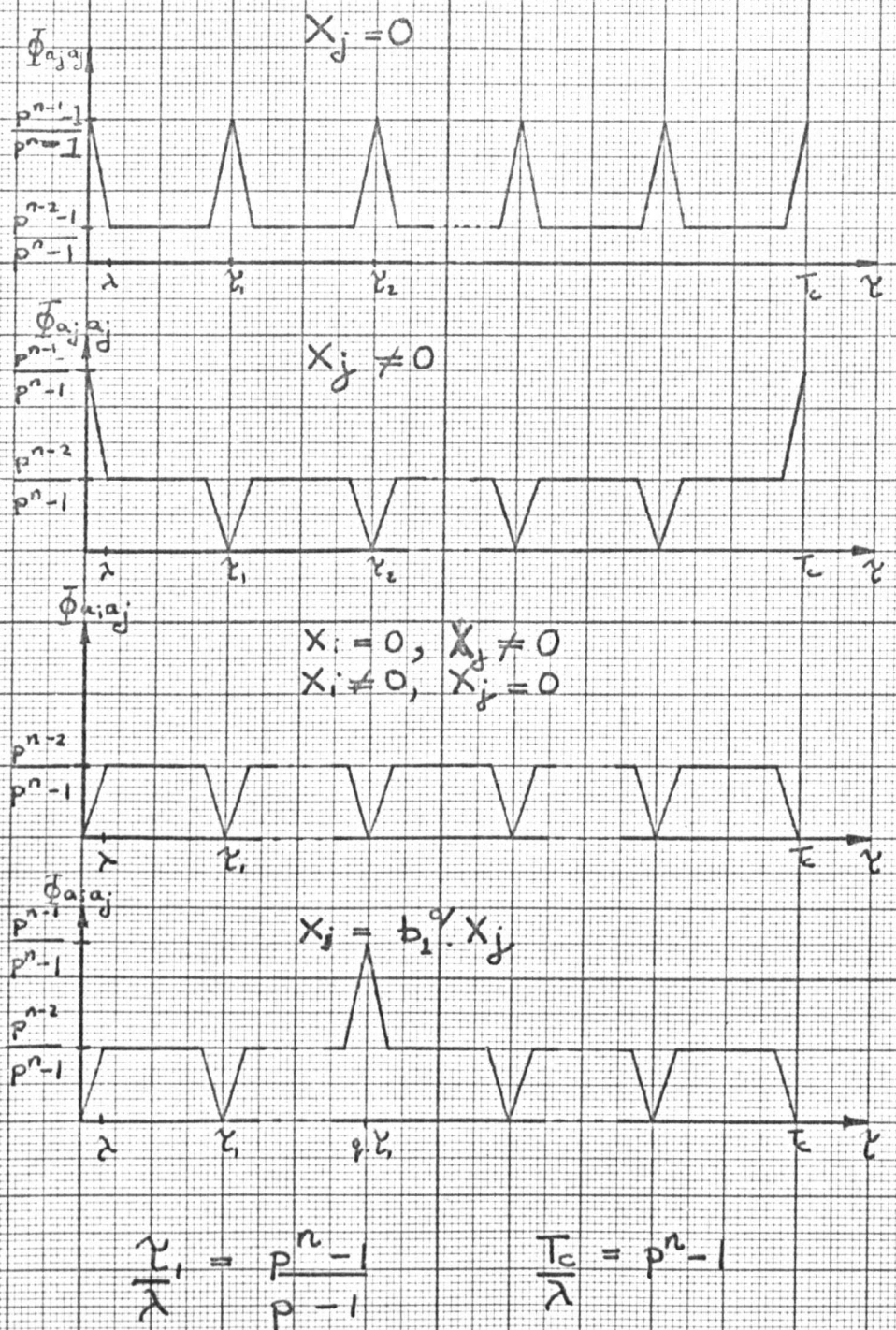

$$\frac{\tau_1}{\lambda} = \frac{p^n - 1}{p - 1} \qquad \frac{T_c}{\lambda} = p^n - 1$$

FIGURE 3·2·6

3.3 Identification Using the p-level m-sequence.

It is clear from figure (3.2.6) that the p-level m-sequence does not meet our specification for a test signal. The cross-correlation between any two components is the sum of a non-zero constant, and a function which has spikes for $\tau = 0, \frac{T_c}{p-1}, \frac{2T_c}{p-1}$ etc

However, consider the identification of the system in section (2.2). For a periodic quantised input signal x(t), and a noise free system, the input-output partial cross-correlation function $\phi_{x3}(\tau,i)$ is given by equation (2.5.6) as

$$\phi_{x3}(\tau,i) = \int_0^{T_c} W(\nu) \sum_{j=0}^{p-1} f_j . \Phi_{a_i a_j}(\tau - \nu) d\nu \qquad 3.3.1$$

where $W(\nu) = 0, \quad \nu \geq T_c$

$\Phi_{a_i a_j}(\tau)$ is the cross-correlation function of a(t,i) and a(t,j)

$f_i = f(X_i)$

The constant term in $\Phi_{a_i a_j}(\tau)$ produces a term C_i in $\phi_{x3}(\tau,i)$ which is independent of τ but dependent on i. Ci depends upon the characteristic of the non-linearity and upon the integral

$$\int_0^{T_c} W(\nu)\, d\nu$$

and is therefore unknown.

We see that if $W(\nu) = 0$, for $\nu \geq \frac{T_c}{p-1}$, then over the range

$0 \leq \tau < \frac{T_c}{p-1}$, the spikes in $\Phi_{a_i a_j}(\tau)$ which are not at the origin have no effect.

Hence, if $W(\nu) = 0$ for $\nu \geq \frac{T_c}{p-1}$ we can use the p-level m-sequence for identification, but we will have to remove the constant term C_i. We will see later how to achieve this.

In appendix (3) we derive an expression for $\phi_{x3}(\tau,i)$ in terms of the parameters of the m-sequence, and those of the system, with the result

$$\phi_{x3}(\tau,0) = \frac{p^{n-1}}{p^n-1} \left\{ (f(o) - f_{av}).W(\tau) + (f_{av} - \frac{f(o)}{p^n-1}) \int_0^{T_c} W(\nu) d\nu \right\} \qquad 3.3.2$$

$$\phi_{x_3}(\tau,i) = \frac{p^{n-i}}{p^n-1}\left\{(f_i - f_{av})W(\tau) + f_{av}\int_0^{Tc} W(\nu)d\nu\right\} \qquad 3.3.3$$

$X_i \neq 0$

provided that (1) $W(\tau)$ has a settling time long compared with λ

(2) $W(\tau) = 0, \quad \tau \geq \left\{\frac{(p^n-1)}{p-1} - 1\right\}\lambda$

and where $f_{av} = \frac{1}{p}\sum_j f_j$

If we were mechanising the identification on a digital computer, we would compute $\phi_{x_3}(k\lambda, i)$ for $k = 0,1,\ldots m$.

where $m = \frac{p^n - 1}{p-1} - 1$

and since we have assumed that $W(m\lambda) = 0$,

$$\phi_{x_3}(k\lambda,0) = \frac{p^{n-1}}{p^n-1}\left\{(f(0) - f_{av}).W(k\lambda) + (f_{av} - \frac{f(0)}{p^n-1})\sum_{j=o}^{m} W(j\lambda)\right\} \qquad 3.3.4$$

$$\phi_{x_3}(k\lambda,i) = \frac{p^{n-1}}{p^n-1}\left\{(f_i - f_{av}).W(k\lambda) + f_{av}\sum_{j=o}^{m} W(j\lambda)\right\} \qquad 3.3.5$$

$X_i \neq 0$

It is clear that

$$\phi_{x_3}(k\lambda,i) - \phi_{x_3}(m\lambda,i) = \frac{p^{n-i}}{p^n-1}\ (f_i - f_{av}).\ W(k\lambda) \qquad 3.3.6$$

for all k, i

If we form a matrix of measurements $[M_{ki}]$ such that

$$M_{ki} = \frac{p^n-1}{p^{n-i}}\left\{\phi_{x_3}(k\lambda,i) - \phi_{x_3}(m\lambda,i)\right\}$$

then $M_{ki} = W(k\lambda).\ (f_i - f_{av})$ 3.3.7

Now we have the same information as we would have had if we had performed the identification with our ideal test signal, except that we are unable to find f_{av} from M_{ij}.

We are unable to find the equivalent gain of the non-linearity either from equation (7) or from equation (2.2.3), but this is unlikely to be a serious drawback in practice.

3.4 The Power Spectrum of the Output of a Non-linearity with p-level m-sequence input.

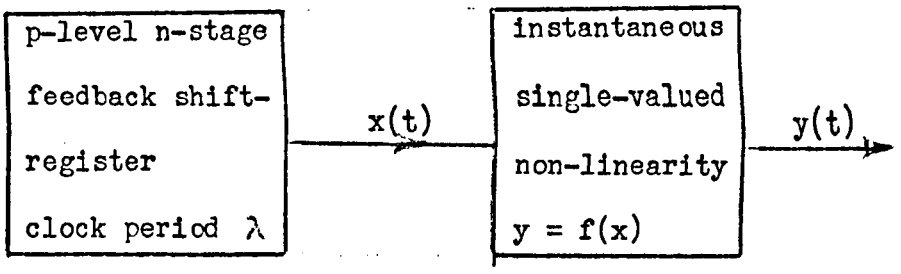

figure 3.4.1

Consider the system of figure (1). We assume that the feedback connections to the shift-register have been made such that x(t) is an m-sequence of period Tc,

$$T_c = (p^n-1)\lambda$$

In appendix (4) we found the autocorrelation functions $\Phi_{xx}(\tau)$ and $\Phi_{yy}(\tau)$ for this case. When $p>2$, $\Phi_{yy}(\tau)$ was found for τ an integer multiple of λ, the clock period, as

$$\underset{\tau=q\tau_1}{\Phi_{yy}(\tau)} = \frac{p^{n-1}}{p^n-1}\left\{ \sum_{l=0}^{p-1} f(\langle B^q.X_J\rangle_p).f_J \right\} - \frac{f_o^2}{p^n-1} \qquad 3.4.1$$

$$\underset{\tau\neq q\tau_1}{\Phi_{yy}(\tau)} = \frac{p^{n-2}}{p^n-1}\left\{ \sum_{l=0}^{p-1} f_l \right\}^2 - \frac{f_o^2}{p^n-1} \qquad 3.4.2$$

where (a) $f_J = f(X_J)$

(b) $\tau_1 = \dfrac{T_c}{p-1}$

(c) $q = 0,1,\ldots. p-2$

(d) B is the delay gain b_o which corresponds to τ_1 (see appendix (2))

We see from equation (2) that when the average value $\frac{1}{p}\sum_{l=0}^{p-1} f_l$ of the non-linearity is zero, and when it has zero output for zero input, then there is no constant level in the autocorrelation function of y(t). Generally this will not be so, and there will be a constant level d in the autocorrelation function $\Phi_{yy}(\tau)$, given by equation (2)

From equation (1) we see that spikes occur regularly at delays λK_q, $q = 0,1,\ldots.$ having heights H_q (see figure (2), so that

$$H_q = \frac{p^{n-1}}{p^n-1}\left\{ \sum_{l=0}^{p-1} f(\langle B^q X_l\rangle_p).f_l - \frac{1}{p}\left(\sum_{l=0}^{p-1} f_l\right)^2 \right\} \qquad 3.4.3$$

$$\lambda K_q = q\frac{T_c}{p-1}$$

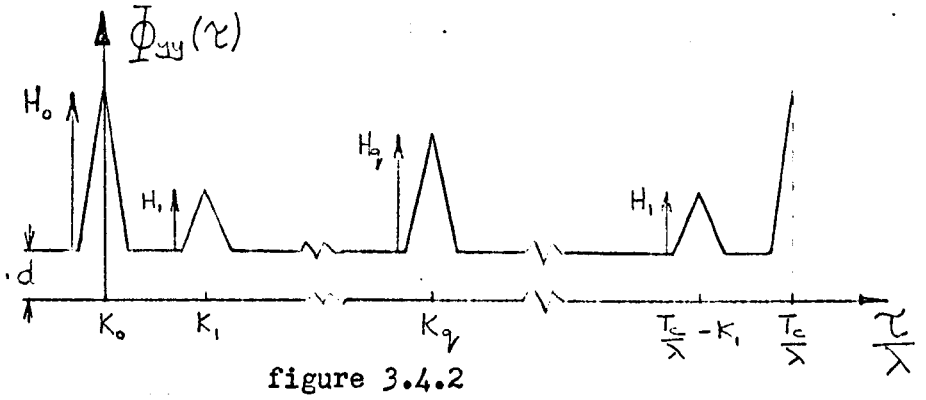

figure 3.4.2

The power spectrum $G''_{yy}(w)$ of y(t) is the sum of an impulse of strength d at zero frequency, due to the constant component d, and $G'_{yy}(w)$, the power spectrum of the spikes alone. $G'_{yy}(w)$ was found in appendix (A.5)

$$G''_{yy}(w) = d.\delta(w) + G'_{yy}(w) \qquad 3.4.5$$

where (a) $G'_{yy}(w) = \operatorname{sinc}^2 \frac{\pi h \lambda}{T_c} . G_{yy}(w)$

(b) $G_{yy}(w) = \left\{ H_o + (-1)^h H_{\frac{p-1}{2}} + 2 \sum_{q=1}^{\frac{p-3}{2}} H_q . g_{yy}(w, K_q) \right\}$

(c) $g_{yy}(w, K_q) = \frac{1}{\lambda} . \cos \frac{2\pi h K_q \lambda}{T_c}$

(d) h is any integer.

(e) $\operatorname{sinc} x \triangleq \frac{\sin x}{x}$

So $G'_{yy}(w)$ is the line spectrum $\operatorname{sinc}^2 \frac{\pi h \lambda}{T_c}$, where h is integral, modulated by a periodic function of h, $G_{yy}(w)$ which has a period in h of (p-1). We need evaluate $G_{yy}(w)$ only for the (p-1) values h = 0,1,....p-2, to determine it for all values of h.

The complete power spectrum of y, in terms of the parameters of the system and of the m-sequence is

$$G''(w) = \delta(w).\left\{ \frac{p^{n-2}}{p^n-1} \left\{ \sum_{i=o}^{p-1} f_i \right\}^2 - \frac{f_o^2}{p^n-1} \right\} + \frac{1}{\lambda} \frac{p^{n-1}}{p^n-1} \operatorname{sinc}^2 \frac{\pi h \lambda}{T_c} \sum_q \left\{ \cos \frac{2\pi h q}{p-1} . \left\{ \sum_{i=o}^{p-1} f(\langle B^q X_i \rangle_p) . f_i - \frac{1}{p} \left(\sum_{i=o}^{p-1} f_i \right)^2 \right\} \right\} \qquad 3.4.6$$

where h is an integer.

In appendix (4) we found that the autocorrelation function of x(t), a p-level m-sequence is given for τ an integer multiple of λ by

$$\Phi_{xx}(q\tau_1) = \frac{p^{n-1}}{p^n-1} \sum_{i=1}^{p-1} \langle B^q \cdot X_i \rangle_p \cdot X_i$$

$$\Phi_{xx}(\tau \neq q\tau_1) = 0,$$

where the symbols have the same meanings as in equation (2).

By the same method that we used to find $G''_{yy}(w)$, we find that

$$G''_{xx}(w) = \frac{1}{\lambda} \cdot \frac{p^{n-1}}{p^n-1} \operatorname{sinc}^2 \frac{\pi h \lambda}{T_c} \sum_{q=0}^{p-2} \left\{ \cos \frac{2\pi h q}{p-1} \sum_{i=0}^{p-1} \langle B^q \cdot X_i \rangle_p \cdot X_i \right\} \qquad 3.4.7$$

and once again we have a modulated sinc^2 function.

An Example

A five level m-sequence is generated by a two stage shift register which has B = 2 and clock period one second. This sequence is the input to a saturation non-linearity y = f(x), given below.

i.e. p = 5, n = 2, B = 2, λ = 1

x	-2	-1	0	1	2
y	-1	-1	0	1	1

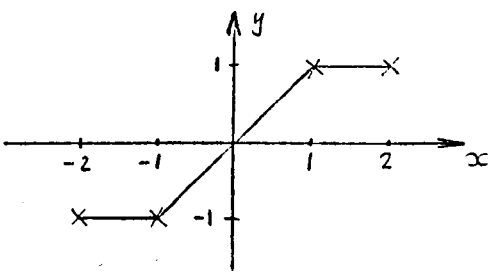

For τ, the delay, a whole number of clock periods, the autocorrelation function of the m-sequence is

$$\Phi_{xx}(q\tau_1) = \frac{p^{n-1}}{p^n-1} \left\{ \sum_{i=1}^{p-1} \langle B^q \cdot X_i \rangle_p \cdot X_i \right\}$$

$$\Phi_{xx}(\tau \neq \tau_s) = 0$$

$$\frac{p^{n-1}}{p^n-1} = \frac{5}{24}$$

$$q = 0, \{\ \} = 4 + 1 + 1 + 4 = 10$$

$$q = 1,3, \{\ \} = -2 + 2 + 2 - 2 = 0$$

$$q = 2, \{\ \} = -10$$

and the autocorrelation function of the m-sequence is the full line in figure (3)

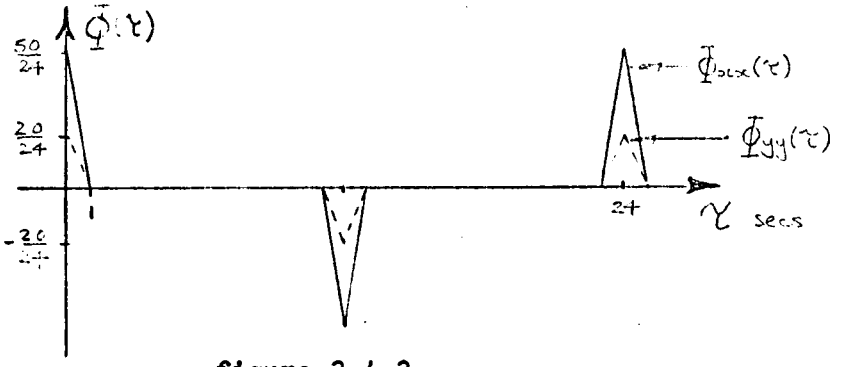

figure 3.4.3

For τ an integer number of clock periods,

$\Phi_{yy}(\tau \neq \tau_s) = 0$, since $f_o = 0$, and $\sum_{i=o}^{p-1} f_i = 0$

$$\Phi_{yy}(q.\tau_1) = \frac{p^{n-1}}{p^n-1}\left\{\sum_{j=o}^{p-1} f(\langle B^q . X_j\rangle_p).f_j\right\} - \frac{f_o^2}{p^n-1}$$

$$\frac{p^{n-1}}{p^n-1} = \frac{5}{24}$$

$$f_o^2 = 0$$

$q = 0, \{\ \} = +1+1+1+1 = 4$

$q = 1, 3, \{\ \} = -1+1+1-1 = 0$

$q = 2, \{\ \} = -1-1-1-1 = -4$

and the autocorrelation function of the output y(t) of the non-linearity is the dotted line in figure (3).

We may now find the functions $G_{xx}(w)$ and $G_{yy}(w)$ using equation (5b)

$$G_{xx}(w) = \frac{5}{24} \times 10\{1 - (-1)^h\} = \frac{100}{24}, \text{ h odd}$$

$$= 0, \text{ h even}$$

$$G_{yy}(w) = \frac{5}{24} \times 4\{1 - (-1)^h\} = \frac{40}{24}, \text{ h odd}$$

$$= 0, \text{ h even}$$

So the power spectrum of x(t) is the function $\text{sinc}^2 \frac{\pi h}{24}$ (see figure (4) modulated by $G_{xx}(w)$ (see figure (5). The power spectrum of y(t) is the same sinc^2 function, modulated by the function $G_{yy}(w)$ (see figure (6).

For this particular non-linearity, the autocorrelation function and power spectrum of the output have the same form as those of the input.

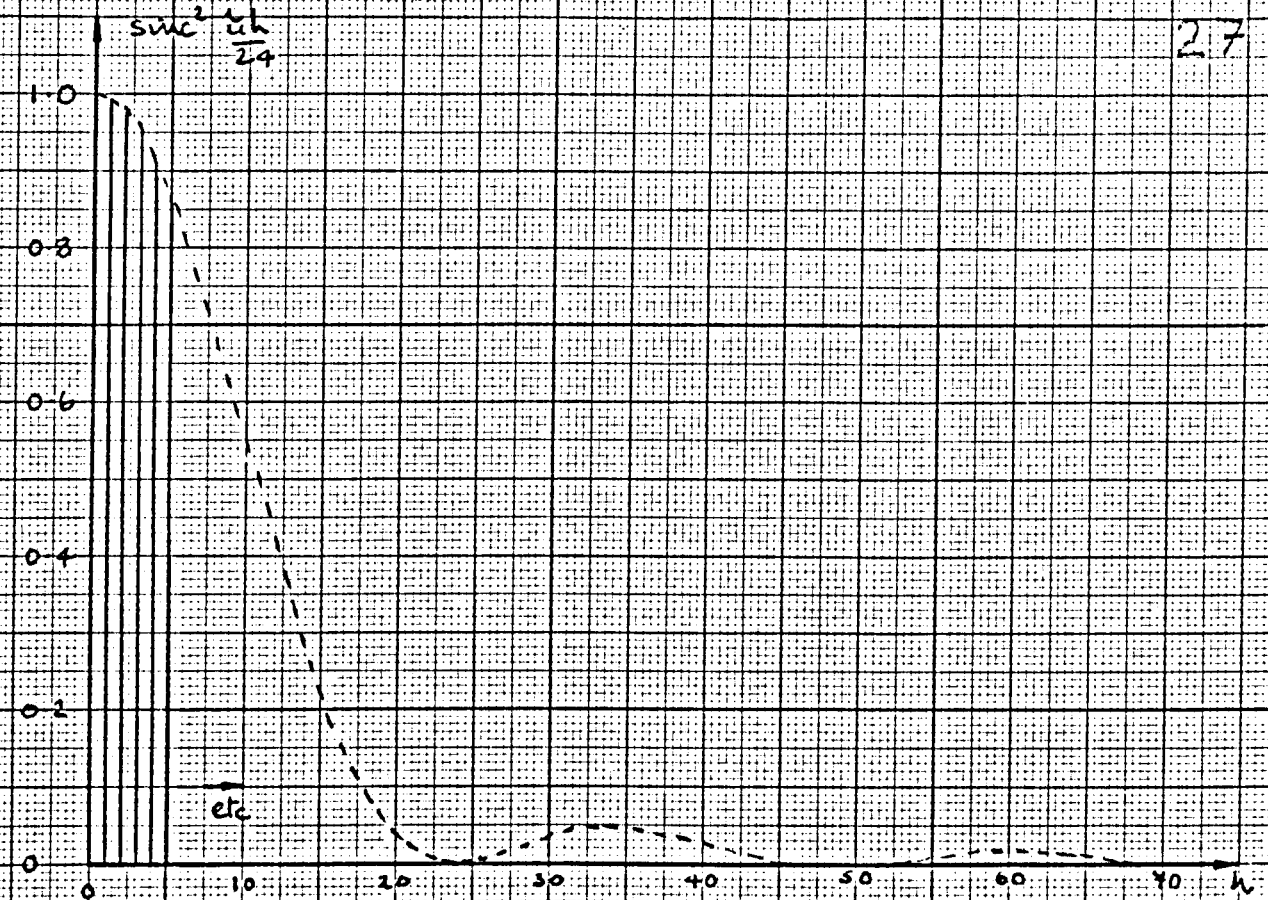

FIGURE 3·4·4

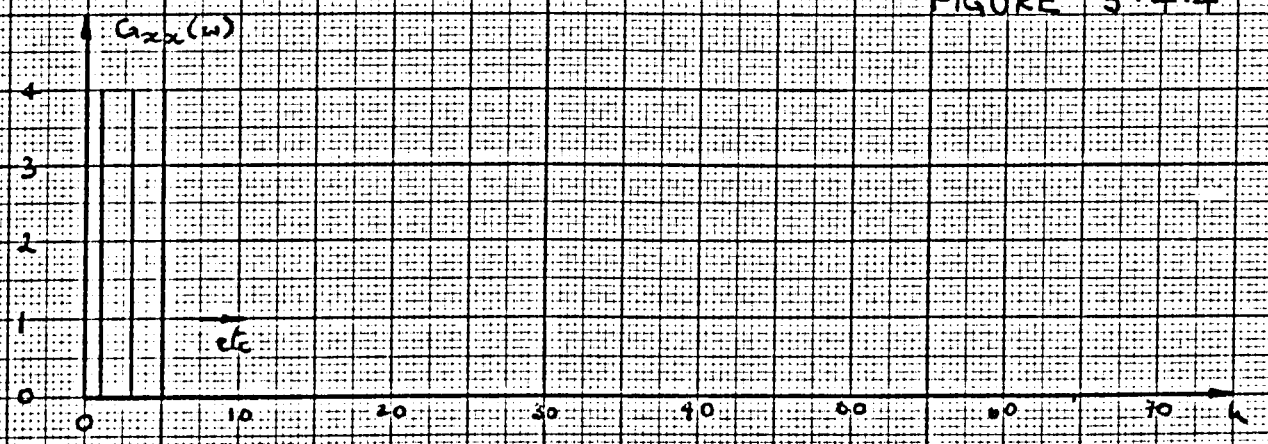

FIGURE 3·4·5

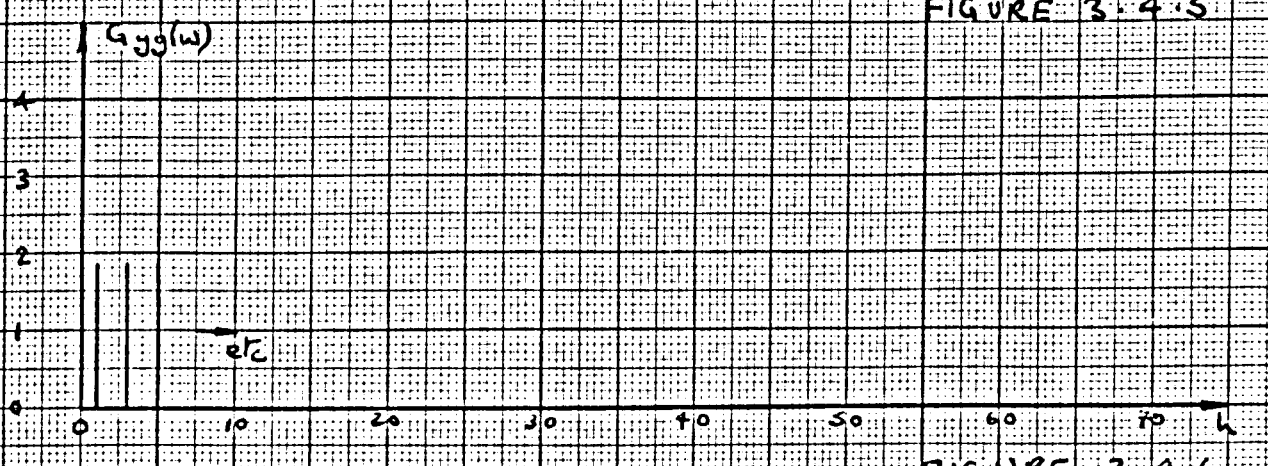

FIGURE 3·4·6

Another Example

We will take the m-sequence of the previous example as the input to a modulus non-linearity, given below.

x	-2	-1	0	1	2
y	2	1	0	1	2

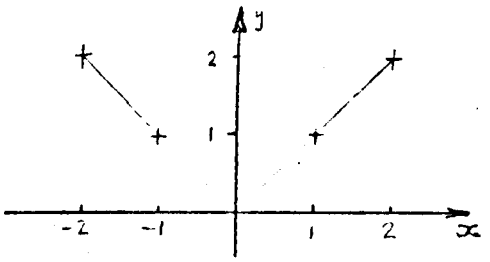

The autocorrelation function of the non-linearity output is

$$\Phi_{yy}(\tau \neq \tau_s) = \frac{p^{n-2}}{p^n-1}\left\{\sum_{i=0}^{p-1} f_i\right\}^2 = \frac{3}{2}$$

(since $f_0 = 0$)

$$\Phi_{yy}(q\tau_1) = \frac{p^{n-1}}{p^n-1}\left\{\sum_{j=0}^{p-1} f(\langle B^q . X_j\rangle_p f_j\right\}$$

$$\frac{p^{n-1}}{p^n-1} = \frac{5}{24}$$

$q = 0, \{\ \} = 4 + 1 + 1 + 4 = 10$

$q = 1,3, \{\ \} = 2 + 2 + 2 + 2 = 8$

$q = 2, \{\ \} = 4 + 1 + 1 + 4 = 10$

The autocorrelation function of y(t) is the dotted line in figure (7). The autocorrelation function of the m-sequence is reproduced as the full line in figure (7), for comparison.

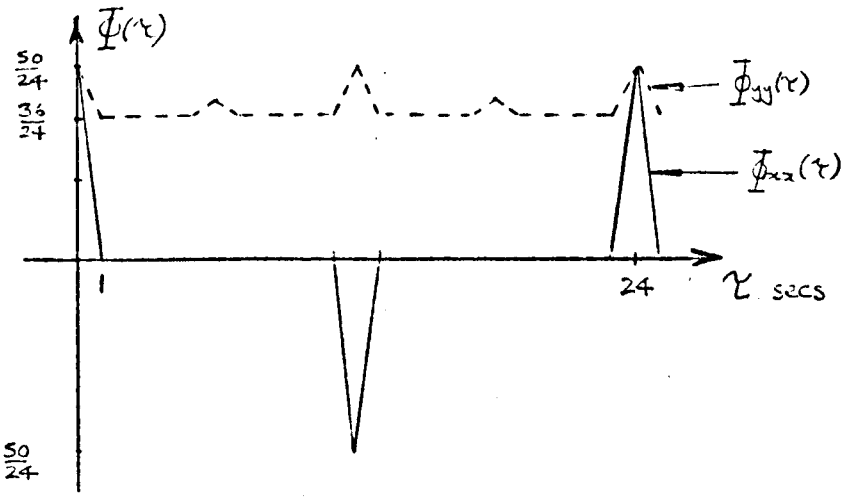

figure 3.4.7

The power spectrum $G_{yy}(w)$ is given by equation (5b)

$$G_{yy}(w) = \frac{1}{24} \{ 14(1 + (-1)^h) + 8 \cos \frac{\pi h}{2} \}$$

$$= \frac{3}{2}, \quad h = 0,4,8,....$$

$$= 0, \quad h = 1,5,9,....$$

$$= \frac{5}{6}, \quad h = 2,6,10,....$$

$$= 0, \quad h = 3,7,11,....$$

$$G''_{yy}(w) = \frac{3}{2} \delta(w) + \text{sinc}^2 \frac{\pi h}{24} \cdot G_{yy}(w)$$

$G_{yy}(w)$ is plotted in figure (9) with $G_{xx}(w)$ in figure (8) for comparison.

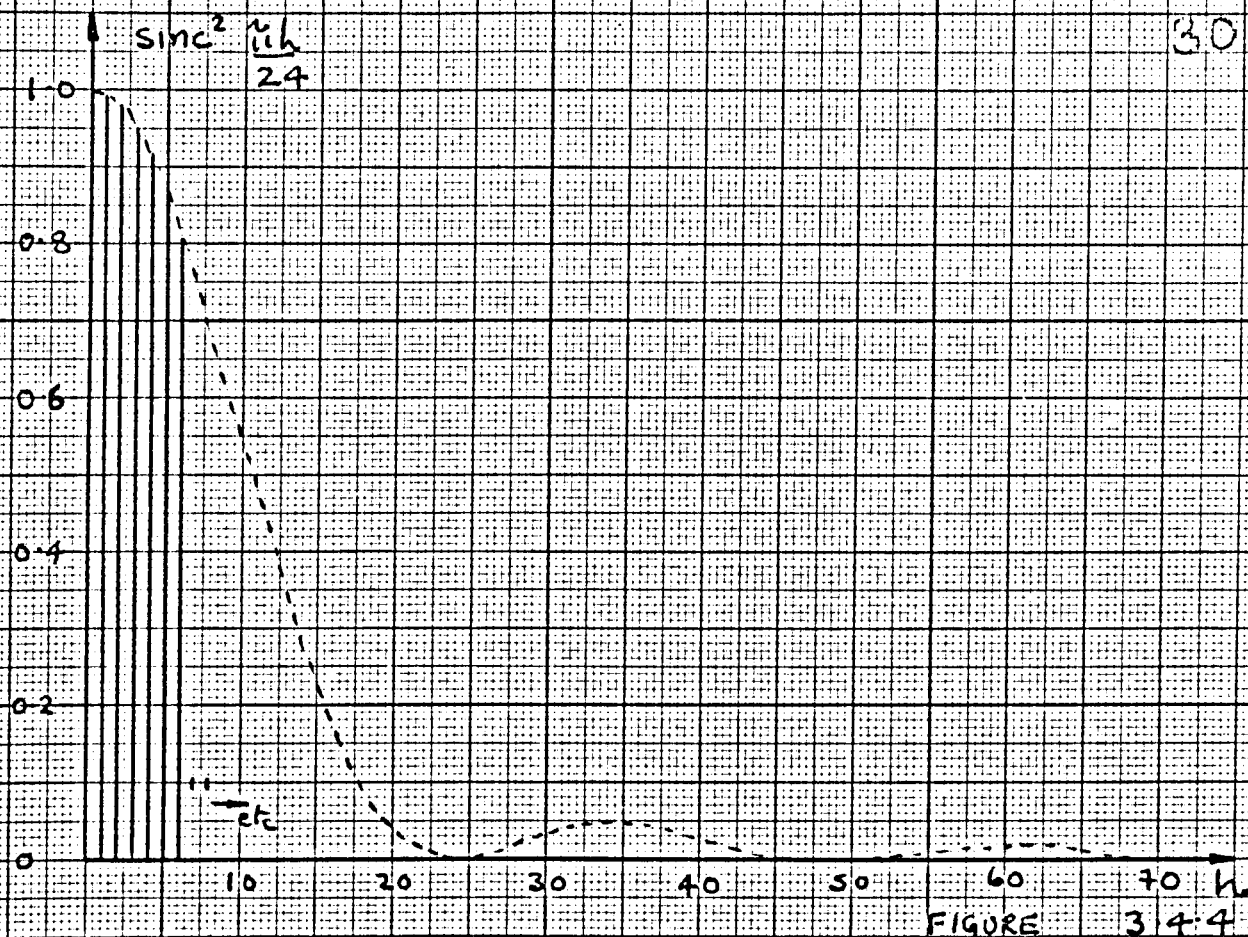

FIGURE 3·4·4

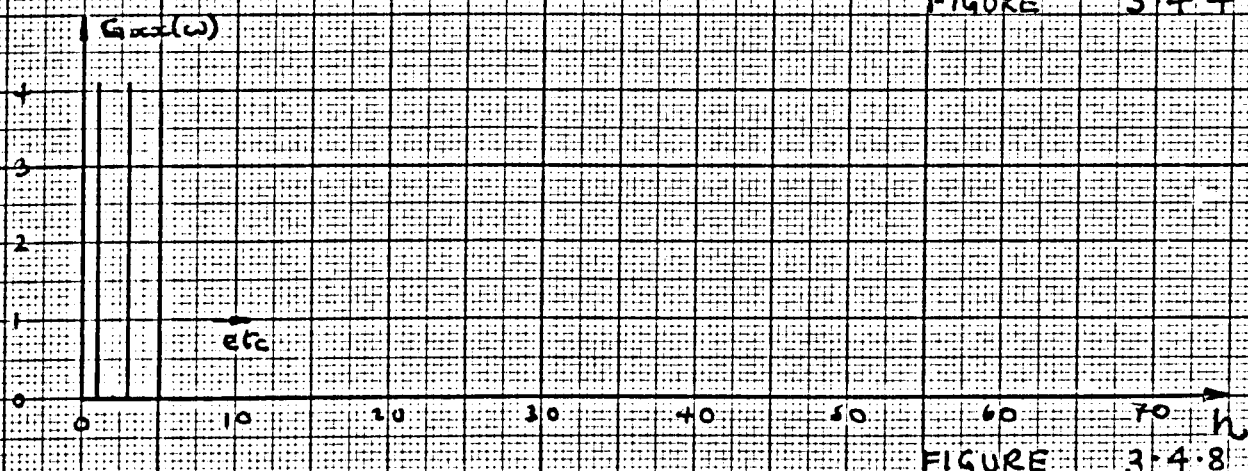

FIGURE 3·4·8

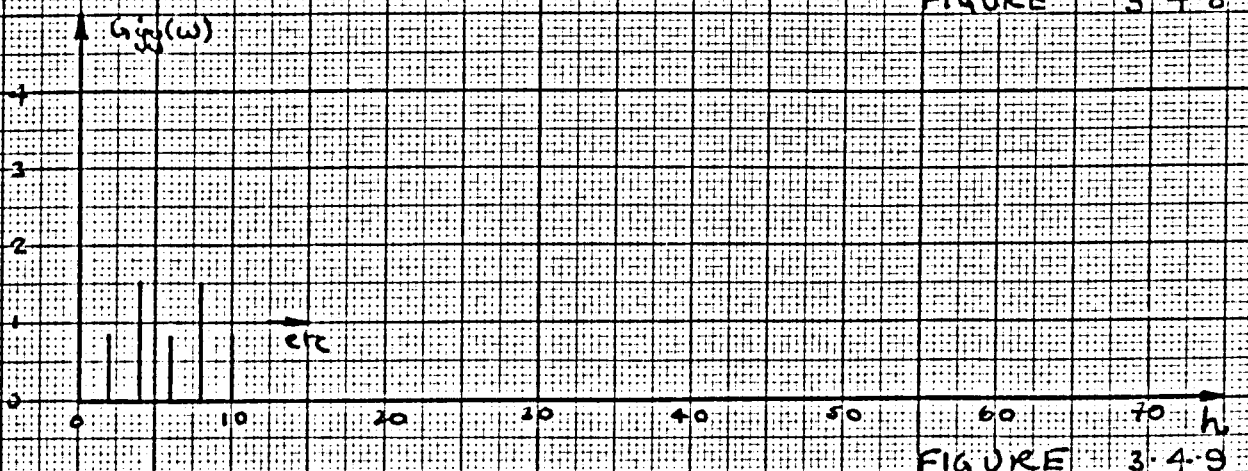

FIGURE 3·4·9

Chapter 4.

4.1 Identification in the presence of noise.

In any experimental situation, the various signals within a system will be contaminated by noise, due to disturbances to the system. Also, any measurements will be contaminated by noise, due in part to the instruments. Let us consider the effect of this on the system of figure (1) which we have been studying.

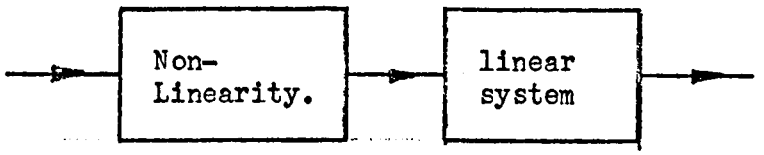

figure 4.1.1

The non-linearity is likely to be an element in which noise injection can only take place at its input or output, a non-linear transducer for example. When this is the case we may represent the non-linearity in the noisy environment as in figure (2)

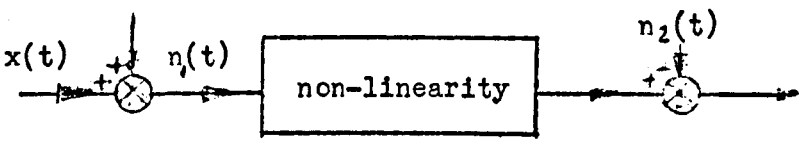

figure 4.1.2

The linear part of the system is more likely to be a distributed dynamic system with noise injection taking place at various points. As it is a linear system, the output will be the sum of the outputs due to each of the inputs (the signal input and the noise inputs), individually. We can therefore represent the linear system in the noisy environment by figure (3)

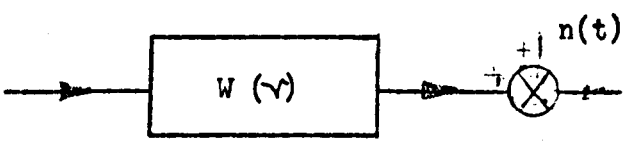

figure 4.1.3

The noise n(t) in figure (3) can take account of all noise sources at the input to the linear system and all noise sources in the measurement of the output. We may consider the entire system as in figure (4)

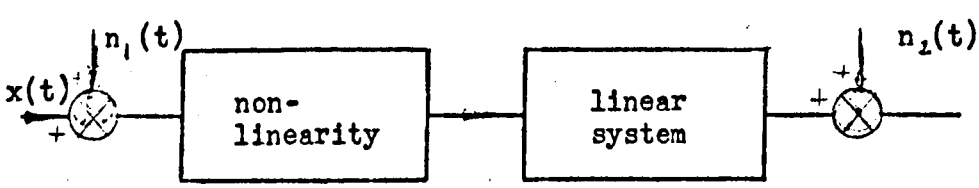

figure 4.1.4

4.2 Identification of a non-linear system when the input test signal is contaminated by noise.

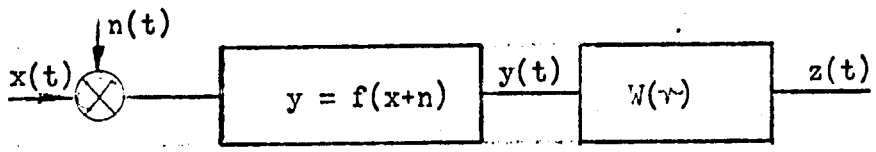

figure 4.2.1

For the sake of completeness, this situation is investigated in appendix (8). If (a) the signal to noise power ratio is high

(b) x(t) and n(t) are uncorrelated

(c) n(t) has zero mean

then the estimate $r_{x3}(\tau,X)$ of $\phi_{x3}(\tau,X)$ is unbiassed,

where

$$r_{x3}(\tau,X) = \frac{1}{T_c}\int_0^{T_c} a(t,X).z(t+\tau)dt$$

The variance of this estimate is found in appendix (8), but the result does not give any insight into the situation, and is therefore not reproduced here.

4.3 Identification of a non-linear system whose output is contaminated by noise.

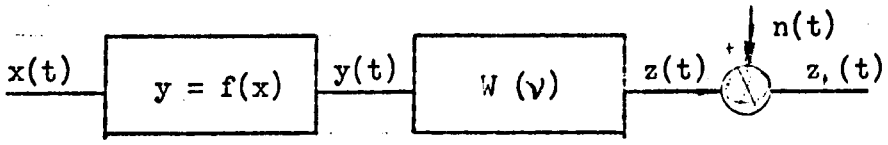

figure 4.3.1

Consider the system of figure (1). This represents the non-linear system which we have considered, and takes account of any noise injection after the output of the non linearity, as we saw in section (4.1)

We make an estimate $r_{x_3}(\tau,X)$ of the partial cross-correlation function $\phi_{x_3}(\tau,X)$, by integrating over one period of the input signal, to give

$$r_{x_3}(\tau,X) = \frac{1}{T_c}\int_0^{T_c} a(t,X).z_1(t+\tau)dt \qquad 4.3.1$$

where $a(t,X)$ is a component of $x(t)$, as defined in section 2.1

In appendix (6) we find that $r_{x_3}(\tau,X)$ is an unbiassed estimate of $\phi_{x_3}(\tau,X)$ if the effective noise input $n(t)$ at the system output

(a) is ergodic

(b) has zero mean value

(c) is uncorrelated with $x(t)$

In the same appendix the variance, σ^2 of the estimate is shown to be

$$\sigma^2 = \frac{2}{T_c^2}\int_0^{T_c} (T_c - \nu).\Phi_{nn}(\nu).\Phi_{aa}(\nu).d\nu \qquad 4.3.2$$

where $\Phi_{nn}(\nu)$ and $\Phi_{aa}(\nu)$ are the autocorrelation functions of $n(t)$ and of $a(t,X)$ respectively.

Clearly σ^2 is independent of τ, and $\Phi_{nn}(\nu)$ is independent of X. When $x(t)$ is an m-sequence, $\Phi_{aa}(\nu)$ is independent of X for all $X \neq 0$, and the variance of our estimate is independent of X and τ. In many cases, the variance for $X = 0$ is similar to that for $X \neq 0$, but this depends upon the autocorrelation function of the noise, and must be checked in each case.

An Example.

Let us consider the identification of the system in figure (1) when x(t) is a p-level m-sequence, and n(t) has the auto-correlation function shown in figure (2)

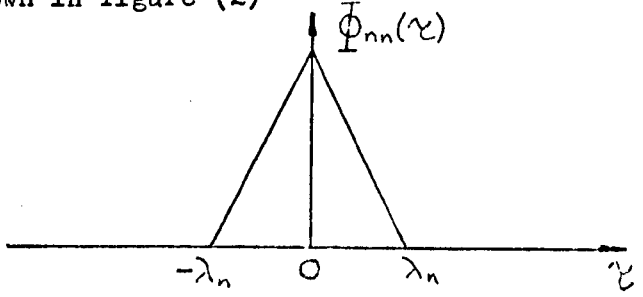

figure 4.3.2

n(t) could be, for example, a random clocked signal or an m-sequence with period longer than that of x(t). In particular it could be a binary m-sequence, which would be useful in a simulation to test the theory that has been developed so far, because of its ease of generation. We will assume that x(t) and n(t) are uncorrelated.

Let us take the very simple case $\lambda_n=\lambda$, the clock period of the m-sequence generator producing x(t)

$$\Phi_{nn}(\tau) = C\left(1 - \frac{|\tau|}{\lambda}\right), \quad |\tau| \leq \lambda$$

$$= 0 \quad , \text{ otherwise}$$

applying equation (2), and inserting the results for a p-level m-sequence we have, for $X \neq 0$,

$$\sigma^2 = \frac{2}{T_c^2}.C.\frac{p^{n-2}}{(p^n-1)}\int_0^{\lambda}(T_c - \nu).(1 - \frac{\nu}{\lambda})\,(p - (p-1)\frac{\nu}{\lambda})\,d\nu$$

$$= \frac{C}{6}\cdot\frac{p^{n-2}}{(p^n-1)^3}\left\{4p^{n+1} + 2p^n - 5p - 3\right\} \qquad 4.3.3$$

for $X = 0$,

$$\sigma^2 = \frac{2}{T_c^2}.C.\frac{p^{n-2}}{(p^n-1)}\int_0^{\lambda}(T_c - \nu).(1 - \frac{\nu}{\lambda})\,(p - (p-1)\frac{\nu}{\lambda})\,d\nu$$

$$- \frac{2}{T_c^2}.C.\frac{1}{(p^n-1)}\int_0^{\lambda}(T_c - \nu).(1 - \frac{\nu}{\lambda})\,d\nu$$

$$= \frac{C}{6}\cdot\frac{1}{(p^n-1)^3}\left\{p^{n-2}(4^{n+1} + 2p^n - 5p - 3) - (6p^n - 8)\right\} \qquad 4.3.4$$

We see that the variance for X = 0 (equation (4), is a small amount less than for $X \neq 0$ (equation (3)). We will not make a large error, therefore, if we take equation (3) as the variance for all X.

4.4 Identification using a p-level m-sequence when the System Output is Contaminated by Noise.

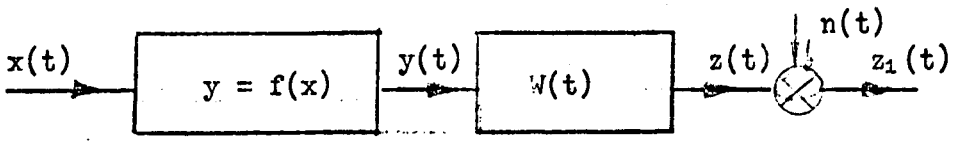

In section (3.3) we considered identification with an m-sequence. In section (4.3) we considered the general effects of noise at the system output. So far we have not asked the question 'Given experimental estimates of the partial correlation function, what are f(x) and W(t)?'. It is the purpose of this section to answer the question, given the following assumptions:-

(1) n(t) is stationary and not correlated to x(t)

(2) The autocorrelation function of n(t) is such that the variance in estimates of the partial correlation function is independent of the level X for which the function is found. (It is in any case the same for all non-zero X, but may differ for X = 0, see equation 4.3.2.)

We saw in section (3.3) (Equation (3.3.6)) that

$$\frac{p^n-1}{p^{n-1}}\left\{\phi_{x_3}(j\lambda,X_i) - \phi_{x_3}(m\lambda,X_i)\right\} = \hat{f}_i . W_j \qquad 4.4.1$$

where λ is the clock period of the m-sequence,

$$W_j = W(j\lambda)$$

$$\hat{f}_i = f(X_i) - f_{av}$$

$$f_{av} = \frac{1}{p}\sum_{i=0}^{p-1} f(X_i)$$

$$W_j = 0, \quad j \geq m$$

Let us define a matrix of measurements $\underset{\sim}{M}$, where

$$\underset{\sim}{M} = [M_{ij}]$$

$$M_{ij} = \left\{r_{x_3}(j\lambda,i) - \mathcal{C}_{x_3}(m\lambda,i)\right\}\frac{p^n-1}{p^{n-1}} \qquad 4.4.2$$

where

$$r_{x_3}(\tau,i) = \frac{1}{T_c}\int_0^{T_c} a(t,X_i).z_1(t+\tau).dt \qquad 4.4.3$$

$$T_c = (p^n - 1)\lambda$$

From our previous work, and assumption (2),

$$M_{ij} = \hat{f}_i \cdot W_j + \epsilon_{ij}$$

where the matrix of errors $[\epsilon_{ij}]$ has elements ϵ_{ij} independent of i and j.

We wish to choose $\hat{f}_i$ and W_j to be the best fit to the data $\underset{\sim}{M}$ in the sense that the variance, C, is minimized where

$$C = \sum_i \sum_j \epsilon^2_{ij} \qquad 4.4.4$$

$$\epsilon^2_{ij} = (M_{ij} - \hat{f}_i \cdot W_j)^2$$

$$\frac{\partial C}{\partial \hat{f}_i} = -2\sum_j M_{ij} \cdot W_j + 2\sum_j \hat{f}_i \cdot W_j^2 = 0 \text{ for C max or min}$$

$$\frac{\partial C}{\partial W_j} = -2\sum_i M_{ij} \cdot \hat{f}_i + 2\sum_i \hat{f}_i^2 \cdot W_j = 0 \text{ for C max or min}$$

Rewriting these last two equations in matrix terms,

$$\frac{\partial C}{\partial \underline{\hat{f}}} = 2(\underline{\hat{f}} \cdot \underline{W}^T \cdot \underline{W} - \underset{\sim}{M}\underline{W}) = 0 \qquad 4.4.5$$

$$\frac{\partial C}{\partial \underline{W}} = 2(\underline{W} \cdot \underline{\hat{f}}^T \underline{\hat{f}} - \underset{\sim}{M}^T \underline{\hat{f}}) = 0 \qquad 4.4.6$$

where $\frac{\partial C}{\partial \underline{\hat{f}}}$, $\underline{W}$ and $\underline{\hat{f}}$ are

$$\frac{\partial C}{\partial \underline{\hat{f}}} = \begin{bmatrix} \frac{\partial C}{\partial \hat{f}_1} \\ \cdots \\ \frac{\partial C}{\partial \hat{f}_2} \\ \vdots \\ \frac{\partial C}{\partial \hat{f}_i} \\ \vdots \end{bmatrix} \quad \underline{W} = \begin{bmatrix} W_1 \\ W_2 \\ \vdots \\ W_j \\ \vdots \end{bmatrix}, \quad \underline{\hat{f}} = \begin{bmatrix} \hat{f}_1 \\ \hat{f}_2 \\ \vdots \\ \hat{f}_i \\ \vdots \end{bmatrix}$$

equations (5) and (6) yield

$$\underset{\sim}{M}\,\underline{W} = \underline{\hat{f}}\,\underline{W}^T\,\underline{W} \qquad 4.4.7$$

$$\underset{\sim}{M}^T\underline{\hat{f}} = \underline{W}\,\underline{\hat{f}}^T\,\underline{\hat{f}} \qquad 4.4.8$$

for which,

$$\underset{\sim}{M}\,\underset{\sim}{M}^T\underline{\hat{f}} = \alpha^2\,\underline{\hat{f}} \qquad 4.4.9$$

$$\underset{\sim}{M}^T\underset{\sim}{M}\,\underline{W} = \alpha^2\,\underline{W} \qquad 4.4.10$$

where

$$\alpha^2 = \underline{W}^T\underline{W}\,\underline{\hat{f}}^T\,\underline{\hat{f}} = |W|^2|\hat{f}|^2 \qquad 4.4.11$$

We would like to know how many solutions for α^2 are common to equations (9) and (10). This is dependent on the ranks of the matrices $\underset{\sim}{M}\underset{\sim}{M}^T$ and $\underset{\sim}{M}^T\underset{\sim}{M}$.

Let us assume that $\underset{\sim}{M}$ is an mxn matrix and that $m \leq n$. (In the rest of this section, we will use m,n and r as parameters of the matrices, and not in their former roles). The other case (that $m > n$) yields a similar result by the same method. Generally we would expect the rank r of $\underset{\sim}{M}$ to be m, but the following is quite general and admits the possibility that $r < m$.

$$r \leq m \leq n$$

$\underset{\sim}{M}\underset{\sim}{M}^T$ is an m x m matrix, and $\underset{\sim}{M}^T\underset{\sim}{M}$ is an n x n matrix. The number of non-zero eigen values in equation (9) is the rank of $\underset{\sim}{M}\underset{\sim}{M}^T$, and the number of non-zero eigen values in equation (10) is the rank of $\underset{\sim}{M}^T\underset{\sim}{M}$.

In text books of matrix algebra it is shown that

(1) the rank of a matrix is unchanged by elementary row operations.

(2) the rank of a matrix is unchanged by elementary column operations.

(3) any number of elementary row operations may be represented by premultiplication by a non-singular matrix.

(4) any number of elementary column operations may be represented by post multiplication by a non-singular matrix.

So, if $\underset{\sim}{M}$ has rank r there is a matrix $\underset{\sim}{P}$ such that

$$\underset{\sim}{P}\underset{\sim}{M} = \begin{bmatrix} \underset{\sim}{A} & \underset{\sim}{R} & \underset{\sim}{B} \\ 0 & 0 & 0 \end{bmatrix}$$

where $\underset{\sim}{R}$ is an r x r non-singular matrix. 4.4.12

hence

$$\underset{\sim}{M} = \underset{\sim}{P}^{-1} \begin{bmatrix} \underset{\sim}{A} & \underset{\sim}{R} & \underset{\sim}{B} \\ 0 & 0 & 0 \end{bmatrix}$$

$$\therefore \quad \underset{\sim}{M}\underset{\sim}{M}^T = \underset{\sim}{P}^{-1} \begin{bmatrix} \underset{\sim}{A} & \underset{\sim}{R} & \underset{\sim}{B} \\ 0 & 0 & 0 \end{bmatrix} \begin{bmatrix} \underset{\sim}{A} & 0 \\ \underset{\sim}{R} & 0 \\ \underset{\sim}{B} & 0 \end{bmatrix} \underset{\sim}{P}^{-1T}$$

$$= \underset{\sim}{P}^{-1} \begin{bmatrix} \underset{\sim}{C} & 0 \\ 0 & 0 \end{bmatrix} \underset{\sim}{P}^{-1T}$$

where $\underset{\sim}{C} = \underset{\sim}{A}\underset{\sim}{A}^T + \underset{\sim}{R}\underset{\sim}{R}^T + \underset{\sim}{C}\underset{\sim}{C}^T \underset{\sim}{B}\underset{\sim}{B}^T$

$\underset{\sim}{R}\,\underset{\sim}{R}^T$ is +ve definite, $\underset{\sim}{A}\,\underset{\sim}{A}^T$ and $\underset{\sim}{C}\,\underset{\sim}{C}^T$ are +ve semi definite so $\underset{\sim}{C}$ is non singular. $\underset{\sim}{C}$ is an r x r submatrix, hence $\underset{\sim}{M}\,\underset{\sim}{M}^T$ is of rank r.

A similar use of elementary column operations shows that $\underset{\sim}{M}^T\underset{\sim}{M}$ is also of rank r.

There are r non-zero eigen values of equation (9) and r non-zero eigen values of equation (10); we must now find how many eigen values are common to both.

Let us assume that $\underline{\xi}$ is an eigen vector of equation (9) and σ^2 is a corresponding eigen value.

i.e. $\underset{\sim}{M}\,\underset{\sim}{M}^T\,\underline{\xi} = \sigma^2\,\underline{\xi}$

premultiplying by $\underset{\sim}{M}^T$,

$$\underset{\sim}{M}^T\underset{\sim}{M}\;\underset{\sim}{M}^T\,\underline{\xi} = \sigma^2\;\underset{\sim}{M}^T\,\underline{\xi}$$

clearly, by comparison of this with equation (10), $\underset{\sim}{M}^T\underline{\xi}$ is an eigen vector of equation (10), and σ^2 is the corresponding eigen value.

We see that all of the r non-zero eigen values of equation (9) are eigen values of equation (10), and so all the non-zero eigen vectors are common to both.

To minimise the computation required, we should find the eigen vectors and eigen values of whichever of equations (9) and (10) has the smaller order. If $m < n$, then $\underset{\sim}{M}\,\underset{\sim}{M}^T$ is m x m and smaller then $\underset{\sim}{M}^T\underset{\sim}{M}$. So the estimation of $\hat{\underline{f}}$ and $\underline{w}$ becomes

(1) find eigenvector and eigenvalue of equation (9) to obtain α^2 and $\hat{\underline{f}}$

(2) premultiply $\hat{\underline{f}}$ by $\underset{\sim}{M}^T$ to obtain $\underline{w}$

(3) scale $\hat{\underline{f}}$ and/or $\underline{w}$ such that $|\hat{\underline{f}}|^2.|\underline{w}|^2 = \alpha^2$.

Unfortunately this will give us r sets of α^2, $\hat{\underline{f}}$ and $\underline{w}$, each one corresponding to a local minimum in the variance $\underset{\sim}{C}$ (see equation (4)). We must therefore evaluate $\underset{\sim}{C}$ for each set to obtain the true minimum.

Remembering that the eigenvalues are related to the sizes of the vectors $\underline{w}$ and $\hat{\underline{f}}$ by equation (11), we see that the eigenvectors corresponding to zero eigenvalues are for this case null-vectors, and so the case of zero eigenvalues is of no interest.

Experimental work was carried out with an analogue simulation of the non - linear system, and also with a digital simulation of the system. The former was unsatisfactory because of a period of unreliability of the analogue computer. The digital simulation yielded results consistent with those predicted.

Conclusion

Chapter 5.

The technique which has been developed in the preceeding chapters allows the characteristics of certain non-linear time-invariant systems to be found in a single experiment. The method is restricted to those systems which may be represented as a non-linear element followed by linear dynamics. The non-linear element must be instantaneous and single-valued. The characteristic of the non-linearity and the impulse response of the dynamics are found simultaneously.

Further work is required on the partial-correlation function, and on its application to identification, particularly in the presence of noise. The following notes summarise the work that is required.

1. An investigation of the application of the method to an extended class of non-linear systems.
2. A comparison of the partial correlation technique with other methods of identification, in the presence of noise. For instance, the relative efficiencies of this method and repetitive experiments with binary signals could be found for various noisey environments. This would be helpful in determining the value of the partial correlation functions in identification.
3. Preliminary experiments* suggest that the identification of non-linear systems by the partial correlation technique is readily implemented by digital computer. Further work is required to establish program requirements, and to compare them with those of other methods.
4. The feasability of finding alternative test signals should be investigated.

* Please see note opposite.

References.

1). Douce, J.L., An Introduction to the Mathematics of Servomechanisms, E.U.P., 1963.

2). West, J.C., Non-linear Signal Distortion Correlation. Internat. J. Control (GB), Vol 2, No. 6, 529-38 (1965)

3). Nuttall, A.H., Theory and Application of the Seperable Class of Random Processes, M.I.T. Technical Report No. 343., May 1958.

4). Zierler, N., Linear Recurring Sequences, J. Soc. Indust. Appl. Maths. Vol. 7, No. 1, p.31.

5). Dickson, L.E., Modern Elementary Theory of Numbers, University of Chicago Press, 1939.

6). Newton, G.C., Gould, L.A., Kaiser, J.F., The Analytical Design of Linear Feedback Controls, Wiley 1957.

Appendix (1)

The Partial Correlation function of the input and output of a non-linear system.

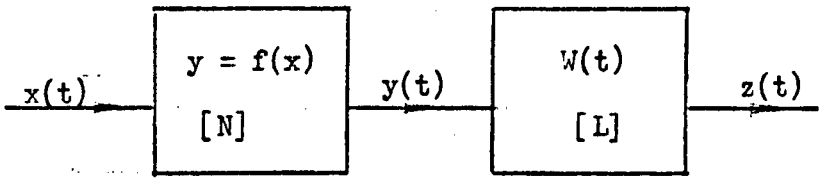

figure A.1.1

Consider the system of figure (1). An instantaneous non-linearity [N] has an output y(t) related to its input x(t) by the equation $y(t) = f(x(t))$ A.1.1

Where f(x) is single-valued (i.e. to each value of x there corresponds one, and only one, value of y).

The output of the non-linearity is applied to the input of a linear dynamic element [L], having an impulse response W(t).

Let us now investigate the result of forming the partial cross-correlation function of the input x(t) and the output z(t), with respect to the input. The partial cross-correlation function $\phi_{xz}(\tau,X)$ was defined for two ergodic signals x(t) and z(t) in section (2.1). It was expressed (equation 2.1.6) in terms of the component signal a(t,X) of x(t) as

$$\phi_{xz}(\tau,X) = \underset{T \to \infty}{\text{limit}} \frac{1}{2T} \int_{-T}^{T} a(t,X).z(t+\tau).dt \qquad A.1.2$$

where

$$x(t) = \int_{-\infty}^{\infty} X.a(t,X).dX \qquad A.1.3$$

Since [L] is linear, we may express the output z(t) in terms of the input y(t) and the impulse response W(t) by the convolution integral,

$$z(t) = \int_{-\infty}^{\infty} W(\nu).\, y(t-\nu).d\nu \qquad A.1.4$$

where ν is a dummy time variable.

By equations (1) and (3),

$$y(t) = \int_{-\infty}^{\infty} f(X).\, a(t,X).dX \qquad A.1.5$$

since by our definition of [N] , the output y of [N] for an input X is f(X)

From (4) and (5)

$$z(t) = \int_{-\infty}^{\infty} W(\nu) \int_{-\infty}^{\infty} f(X).a(t - \nu,X).dX.d\nu \qquad \text{A.1.6}$$

So from (2) and (6)

$$\phi_{x_3}(\tau,X) = \lim_{T \to \infty} \frac{1}{2T} \int_{-T}^{T} a(t,X). \int_{-\infty}^{\infty} W(\nu)$$

$$\int_{-\infty}^{\infty} f(X_1).\ a(t + \tau - \nu,X_1)dX_1.d\nu.dt \qquad \text{A.1.7}$$

Changing the order of integration we get,

$$\phi_{x_3}(\tau,X) = \int_{-\infty}^{\infty} W(\nu) \int_{-\infty}^{\infty} f(X_1) \left\{ \lim_{T \to \infty} \frac{1}{2T} \int_{-T}^{T} a(t,X).\right.$$

$$\left. a(t + \tau - \nu,X_1).dt \right\} \ dX_1.d\nu \qquad \text{A.1.8}$$

Now, we saw in section (2.1) that the term in curly brackets is the cross-correlation function, $\Phi_{aa_1}(\tau)$, of a (t,X) and $a(t,X_1)$, and that it is also the joint probability density function $p_X\ (X,X_1,\tau - \nu)$, so

$$\phi_{x_3}(\tau,X) = \int_{-\infty}^{\infty} W(\nu) \int_{-\infty}^{\infty} f(X_1).\Phi_{aa_1}(\tau - \nu).dX_1.d\nu \qquad \text{A.1.9}$$

or

$$\phi_{x_3}(\tau,X) = \int_{-\infty}^{\infty} W(\nu) \int_{-\infty}^{\infty} f(X_1).\ p_X\ (X,X_1,\tau - \nu).dX_1.d\nu \qquad \text{A.1.10}$$

Equations (9) and (10) give us a relationship between the partial cross-correlation function, the characteristics of the system W(t) and f(x) and the amplitude distribution of the input signal.

Appendix (2)

The Cross-correlation between the components of a p-level m-sequence.

All the results obtained in this appendix may be found in Zierler's paper [4]. An alternative, more physical approach is presented here, as Zierler's paper is not easy to read, and the results are important to this thesis.

Consider the m-sequence c(t) generated by a p-level n-stage shift register having feedback gains (a_1, a_2 . . . a_n), and clock period 1 unit. p is a prime. c(t) may take any integer value in the range $0 \leqslant c(t) \leqslant p-1$, or in the range $-\frac{p-1}{2} \leqslant c(t) \leqslant \frac{p-1}{2}$ or any other range for which modulo p arithmetic has been defined. The work of this appendix is applicable to all of these cases.

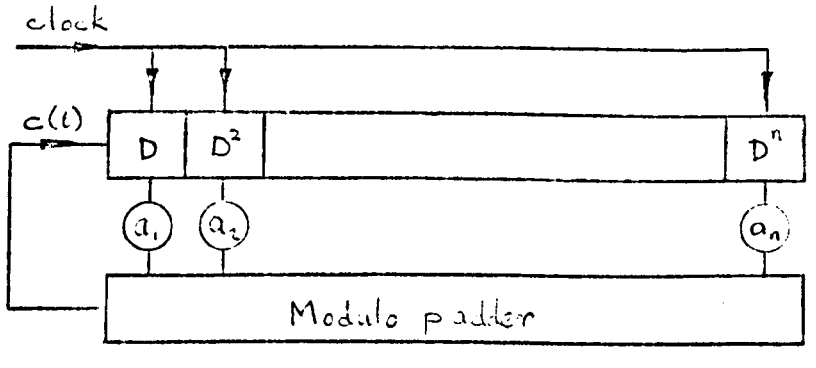

figure A.2.1

If we define a delay operator D, by the relation

$D^k(c(t)) = c(t - k)$

then we may write the following equation to describe the behaviour of the feedback shift register.

$$c(t) = \langle (a_n D^n + a_{n-1} D^{n-1} + \ldots a_1 D)c(t) \rangle_p \qquad \text{A.2.1}$$

where the symbol $\langle \ldots . \rangle_p$ is used to mean that the operations between the brackets $\langle$ and $\rangle$ are carried out modulo p.

Any delayed version $c(t - \tau)$, of c(t) where τ is an integral number of clock periods may be formed by linear modulo p operations upon the outputs of the shift register. That is,

$$c(\langle t - \tau \rangle_N) = \langle (b_{n-1} D^{n-1} + \ldots\ldots + b_0)c(t) \rangle_p \qquad \text{A.2.2}$$

for all τ , where N is the number of elements in the sequence,

$N = p^n - 1$

Now, all states of the shift register except the null state occur once in every period, hence $c(t - \tau)$ is statistically independent of $c(t)$ unless,

$$\left.\begin{aligned} &b_{n-1} = b_{n-2} = b_{n-3} = \cdots = b_1 = 0 \\ &\langle b_0 \rangle_p \neq 0 \end{aligned}\right\} \qquad \text{A.2.3}$$

when equations (3) are satisfied, $c(\langle t - \tau \rangle_N)$ is completely determined by b_0. We require therefore, the values of τ for which the condition equations (3) holds. Let these values of τ be called the 'special delays' τ_s.

If we substitute the equations (3) into equation (2) we get

$$c(\langle t - \tau_s \rangle_N) = \langle b_0 c(t) \rangle p$$

therefore

$$\begin{aligned} c(\langle t - 2\tau_s \rangle_N) &= \langle b_0 c(t - \tau_s \rangle_N) \rangle p \\ &= \langle b_0^2 \, c(t) \rangle p \end{aligned}$$

and by induction we find

$$c(\langle t - m\tau_s \rangle_N) = \langle b^m \, c(t) \rangle p \qquad \text{A.2.4}$$

Fermat's theorem [5] states that for all b_0,

$$\langle b_0^{p-1} \rangle p = 1 \qquad \text{A.2.5}$$

Hence, substituting $m = p-1$ into equation (4),

$$\left.\begin{aligned} c(\langle t - (p-1)\tau_s \rangle_N) &= \langle b_0^{p-1} \, c(t) \rangle p \\ &= c(t) \end{aligned}\right\} \qquad \text{A.2.6}$$

It is important to notice that equation (6) is not a condition governing the values of b_0, which may take any integer value, but it is a condition upon the value of τ_s, and implies that

$$\langle (p-1)\tau_s \rangle_N = 0 \qquad \text{A.2.7}$$

from which,

$$\langle \tau_s \rangle_N = q \cdot \frac{(p^n - 1)}{(p-1)}, \quad q = 0, 1 \ldots\ldots p-2 \qquad \text{A.2.8}$$

Equation (8) tells us that there are $(p-1)$ special delays in each period, (p^n-1) elements, of the sequence. We note that there are $(p-1)$ non-zero values of b_0, modulo p.

The smallest positive value of τ_s is

$$\tau_s = \frac{(p^n-1)}{(p-1)} = \tau_1 \text{ say}$$

and all other special delays are integer multiples of τ_1.

Let the value of the delay gain b_o corresponding to a special delay τ_1 be B. Hence

$$\langle B\, c(t)\rangle_p = c\left(\left\langle t - \frac{(p^n-1)}{(p-1)}\right\rangle_N\right)$$

and so, by equation (4),

$$\langle B^q\, c(t)\rangle_p = c(\langle t - q\,\tau_1\rangle_N) \qquad \text{A.2.9}$$

If $p > 2$, since p is a prime, p is odd and (p-1) is always divisable by 2. So for all p prime >2 there is a special delay τ_s, such that :

$$\tau_s = \frac{p^n-1}{2}$$

and the corresponding value of b_o is $\langle B^{\frac{p-1}{2}}\rangle_p$

Clearly the value of b_o corresponding to $\tau_s = p^n-1$ is unity since $c(t - (p^n-1)) = c(t)$ therefore

$$\langle (B^{\frac{p-1}{2}})^2\rangle_p = 1$$

and taking the square root of each side,

$$\langle B^{\frac{p-1}{2}}\rangle_p = \pm 1$$

hence, since $\langle B^{\frac{p-1}{2}}\rangle_p \neq 1$

(this would imply that the period was actually $\frac{p^n-1}{2}$)

$$\langle B^{\frac{p-1}{2}}\rangle_p = -1$$

or

$$B = \langle \sqrt{-1}\rangle_p. \qquad \text{A.2.10}$$

We notice that this implies that for any p prime >2, the second half of a p-level m-sequence is (-1) times the first half.

Unfortunately there are $\frac{p-1}{2}$ solutions to equation (10), but we know some properties of B which help us to determine it. They are

(1) $B^q \neq -1$ for any $q < \frac{p-1}{2}$

(2) $B^q \neq 1$ for any $q < p-1$

i.e. B is a primitive (p-1)th root of unity.

(3) A single stage p-level shift register generates a sequence with period (p-1), which contains each level, except zero, once and only once, and zero does not occur see figure (2). B must be a useful feedback gain for such a register

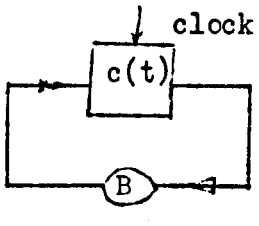

$$c(t) = \langle B\ c(t-1) \rangle_p$$

figure A.2.2

(4) It is clear from property (3), that the values of B will occur in pairs B and B′ such that

$$\langle B\ B' \rangle_p = 1$$

since the sequence generated by a shift register with feedback gain B′ will be the time - reverse of the sequence generated by a register with feedback gain B.

In paragraph (2.3) a component signal a(t,i) was defined for a quantised signal c(t) such that

$a(t,i) = 1$ when $c(t) = X_i$

$= 0$ otherwise

We require the cross-correlation function $\Phi_{a_i a_j}(\tau)$ between two such signals a(t,i) and a(t,j) for all i,j = o,1... p-1

$$\Phi_{a_i a_j}(\tau) = E\{ a(t,i).\ a(t-\tau, j)\}$$

Let us consider values of τ which are integer multiples of the clock period, which we will take as unity. Two different cases are apparent.

Case (1) $\tau = \tau_s = q\,\tau_1$

Equation (9) states

$$\langle B^q c(t)\rangle_p = c(\langle t - q\tau_1\rangle_N)$$

so for every j, q there corresponds a single value of i such that

$$\left.\begin{aligned} a(t,j) &= a(\langle t - q\tau_1\rangle_N, i) \\ \langle B^q X_j\rangle &= X_i \end{aligned}\right\} \qquad \text{A.2.11.}$$

If $X_j = 0$, then clearly from equation (11)

$$a(t,j) = a(\langle t - q\tau_1\rangle_N, j) \qquad \text{A.2.12}$$

for all q.

This means that for $X_j = 0$, a(j,t) is periodic, and has a period of $\left(\frac{p^n-1}{p-1}\right)$ clock periods.

Case (2) $\tau \neq \tau_s$

We have seen that equations (3) do not hold for a non-special delay, so $c(t-\tau)$ is independent of c(t). Also, there are p^{n-1} occurrences of the level $X_j \neq 0$ and $(p^{n-1}-1)$ zeros in each period. So,

$$P\{ c(t) = X_j \neq 0\} = \frac{p^{n-1}}{p^n-1}$$

$$P\{ c(t) = 0\} = \frac{p^{n-1}-1}{p^n-1}$$

where, by P{ (statement)} we mean "the probability that the (statement) is true".

$$P\{ c(t) \neq 0, \text{ and } c(t-\tau) = X_j\} = \frac{1}{p} \text{ for all } X_j$$

We see from equation (12) that having located a zero, we have located (p-1) zeros, so, given that c(t) = 0

$$P\{ c(t-\tau) = 0\} = \frac{p^{n-1}-1-(p-1)}{p^n-1-(p-1)}$$

$$= \frac{p^{n-2}-1}{p^{n-1}-1}$$

$$P\{ c(t-\tau) = X_j \neq 0\} = \frac{1}{p-1}\left(1 - \frac{p^{n-2}-1}{p^{n-1}-1}\right)$$

$$= \frac{p^{n-2}}{p^{n-1}-1}$$

Hence $\Phi_{a_i a_i}(\tau_s) = \frac{p^{n-1}-1}{p^n-1}$, $X_i = 0$

$$\Phi a_i a_i(\tau \neq \tau_s) = \frac{p^{n-2}-1}{p^n-1} \quad , \quad X_i = 0$$

$$\Phi a_i a_j(\tau_s) = \frac{p^{n-1}}{p^n-1} \quad , \quad X_j = B^q X_i \neq 0, \ \tau_s = q\tau_i$$

$$= 0 \quad , \quad \text{otherwise}$$

$$\Phi a_i a_j(\tau \neq \tau_s) = \frac{p^{n-2}}{p^n-1} \quad , \quad X_i \neq 0 \ \underline{\text{or}} \ X_j \neq 0$$

So far we have assumed that τ is a whole number of clock periods. In appendix (7) it is shown that a clocked signal has an autocorrelation function which changes linearly between a delay which is a whole number of clock periods, and the next delay which is a whole number of clock periods.

We may generalize the results obtained so far in terms of a clock period λ and any delay τ. We simplify the equations by writing $(\tau' = \tau - q\tau_i)$, then

for $\lambda \leqslant |\tau'| \leqslant \frac{p^n-1}{p-1}\lambda$

$$\Phi a_i a_j(\tau') = \frac{p^{n-2}}{p^n-1} \qquad X_i \neq 0 \ \text{ or } X_j \neq 0$$

$$= \frac{p^{n-2}-1}{p^n-1} \qquad X_i = X_j = 0$$

for $0 \leqslant |\tau'| \leqslant \lambda$

$$\Phi a_i a_j(\tau') = \frac{|\tau'|}{\lambda} \cdot \frac{p^{n-2}}{p^n-1}, \qquad X_i \neq B^q X_j$$

$$= \frac{p^{n-2}}{p^n-1}\left\{1 + (p-1)\left(1 - \frac{|\tau'|}{\lambda}\right)\right\}, \ X_i = B^q X_j \neq 0$$

$$= \frac{1}{p^n-1}\left\{p^{n-2}\left(1 + (p-1)\left(1 - \frac{|\tau'|}{\lambda}\right)\right) - 1\right\}, \ X_i = X_j = 0$$

These results are summarised in figure 3.2.6

Appendix (3)

Identification using a p-level m-sequence.

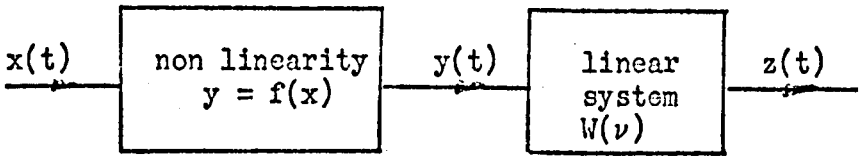

figure A.3.1

For the system shown in figure (1), the partial cross-correlation function $\phi_{x3}(\tau,X)$ was found to be (equation A.1.9)

$$\phi_{x3}(\tau,X) = \int_{-\infty}^{\infty} W(\nu) \int_{X_1=-\infty}^{\infty} f(X_1).\, \varphi aa_1\,(\tau - \nu)\, dX_1.d\nu \qquad A.3.1$$

where $\varphi aa_1(\tau)$ is the cross correlation function between the component signals $a(t,X)$ and $a(t,X_1)$ as defined in paragraph (2.1)

For a p-level m-sequence, which is a periodic quantised signal, equation (1) becomes

$$\phi_{x3}(\tau,i) = \int_{-\infty}^{\infty} W(\nu) \sum_{j=0}^{p-1} f_j.\varphi a_i a_j(\tau - \nu).d\nu \qquad A.3.2$$

where $\phi_{x3}(\tau,i)$ is the partial cross-correlation function between $x(t)$ and $z(t)$ with respect to the level X_i of $x(t)$, and $\varphi a_i a_j(\tau)$ is the cross-correlation function between the two component signals $a(t,i)$ and $a(t,j)$.

$$a(t,i) = 1 \quad , \quad x(t) = X_i$$
$$= 0 \quad , \quad \text{otherwise}$$

for all of the p possible levels X_i

$$f_i = f(X_i)$$

$$\text{Let } Tm = \left\{\frac{p^n-1}{p-1} \text{ ---} 1\right\}\lambda$$

then if $W(\nu) = 0$ for $\nu \geq Tm$, and $\nu < 0$,

$$\phi_{x3}(\tau,i) = \int_{0}^{Tm} W(\nu) \sum_{j=0}^{p-1} f_j\, \varphi a_i a_j(\tau - \nu)\, d\nu \qquad A.3.3$$

$\varphi a_i a_j(\tau)$ was found in appendix (2). For the range $-Tm \leq \tau \leq Tm$, the results were:-

$$\left.\begin{array}{l} \lambda \leq |\tau| \leq Tm \\ X_i \neq 0 \text{ or } X_j \neq 0 \end{array}\right\} \quad \varphi a_i a_j(\tau) = d, \text{ a constant, } = \frac{p^{n-2}}{p-1}$$

$$\left.\begin{array}{l}\lambda \leq |\tau| \leq Tm \\ X_i = X_j = 0\end{array}\right\} \quad \Phi a_i a_j(\tau) = d_{oo}, \text{ a constant} = \frac{p^{n-2}-1}{p^n-1}$$

$$\left.\begin{array}{l}0 \leq |\tau| \leq \lambda \\ X_i \neq X_j\end{array}\right\} \quad \Phi a_i a_j(\tau) = \frac{|\tau|}{\lambda}.d$$

$$\left.\begin{array}{l}0 \leq |\tau| \leq \lambda \\ X_i = X_j \neq 0\end{array}\right\} \quad \Phi a_i a_j(\tau) = d + h_o\left\{1 - \frac{|\tau|}{\lambda}\right\}$$

$$\left.\begin{array}{l}0 \leq |\tau| \leq \lambda \\ X_i = X_j = 0\end{array}\right\} \quad \Phi a_i a_j(\tau) = d_{oo} + h_o\left\{1 - \frac{|\tau|}{\lambda}\right\}$$

where $h_o = \frac{(p-1)}{(p^n-1)} . p^{n-2}$ A.3.4

Therefore, $\sum_{j=0}^{p-1} f_j . \Phi a_i a_j(\tau - \nu)$ is a constant for $\lambda \leq |\tau - \nu| \leq Tm$, so it is convenient to rewrite equation (3) in terms of a new variable u where

$$\left.\begin{array}{l}u = \tau - \nu \\ du = -d\nu\end{array}\right\} \quad \text{A.3.5}$$

$$\phi_{x_i}(\tau, i) = \int_{\tau - T_m}^{\tau} W(\tau - u).d.\sum_{j=0}^{p-1} f_j.du \quad (A)$$

$X_i \neq 0$

$$- \int_{-\lambda}^{\lambda} W(\tau - u).d.\left\{\sum_{j=0}^{p-1} f_j - f_i\right\}.du \quad (B)$$

$$+ \int_{-\lambda}^{\lambda} W(\tau - u).d.\frac{|u|}{\lambda}.\left\{\sum_{j=0}^{p-1} f_j - f_i\right\}du \quad (C)$$

$$+ \int_{-\lambda}^{\lambda} W(\tau - u).h_o.(1 - \frac{|u|}{\lambda}).f_i.du \quad (D)$$

A.3.5

If λ is short compared with the system settling time, the terms of equation (5) become

$$B = -W(\tau).d.\left\{\sum_{J=0}^{p-1} f_j - f_i\right\}.2\lambda$$

$$C = W(\tau).d\left\{\sum_{J=0}^{p-1} f_j - f_i\right\}\frac{2}{\lambda}.\frac{\lambda^2}{2}$$

$$D = W(\tau).h_o.f_i.2(\lambda - \frac{\lambda^2}{2\lambda})$$

Hence when λ is small compared with the system settling time,

$$\phi_{x_3}(\tau,i)_{X_i \neq 0} = d.\sum_{j=0}^{p-1} f_j \int_0^{T_m} W(\nu)\, d\nu + W(\tau).\left\{ h_o.\lambda.f_i - d.\lambda.\left(\sum_{j=0}^{p-1} f_j - f_i \right) \right\} \qquad A.3.7$$

$$\phi_{x_3}(\tau,i)_{X_i \neq 0} = d.\sum_{j=0}^{p-1} f_j \int_0^{T_m} W(\nu)\, d\nu + W(\nu)\left\{ (h_o + d).f_i - d.\sum f_i \right\}\lambda \qquad A.3.8$$

If we define the 'average value' f_{av} of the non linearity as

$$f_{av} = \frac{1}{p}\sum_{j=0}^{p-1} f_j$$

then, when we substitute this, and expressions for d and h_o from (4), into equation (8), we get

$$\phi_{x_3}(\tau,i)_{X_i \neq 0} = \frac{p^n-1}{p^n-1}\left\{ W(\tau).\lambda.(f_i - f_{av}) + f_{av}\int_0^{T_m} W(\nu)d\nu \right. \qquad A.3.9$$

When $X_i = 0$, the term (A) in equation (6) is replaced by

$$(A') = \int_{\tau - T_m}^{\tau} W(\tau - u).\left\{ d\sum f_j + (d_{oo} - d)f_i \right\} du$$

The other terms are unchanged, so

$$\phi_{x_3}(\tau,i)_{X_i = 0} = \frac{p^{n-1}}{p^n-1}\left\{ W(\tau).\lambda.(f(o) - f_{av}) + (f_{av} - \frac{f(o)}{p^n-1}) \int_0^{T_m} W(\nu)d\nu \right\} \qquad A.3.10$$

Equations (9) and (10) give us $\phi_{x_3}(\tau,i)$ when $W(\nu) = 0$ for

$$\nu \geq T_m = \left(\frac{(p^n-1)}{p-1} - 1 \right)\lambda$$

Appendix (4)

The autocorrelation function of the output of a non-linearity with p-level m-sequence input.

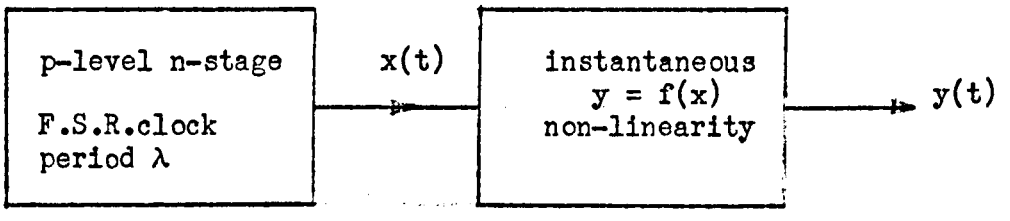

figure A.4.1

We wish to know the autocorrelation function $\Phi_{yy}(\tau)$ of the output y(t) of a single-valued instantaneous non-linearity in response to an input signal x(t) which is a p-level m-sequence.

Remembering that p must be prime, let x(t) take the levels $X_0, X_1, \ldots X_{p-1}$. x(t) is periodic, The period is

$$T_c = \lambda.(p^n-1)$$

One of the levels X_i of x(t) will be zero, so we may without loss of generality choose $X_0 = 0$. If $p > 2$ we may choose $X_1, X_2 \ldots X_{p-1}$ such that they are symmetrically disposed about $X_0 = 0$. We then have

$$-\frac{p-1}{2} \leqslant x(t) \leqslant \frac{p-1}{2}$$

and

$$\sum_{j=0}^{p-1} X_j = 0 \qquad \text{A.4.1}$$

It is useful to recall some of the results for quantised periodic signals from paragraph (2.5)

$$x(t) = \sum_{i=0}^{p-1} X_i . a(t,i) \qquad \text{A.4.2}$$

where a(t,i) is a component signal of x(t) as defined in section (2.3),

$$a(t,i) = 1 \qquad \text{when } x(t) = X_i$$

$$= 0 \qquad \text{otherwise}$$

The partial correlation function $\phi_{xy}(\tau,i)$ of x(t) and y(t) is

$$\phi_{xy}(\tau,i) = \frac{1}{T_c}\int_0^{T_c} a(t,i).y\ (t+\tau)dt \qquad \text{A.4.3}$$

since x(t) is ergodic.

The full crosscorrelation function $\Phi_{xy}(\tau)$ of x(t) and y(t) is

$$\Phi_{xy}(\tau) = \sum_{i=0}^{p-1} X_i \cdot \phi_{xy}(\tau,i) \qquad A.4.4$$

We find in appendix (7) that for a clocked signal x(t), $\phi_{xy}(\tau,i)$ changes linearly from $\phi_{xy}(j\lambda,i)$ to $\phi_{xy}((j+1)\lambda,i)$ for all j, i, so there is no need for us to consider values of τ which are not integral multiples of the clock period.

Let us first find the autocorrelation function $\Phi_{xx}(\tau)$ of the m-sequence x(t), by substituting y = x into equation (4)

$$\begin{aligned}\Phi_{xx}(\tau) &= \sum_{i=0}^{p-1} X_i \cdot \phi_{xx}(\tau,i) \\ &= \sum_{i=0}^{p-1} X_i \cdot \frac{1}{T_c} \cdot \int_0^{T_c} a(t,i) \cdot \sum_{j=0}^{p-1} X_j \cdot a(t+\tau,j)\,dt \\ &= \sum_{i=0}^{p-1}\sum_{j=0}^{p-1} X_i \cdot X_j \cdot \frac{1}{T_c}\int_0^{T_c} a(t,i)\cdot a(t+\tau,j)\,dt \\ &= \sum_{i=0}^{p-1}\sum_{j=0}^{p-1} X_i \cdot X_j \cdot \Phi_{a_i a_j}(\tau) \qquad A.4.5\end{aligned}$$

where $\Phi_{a_i a_j}(\tau)$ is the cross correlation function between a(t,i) and a(t,j) This was found in appendix (2) and the results are shown in figure (3.2.6)

for $\tau = \tau_s = q\ \tau_1 = q.\lambda.\frac{p^n-1}{p-1}$,

$\Phi_{a_i a_j}(q\ \tau_1) = 0$ for all X_j except $X_j = \langle B^q X_i \rangle_p$

$= \frac{p^{n-1}}{p^n-1}$ for $X_j = \langle B^q X_i \rangle_p \neq 0$

$= \frac{p^{n-1}-1}{p^n-1}$ for $X_j = X_i = 0$

$\Phi_{a_i a_j}(\tau) = \frac{p^{n-2}}{p^n-1}$ for all i,j except $i = j = 0$

$\tau \neq \tau_s$

$= \frac{p^{n-1}-1}{p^n-1}$ for $i = j = 0$

where B is the delay gain corresponding to a delay τ_1, as defined in appendix (A.2)

We chose $X_0 = 0$, so we may rewrite equation (5) as

$$\Phi_{xx}(\tau) = \sum_{i=1}^{p-1}\sum_{j=1}^{p-1} X_i \cdot X_j \cdot \Phi_{a_i a_j}(\tau) \qquad A.4.6$$

and substituting the expressions for $\Phi a_i a_j(\tau)$ into equation (6)

$$\Phi_{xx}(\tau) = \frac{p^{n-2}}{p^n-1} \sum_{i=1}^{p-1} \sum_{j=1}^{p-1} X_i . X_j \qquad \text{A.4.7}$$

$\tau \neq \tau_s$

But $\sum_{i=0}^{p-1} X_i = 0$ (by equation (1))

$\therefore$ since $X_o = 0$

$$\sum_{i=1}^{p-1} X_i = 0$$

$$\therefore \quad \Phi_{xx}(\tau) = 0 \qquad \text{A.4.8}$$

$\tau \neq \tau_s$

since $\Phi a_i a_j(q\tau_1) = 0$, $X_j \neq \langle B^q . X_i \rangle_p$

when $\tau = q\tau_1$, equation (6) becomes

$$\Phi_{xx}(q\tau_1) = \frac{p^{n-1}}{p^n-1} \sum_{i=1}^{p-1} X_i \langle B^q . X_i \rangle_p \qquad \text{A.4.9}$$

Now we have completely specified the auto correlation function of the m-sequence. We see that it has a spike every time

$\tau = q\tau_1$,

$\tau_1 = \frac{p^n-1}{p-1} . \lambda$

$q = 0, 1, \ldots P-2$

we also see that for p>2 the auto correlation function has zero mean value.

Let us return to the output of the non-linearity. We have chosen it to be instantaneous and single valued, so every time the input is X_i, the output is $f(X_i)$. For simplicity let us write

$$f(X_i) = f_i$$

The input is $x(t) = \sum_{i=o}^{p-1} X_i . a(t,i)$

so the output is

$$y(t) = \sum_{i=o}^{p-1} f_i . a(t,i) \qquad \text{A.4.10}$$

We shall follow the same procedure to find $\Phi_{yy}(\tau)$ as we used to find $\Phi_{xx}(\tau)$. Equivalent to equation (5) we have

$$\Phi_{yy}(\tau) = \sum_{i=o}^{p-1} \sum_{j=o}^{p-1} f_i . f_j . \Phi a_i a_j(\tau) \qquad \text{A.4.11}$$

In general $f_0 \neq 0$, so we cannot change the limits of the summations as we did for $\Phi_{xx}(\tau)$. Using the results from appendix (A.2) quoted above,

$$\Phi_{yy}(q\tau_1) = \frac{p^{n-1}}{p^n-1} \sum_{j=0}^{p-1} f(\langle B^q X_j \rangle_p).f_j + f_0^2 \left\{ \frac{p^{n-1}-1}{p^n-1} - \frac{p^{n-1}}{p^n-1} \right\}$$

$$= \frac{p^{n-1}}{p^n-1} \sum_{j=0}^{p-1} f(\langle B^q X_j \rangle_p).f_j - \frac{f_0^2}{p^n-1} \qquad \text{A.4.12}$$

$$\Phi_{yy}(\tau) \quad = \frac{p^{n-2}}{p^n-1} \sum_{i=0}^{p-1} \sum_{j=0}^{p-1} f_i.f_j + f_0^2 \left\{ \frac{p^{n-2}-1}{p^n-1} - \frac{p^{n-2}}{p^n-1} \right\}$$

$\tau \neq \tau_s$

$$= \frac{p^{n-2}}{p^n-1} \left\{ \sum_{i=0}^{p-1} f_i \right\}^2 - \frac{f_0^2}{p^n-1} \qquad \text{A.4.13}$$

We notice that if the non-linearity is replaced by a unit linear gain, y = x, the expressions for $\Phi_{yy}(\tau)$ reduce to those for $\Phi_{xx}(\tau)$ as we expect.

We can rewrite equation (13) in terms of f_{av}, the average value of the non-linearity, as

$$\Phi_{yy}(\tau) \quad = \frac{p^n}{p^n-1} . f_{av}^2 - \frac{f_0^2}{p^n-1}$$

$\tau \neq \tau_s$

this is the mean value of the auto correlation function $\Phi_{yy}(\tau)$

Examples of the application of these results appear in section (3.4)

Appendix (5)

The power spectrum of a signal having a periodic, spikey auto correlation function.

When a signal is constrained to change its value only at regularly spaced clock instants, it has an auto correlation function which changes linearly between delays of adjacent whole numbers of clock periods.

i.e. for a clocked signal x(t) having a clock period λ

$$\Phi_{xx}((i + \Delta)\lambda) = \Phi_{xx}(i\lambda) + \Delta\,(\Phi_{xx}((i + 1)\lambda) - \Phi_{xx}(i\lambda)) \qquad \text{A.5.1}$$

$$0 \leq \Delta \leq 1$$

(This result is found in appendix (7)

In consequence, the feature shown in figure (A.5.1) is common in the auto correlation functions of clocked signals.

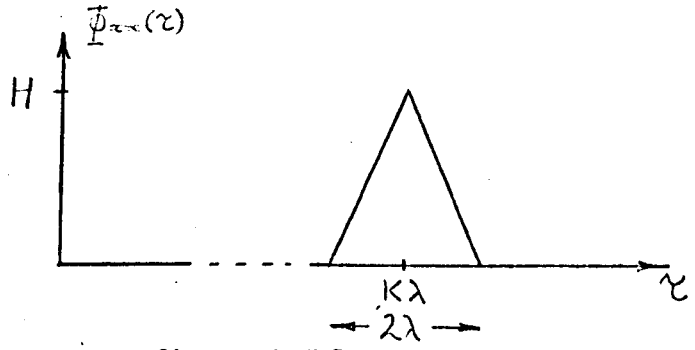

figure A.5.1

We will describe this feature as 'a spike of height H at time $\tau = K\lambda$. Clearly such a spike is an approximation to an impulse of strength $H\lambda$.

If the clocked signal x(t) is periodic, then the autocorrelation function will be periodic. Features other than spikes may be present, for example a steady level. We may find the power spectrum corresponding to each of these features separately, since the fourier transform is a linear operation. The total power spectrum will be the sum of these component spectra.

Let us consider, then, the autocorrelation function shown in figure (2)

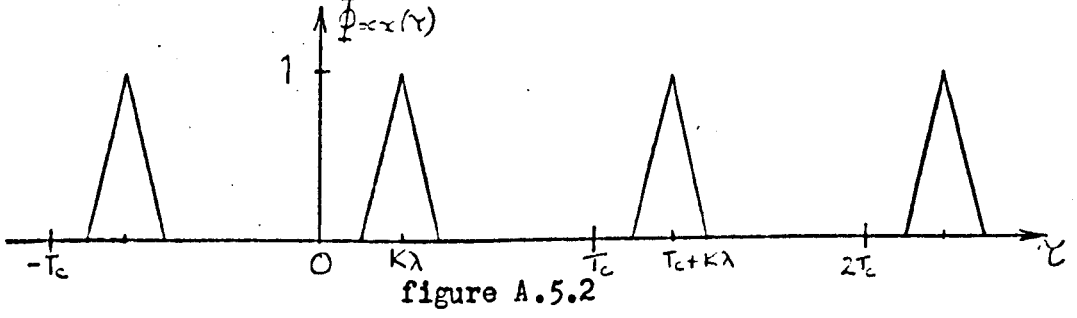

figure A.5.2

This autocorrelation function is of course unrealisable, since $\Phi_{xx}(\tau) = \Phi_{xx}(-\tau)$, $\Phi_{xx}(0) \geq \Phi_{xx}(\tau)$ for all τ. Nevertheless, it is convenient to find the power spectrum due to this train of spikes, and then, as outlined above, to use it to find the complete spectrum.

For $0 \leq K\lambda \leq T_c - \lambda$

$$\begin{aligned}
\Phi_{xx}(\tau) &= 0, && 0 \leq \tau \leq (K-1)\lambda \\
&= 0, && (K+1)\lambda \leq \tau \leq T_c \\
&= (\tau/\lambda) - K + 1, && (K-1)\lambda \leq \tau \leq K\lambda \\
&= K + 1 - (\tau/\lambda), && K\lambda \leq \tau \leq (K+1)\lambda
\end{aligned} \qquad \text{A.5.1}$$

To find $\Phi_{xx}(\tau)$ for K outside the range $0 \leq K\lambda \leq T_c - \lambda$, we use equations(1) and

$$\Phi_{xx}(\tau + NT_c) = \Phi_{xx}(\tau)$$

for all τ and all integer N A.5.2

The component $g'_{xx}(w,K)$ of the power spectrum $G'_{xx}(w)$ due to a spike of unit height in $\Phi_{xx}(\tau)$ at $\tau = (NT_c + K\lambda)$ for N,K integers is given by

$$g'_{xx}(w,K) = \int_{(K-1)\lambda}^{K\lambda} \left(\frac{\tau}{\lambda} \operatorname{Cos} \alpha\tau + (1-K) \operatorname{Cos} \alpha\tau\right) d\tau - \int_{K\lambda}^{(K+1)\lambda} \left(\frac{\tau}{\lambda} \operatorname{Cos} \alpha\tau - (1+K) \operatorname{Cos} \alpha\tau\right) d\tau$$

where $\alpha = \dfrac{2\pi h}{T_c}$ $\quad h = 1, 2 \ldots.$

evaluating the integrals,

$$g'_{xx}(w,K) = \frac{1}{\lambda} \cdot \operatorname{Cos} \alpha K\lambda \cdot \operatorname{Sinc}^2 \frac{\alpha\lambda}{2}$$

where $\operatorname{sinc} x \triangleq \dfrac{\sin x}{x}$

$$\therefore \quad g'_{xx}(w,K) = \frac{1}{\lambda} \operatorname{Cos} \frac{2\pi hK\lambda}{T_c} \operatorname{sinc}^2 \frac{\pi h\lambda}{T_c}$$

We notice that $\operatorname{sinc}^2 \dfrac{\pi h\lambda}{T_c}$ is independent of K, and will therefore occur in the power spectrum component due to each spike in the autocorrelation function. Let us define a new variable $g_{xx}(w,K)$ which is the envelope of the sinc^2 function in $g'_{xx}(w,K)$

$$g'_{xx}(w,K) = g_{xx}(w,K) \cdot \operatorname{sinc}^2 \frac{\pi h\lambda}{T_c}$$

If we define a corresponding quantity for the complete power spectrum, we get

$$G'_{xx}(w) = G_{xx}(w) \cdot \operatorname{sinc}^2 \frac{\pi h \lambda}{Tc}$$

so clearly when the full autocorrelation function consists of spikes of height

$$H_o, H_1 \ldots H_m \quad \text{at} \quad \tau = K_o\lambda, K_1\lambda \ldots K_m\lambda$$

$$0 \leq K_l \leq (Tc - \lambda)$$

then

$$G_{xx}(w) = \sum_{l=o}^{m} H_l \cdot g_{xx}(w.K_l)$$

We know that for a realisable signal

$$\Phi_{xx}(NTc \pm \tau) = \Phi_{xx}(\tau)$$

N integer

$\therefore$ where $K_r \lambda = Tc - K_q \lambda$

$H_q = H_r$

and H_q must exist if H_r exists

Also, $\operatorname{Cos} 2\pi h \cdot \frac{(Tc - K_q\lambda)}{Tc} = \operatorname{Cos} 2\pi h \cdot \frac{K_q\lambda}{Tc}$

$$g_{xx}(w, K_q) = g_{xx}(w, K_r)$$

In particular, for a p-level m-sequence, or the output of a non-linearity with a p-level m-sequence as its input,

$$\frac{K_q\lambda}{Tc} = 0, \frac{1}{p-1}, \ldots \frac{p-2}{p-1}$$

So, for a signal as above,

$$G'_{xx}(w) = \operatorname{Sinc}^2 \frac{\pi h \lambda}{Tc} \left\{ H_o + H_{\frac{p-1}{2}} (-1)^h + 2 \sum_{q=1}^{\frac{p-3}{2}} H_q \cdot g_{xx}(w, K_q) \right\} \qquad A.5.5$$

Notice that the term in curly brackets is periodic in h, period (p-1). This term is $G_{xx}(w)$, and we need only evaluate it for h = 0,1... p-2.

Examples of the application of these results are given in section (3.4)

Appendix (6).

Identification of a non-linear system when measurements of the output are contaminated by noise.

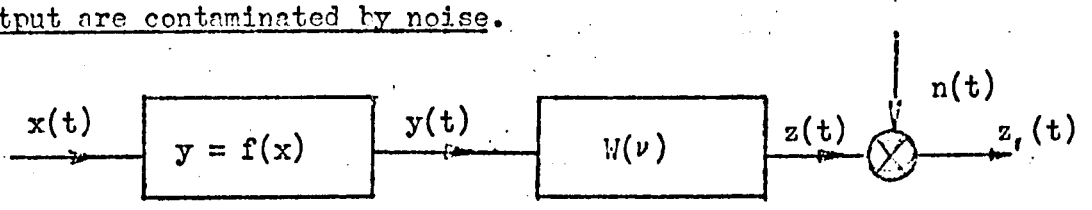

figure A.6.1.

Once again we will consider the system of paragraph (2.2) We will now investigate the problem of identifying the system when the output z(t) is contaminated by noise n(t) which is stationary and uncorrelated to the input x(t). Let the measurable output be $z_1(t)$.

$$z_1(t) = z(t) + n(t)$$

We will consider the outcome of a hypothetical experiment in which we make an estimate $r_{x31}(\tau,X)$ of the partial cross correlation function $\phi_{x3}(\tau,X)$. In this experiment we will take the time average over one period of the input signal, so

$$r_{x31}(\tau,X) = \frac{1}{Tc}\int_0^{Tc} a(t,X).\, z_1(t+\tau)\, dt \qquad A.6.1$$

$$= \frac{1}{Tc}\int_0^{Tc} a(t,X).z(t+\tau)dt + \frac{1}{Tc}\int_0^{Tc} a(t,X).n(t+\tau)dt$$

$$r_{x31}(\tau,X) = \phi_{x3}(\tau,X) + \frac{1}{Tc}\int_0^{Tc} a(t,X).\, n(t+\tau)dt$$

$$= \phi_{x3}(\tau,X) + \epsilon(\tau,X) \qquad A.6.2$$

So the expected value of our estimate is

$$E\{r_{x31}(\tau,X)\} = \phi_{x3}(\tau,X) + E\{\epsilon(\tau,X)\}$$

but we assumed that x(t) and n(t) are uncorrelated, so a(t,X) and n(t) are uncorrelated, so

$$E\{\epsilon(\tau,X)\} = \frac{1}{Tc}\int_0^{Tc} E\{a(t,X).n(t+\tau)\}\, dt$$

$$E\{\epsilon(\tau,X)\} = \frac{1}{T_c}\int_0^{T_c} E\{a(t,X)\}\, E\{n(t+\tau)\}\, dt$$

Let us assume that $E\{n(t)\} = 0$. If this is not so, we will have the same result as when we carry out the technique outlined in paragraph (3.3) for removing the bias from our measurements. We will not be able to distinguish between the average value f_{av} of the non linearity and the mean of the noise at the output.

So, with the assumption that $E\{n(t)\} = 0$

$E\{\epsilon(\tau,X)\} = 0$

We see that our estimate, $r_{x31}(\tau,X)$ of the partial correlation function $\phi_{x3}(\tau,X)$ is unbiassed if the noise contamination is unbiassed.

Let us now assess the variance of our estimate.

Variance in our estimate of $\phi_{x3}(\tau,X) \triangleq E\{\epsilon^2(\tau,X)\}$

$$\epsilon^2(\tau,X) = \frac{1}{T_c^2}\iint_0^{T_c} a(t_1,X).a(t_2,X).n(t_1+\tau).n(t_2+\tau)dt_1dt_2$$

$$E\{\epsilon^2(\tau,X)\} = \frac{1}{T_c^2}\iint_0^{T_c} E\{a(t_1,X).a(t_2,X)\}.E\{n(t_1+\tau).n(t_2+\tau)\}dt_1dt_2$$

$n(t)$ is stationary, so

$E\{n(t_1+\tau).\, n(t_2+\tau)\} = E\{n(t_1).\, n(t_2)\}$

$$E\{\epsilon^2(\tau,X)\} = \frac{1}{T_c^2}\iint_0^{T_c} \Phi_{aa}(t_1-t_2)\, \Phi_{nn}(t_1-t_2)\, dt_1dt_2$$

where $\Phi_{aa}(\tau)$ and $\Phi_{nn}(\tau)$ are the auto correlation functions of $a(t,X)$ and $n(t)$ respectively.

let $t_1 - t_2 = v$

$dt_1 = dv$

$$E\{\epsilon^2(\tau,X)\} = \frac{1}{T_c^2}\int_0^{T_c}\int_{t_2}^{T_c-t_2} \Phi_{aa}(v)\, \Phi_{nn}(v)\, dv\, dt_2$$

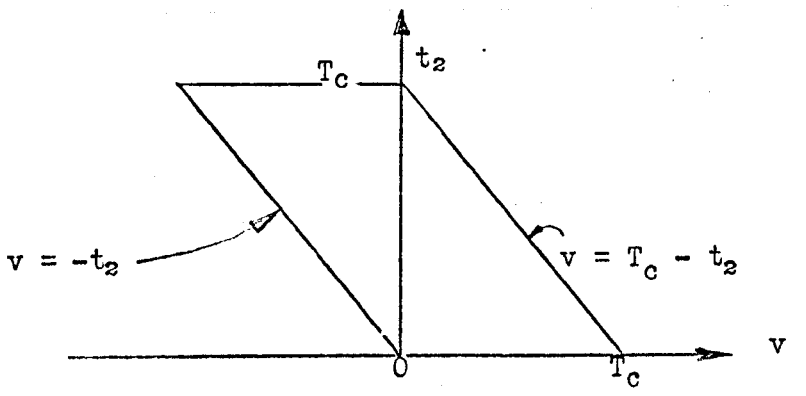

figure A.6.2. - Area of integration.

changing the order of integration,

$$E\{\epsilon^2(\tau,X)\} = \frac{1}{T_c^2}\left\{\int_{-T_c}^{0}\int_{-v}^{T_c} + \int_{0}^{T_c}\int_{0}^{T_c-v}\right\}\Phi_{aa}(v)\,\Phi_{nn}(v)\,dt_2dv$$

$$= \frac{1}{T_c^2}\int_{-T_c}^{0}(T_c + v)\,\Phi_{nn}(v)\,\Phi_{aa}(v)\,dv$$

$$+ \frac{1}{T_c^2}\int_{0}^{T_c}(T_c - v)\,\Phi_{nn}(v)\,\Phi_{aa}(v)\,dv$$

But, $\Phi_{nn}(-v) = \Phi_{nn}(v)$

$\Phi_{aa}(-v) = \Phi_{aa}(v)$

So $$E\{\epsilon^2(\tau,X)\} = \frac{2}{T_c^2}\int_{0}^{T_c}(T_c - v)\,\Phi_{nn}(v)\,\Phi_{aa}(v)\,dv \qquad \text{A.6.3.}$$

We cannot go any further in estimating the variance without a knowledge of $\Phi_{nn}(v)$ and $\Phi_{\underset{\sim}{a}\underset{\sim}{a}}(v)$, but we can see that it is independent of τ, although it is dependent on X.

Appendix (7)

The Autocorrelation Function of a Clocked Signal.

We require the auto-correlation function of an ergodic clocked signal for all delays, when we know its value only for delays which are integer multiples of the clock period. (A clocked signal is one which may change its value only on the occurrence of regularly spaced clock pulses). We will follow the method used by Newton Gould and Kaiser[6] (chapter (3)) for binary signals.

We know - (1) for all τ, $\Phi_{xx}(\tau) = E\{x(t).x(t-\tau)\}$

(2) $\Phi_{xx}(i\lambda)$ and $\Phi_{xx}((i+1)\lambda)$ for all i

where λ is the clock period.

We require $\Phi_{xx}((i+\Delta)\lambda)$, $\quad 0 \leq \Delta < 1$

Now, for a fraction of time Δ,

$$E\{x(t).x(t-(i+\Delta)\lambda)\} = \Phi_{xx}(i\lambda)$$

for a fraction of time $(1-\Delta)$,

$$E\{x(t).x(t-(i+\Delta)\lambda)\} = \Phi_{xx}((i+1)\lambda)$$

therefore

$$\Phi_{xx}((i+\Delta)\lambda) = \Delta\,\Phi_{xx}(i\lambda) + (1-\Delta).\Phi_{xx}((i+1)\lambda)$$

or

$$\Phi_{xx}((i+\Delta)\lambda) = \Phi_{xx}(i\lambda) + \Delta(\Phi_{xx}(i+1)\lambda - \Phi_{xx}(i\lambda)) \qquad A.7.1$$

Hence, the auto-correlation function of a clocked signal changes linearly between a delay of one integral multiple of a clock period, and the next integral multiple, as the delay is varied.

Appendix (8)

Identification of a Non-linear System when the Input Test Signal is Contaminated by Noise.

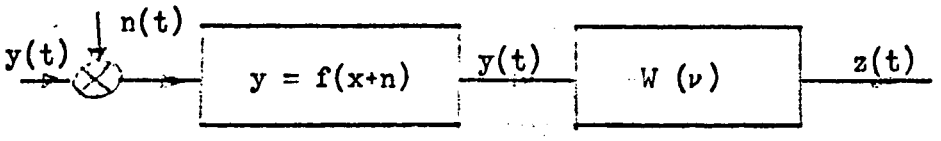

figure A.8.1

Consider an experiment in which we make an estimate $r_{x_3}(\tau,X)$ of the partial cross-correlation function, $\phi_{x_3}(\tau,X)$ between x(t) and z(t) for the system shown in figure 1. We will take the time average over one period of the input signal x(t).

$$r_{x_3}(\tau,X) = \frac{1}{T_c}\int_0^{T_c} a(t,X).z(t+\tau)dt \qquad \text{A.8.1}$$

We will assume that n(t) (a) is stationary

(b) is uncorrelated with x(t)

(c) has zero mean value

(d) has power small compared with that of x(t)

It follows from assumption (d) that

$$y(t) = f(x(t)) + n(t).\, f'(x(t)) \qquad \text{A.8.2}$$

where

$$f' = \frac{df(x)}{dx}$$

$$z(t) = \int_{-\infty}^{\infty} W(\nu).\, y(t-\nu)d\nu$$

$$= \int_{-\infty}^{\infty} W(\nu).\int_{-\infty}^{\infty} (f(X_1) + n(t-\nu).f'(X_1)).a(X_1,t-\nu).dX_1.d\nu \qquad \text{A.8.3}$$

hence

$$r_{x_3}(\tau,X) = \frac{1}{T_c}\int_0^{T_c} a(t,X).\int_{-\infty}^{\infty} W(\nu)\int_{-\infty}^{\infty} (f(X_1)+n(t+\tau-\nu).f'(X_1)).$$
$$a((t+\tau-\nu),X_1)\, dX_1.d\nu.dt$$

$$= \frac{1}{T_c}\int_{-\infty}^{\infty} W(\nu)\int_{-\infty}^{\infty}\int_0^{T_c} (f(X_1) + n\,(t+\tau-\nu).f'(X_1)).$$
$$a(t,X).\, a(t+\tau-\nu,\, X_1).dt.dX_1.d\nu$$

$$= \phi_{x_3}(\tau,X) + \epsilon(\tau,X) \qquad \text{A.8.4}$$

where

$$\epsilon(\tau,X) = \frac{1}{T_c}\int_{-\infty}^{\infty} W(\nu).\int_{-\infty}^{\infty}\int_{0}^{T_c} f'(X_1).\, n(t+\tau-\nu).a(t,X).a(t+\tau-\nu,X_1)\, dt.dX_1.d\nu$$

A.8.5

We require the expected value $E\{\epsilon(\tau,X)\}$ of $\epsilon(\tau,X)$, the error in our estimate of the partial correlation function.

$$E\{\epsilon(\tau,X)\} = \frac{1}{T_c}\int_{-\infty}^{\infty} W(\nu)\int_{-\infty}^{\infty} E\{\int_{0}^{T_c} f'(X_1).n(t+\tau-\nu).a(t,X).\, a(t+\tau-\nu,X_1)dt.\}dX_1.d\nu.$$

But we assumed that n(t) and x(t) are uncorrelated, so

$$E\{\epsilon(\tau,X)\} = \frac{1}{T_c}\int_{-\infty}^{\infty} W(\nu)\int_{-\infty}^{\infty} f'(X_1).E\{n(t)\}\, E\{\int_{0}^{T_c} a(t,X).a(t+\tau-\nu,X_1)\, dt\}.dX_1.d\nu.$$

But, by assumption $E\{n(t)\} = 0$, so $E\{\epsilon(\tau,X)\} = 0$.

Hence we see that

$$E\{r_{x_3}(\tau,X)\} = \phi_{x_3}(\tau,X) \qquad \text{A.8.6}$$

and our estimate of the partial correlation function is unbiassed when our assumptions hold.

We see from equation (5), that

$$\epsilon^2(\tau,X) = \frac{1}{T_c^2}\int_{-\infty}^{\infty}\int\int\int\int W(\nu_1).W(\nu_2).f'(X_1).f'(X_2).\beta\, .d\nu_1.d\nu_2.dX_1.dX_2$$

A.8.7

where $\beta = \int_0^{T_c} n(t_1+\tau-\nu).a(t_1,X).a(t_1+\tau-\nu_1,X_1)dt_1.$

$$\int_0^{T_c} n(t_2+\tau-\nu).a(t_2,X).a(t_2+\tau-\nu_2,X_2)dt_2. \qquad \text{A.8.8}$$

The variance of our estimate of the partial cross-correlation function is $E\{\epsilon^2(\tau,X)\}$.

$$E\{\epsilon^2(\tau,X)\} = \frac{1}{T_c^2}\int_{\infty}^{\infty}\int\int\int\int W(\nu_1).W(\nu_2).f'(X_1).f'(X_2).E\{\beta\}.d\nu_1.d\nu_2.dX_1.dX_2.$$

A.8.9

from equation (8) and our assumption that n(t) and x(t) are uncorrelated, we find

$$E\{\beta\} = E\{\int_0^{T_c}\int n(t_1-\nu_1).n(t_2-\nu_2).dt_1.dt_2\}.$$

$$E\{\int_0^{T_c}\int a(t_1,X).a(t_2,X).dt_1.dt_2\}.$$

$$E\{\int_0^{T_c}\int a(t_1-\nu_1,X_1).a(t_2-\nu_2,X_2)dt_1.dt_2\}$$

$$E\{\beta\} = \int_0^{T_c}\int \Phi_{nn}(t_2 + t_1 + \nu_1 - \nu_2).dt_2.dt_1 . \int_0^{T_c}\int \Phi_{aa}(t_2 - t_1).dt_2.dt_1 .$$

$$\int_0^{T_c}\int \Phi_{a_1a_2}(t_2 - t_1 + \nu_1 - \nu_2)dt_2.dt_1 . \qquad \text{A.8.10}$$

where $\Phi_{nn}(\tau)$ and $\Phi_{aa}(\tau)$ are the autocorrelation functions of n(t) and a(t,X) respectively, and $\Phi_{a_1a_2}(\tau)$ is the cross correlation function between $a(t,X_1)$ and $a(t,X_2)$.

Consider the first double integral of equation (10)

let $t_2 - t_1 = u$

$dt_2 = du$

$\nu_1 - \nu_2 = \nu$

~~Area of integration.~~

$$\int_0^{T_c}\int = \int_0^{T_c} \int_{-t_1}^{T_c - t_1} \Phi_{nn}(\nu + u)du\, dt_1$$

changing the order of integration

$$\int\int = \int_{-T_c}^{0} \int_{-u}^{T_c} + \int_0^{T_c} \int_0^{T_c - u} \Phi_{nn}(\nu + u)dt_1 du$$

$$= \int_{-T_c}^{0} (T_c + u)\Phi_{nn}(\nu + u)du + \int_0^{T_c} (T_c - u)\,\Phi_{nn}(\nu + u)du$$

$$= \int_0^{T_c} (T_c - u)\,(\Phi_{nn}(\nu + u) + \Phi_{nn}(\nu - u))du$$

Exactly the same procedure yields a similar expression for the third double-integral. The second is found by the same procedure, as

$$\int_0^{T_c} (T_c - u)\,(\Phi_{aa}(u) + \Phi_{aa}(-u))du$$

$$= 2\int_0^{T_c} (T_c - u)\Phi_{aa}(u)du$$

since $\Phi_{aa}(u) = \Phi_{aa}(-u)$.

Hence,

$$E\{\beta\} = 2\int_0^{T_c} (T_c - u).(\Phi_{nn}(\nu + u) + \Phi_{nn}(\nu - u))du \int_0^{T_c} (T_c-u)\Phi_{aa}(u)du$$

$$\int_0^{T_c} (T_c - u)(\Phi_{a_1a_2}(\nu + u) + \Phi_{a_1a_2}(\nu - u))du \qquad \text{A.8.11}$$

Equations (9) and (11) together give us the variance of our estimate of the partial cross-correlation function. When x(t) is a p-level m-sequence equation (9) is replaced by equation (12)

$$E\{\epsilon^2(\tau,X)\} = \frac{1}{T_c^2}\sum_{i=0}^{p-1}\sum_{j=0}^{p-1}\int_0^{T_c/p-1}\int W(\nu_1)W(\nu_2)f'(X_i).f'(X_j).E\{\beta\}.d\nu_1 d\nu_2. \qquad A.8.12.$$

SECTION 2.

AN EYE POSITION TRANSDUCER

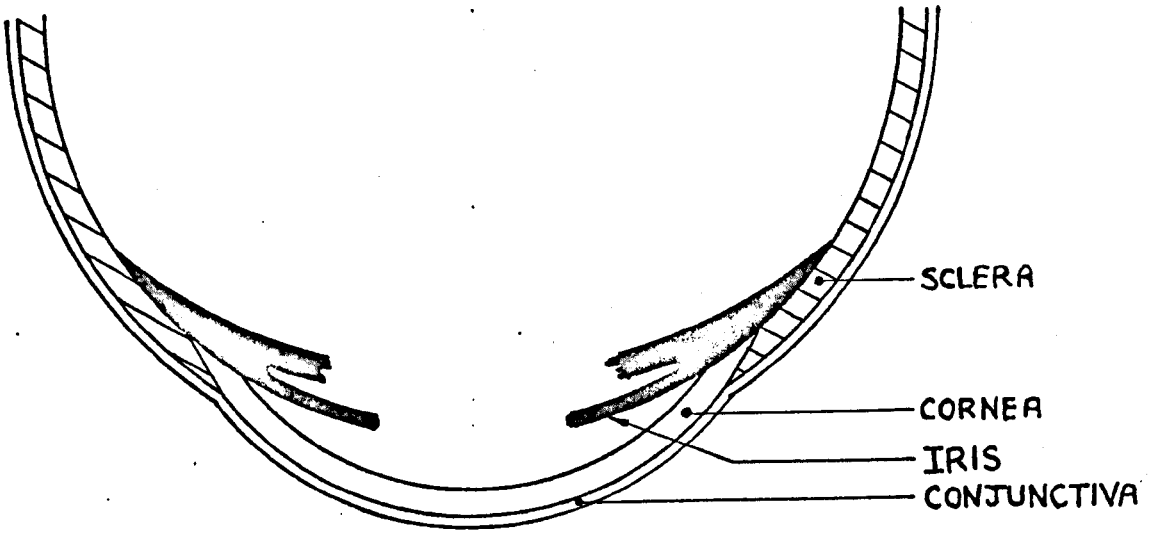
SCLERA
CORNEA
IRIS
CONJUNCTIVA

Chapter 1.

The human eyeball is normally in continual motion as it scans the field of view. This motion consists of rotations about two axes – a vertical one, and a horizontal one which is normal to the optic axis. These movements are controlled mainly by four muscles which are attached tangentially to the eyeball and act in the 'into the head' direction. They are arranged one above, one below and one on either side of the eye (see figure 1.1). A pad of fat behind the eyeball provides a bearing surface, and the necessary 'out of the head' reaction force to maintain equilibrium. In addition to these scanning movements, there are two major movements which are less noticeable. First, the tensing of all of the four muscles together compresses the pad of fat, and the eyeball is translated in the 'into the head' direction, and vice versa. This is observed when an object is brought close to the eye, for instance when removing a foreign body from under an eyelid. Secondly, the eyeball rotates about the optic axis under the control of two more muscles which, by running in 'pulleys' in the scull, apply forces obliquely. This movement is observed when the head is tilted; the eyeball rotates in the opposite sense so that the images of vertical objects remain vertical.

Several sections of the scientific community have found a need to measure the scanning movements, and to record the movements as functions of time. As a result, experimenters from various disciplines have constructed transducers to measure eye movements. The main interest has come from the following groups.

(a) Physicians who require a diagnostic aid, and who wish to study the effectiveness of treatments that they have given for occulo-motor diseases

(b) Physiologists and bio-engineers who wish to study the behaviour of the normal eyeball.

(c) Psychologists who are interested in the scanning behaviour of the eye, for example in driving or reading.

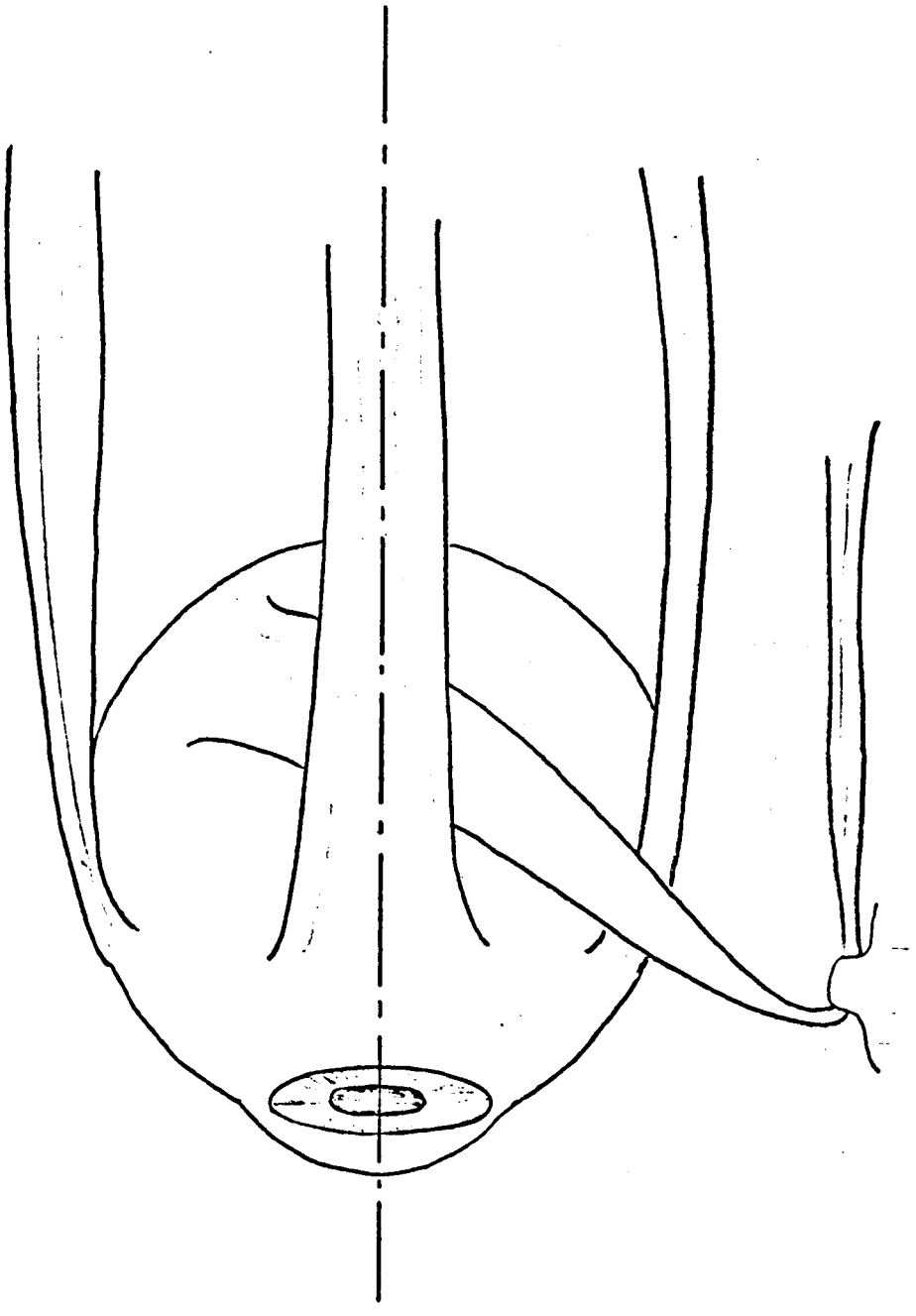

FIGURE 1.1-The Muscles Controlling the Eye (Schematic Plan View)

(d) Engineers who are arranging instruments or controls so that they may be used to the best advantage, or who wish to use the eyeball as an additional information input to a machine, for example, to improve tracking with a telescope, or as a typing aid for the disabled.

Young[1] presents a survey of the methods that have been used to measure eyeball movements, and their performance and accuracy. He also reports on a system which he, and his co-workers at the Massachussetts Institute of Technology (MIT), designed in 1961. This system exploits the variation in reflectivity over the surface of the eyeball. Figure (1.3) shows the salient features of the instrument. Two circular patches of light are thrown onto the eye by the filament lamps. Each of the two photo resistors is directed towards one of the patches of light, and produces an output which is proportional to the light flux reflected by the eye. The difference in the outputs of the two photo-resistors is proportional to the rotation of the eye about its vertical axis.

Because the cadmium sulphide photo resistors have a limited frequency response, this system may only be used to measure components of eyeball movements up to about 10 Hz.

In the summer of 1966, I spent some time at the National Physical Laboratory (NPL), Teddington, and became familiar with a development of Young's device which had been made by Plumb[2] (figure 1.4). Plumb's requirement was for a device which he could use in total darkness, and which would measure eyeball rotation only about a vertical axis. Also he required the instrument to have a high frequency response.

So that his subject would remain in a state of dark adaption, Plumb replaced the two filament lamps by gallium arsenide diodes, and the photo-resistors by silicon photo-transistors. The diodes, when reverse-biased, are monochromatic sources of near infra-red (wavelength 0.9μ). The photo-transistors have a high sensitivity to radiation of this wavelength, as well as to visible light towards the red end of

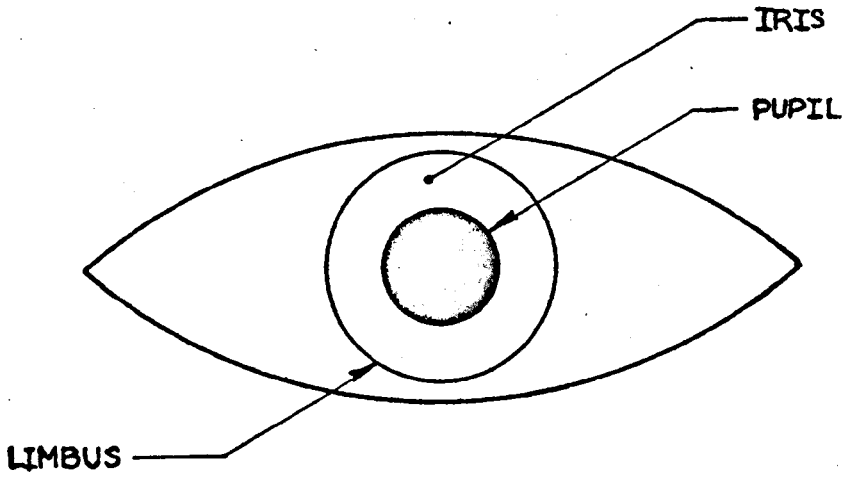

FIGURE 1.2

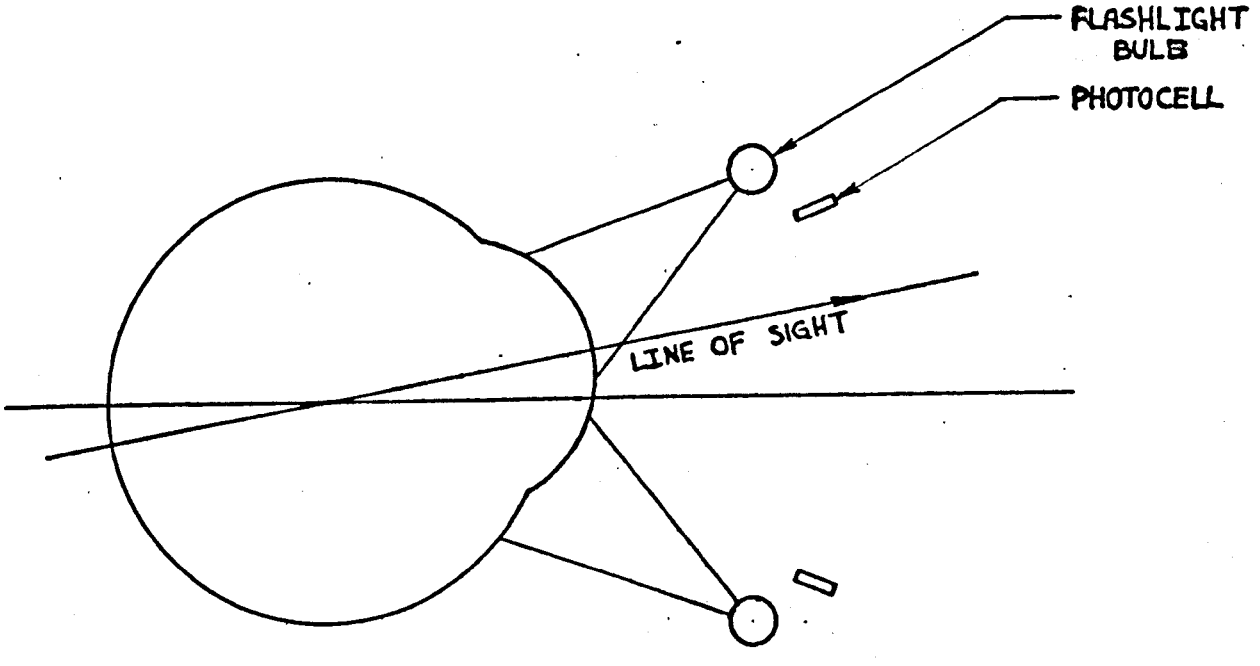

FIGURE 1.3

YOUNG'S DEVICE

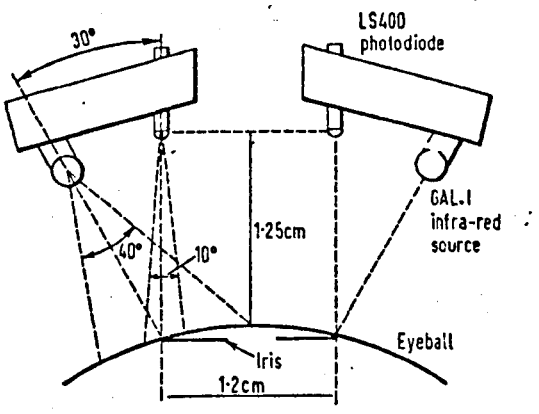

Figure 1.4

PLUMB'S DEVICE.

the spectrum. Because the silicon photo-transistor has a very much faster rise time than a photo-resistor, Plumb's version is capable of recording eye movements of considerably higher frequency than is Young's.

The wide spectral response of the photo-transistors (extending through the visible spectrum and well into the infra-red spectrum) meant that Plumb's device could not be used except in total darkness. On my return to the University of Warwick, I started work on a modified version of the transducer which would allow its use in any lighting conditions. At the same time Hughes[3] was working on a similar improvement to the same device for the British Aircraft Corporation. This latter work was later suspended because the problems involved in setting-up the instrument made it unsuitable for the proposed tracking application.

Chapter 2. The design and development of a transducer based on the N.P.L. version of Young's instrument.

The NPL transducer was constructed so that the special relationship between the infra-red sources and the photo-transistors was fixed by the frame on which they were carried. The frame was supported by a travelling microscope stand (see figure 2.0.1.). The stand was provided with slides and scales which allowed the transducer to be moved along the three axes (x, y, z in fig 1) and the movements to be measured.

The subject's head was held stationary by means of a dental bite which was firmly secured to the supporting table. The time required to readjust the apparatus, following a change in subject, was considerably reduced by recording the setting of the microscope stand for each subject.

Initially I constructed a copy of the NPL transducer that was supported on a spectacle frame so that the subject would not have the tiring restraint of the bite. The photo-transistors and gallium arsenide diodes were supported on a frame which allowed the geometry to be altered easily, and clamped firmly after adjustments were made. The performance of this copy was not as good as that of the NPL version, and this was later attributed to the considerable variation in characteristics between one photo-transistor and another of the same type, and to variation in the reflective properties of the eyeball, between one subject and another.

A considerable amount of experimentation lead to the following conclusions about the NPL version.

(1) The geometry quoted by Plumb is not optimum

(2) The performance is very sensitive to small changes in geometry.

(3) Errors are introduced as a result of the movement of the subject's eyelids.

(4) It is reasonable to use the device to operate an electric typewriter, while the subject looks at a matrix of letters.

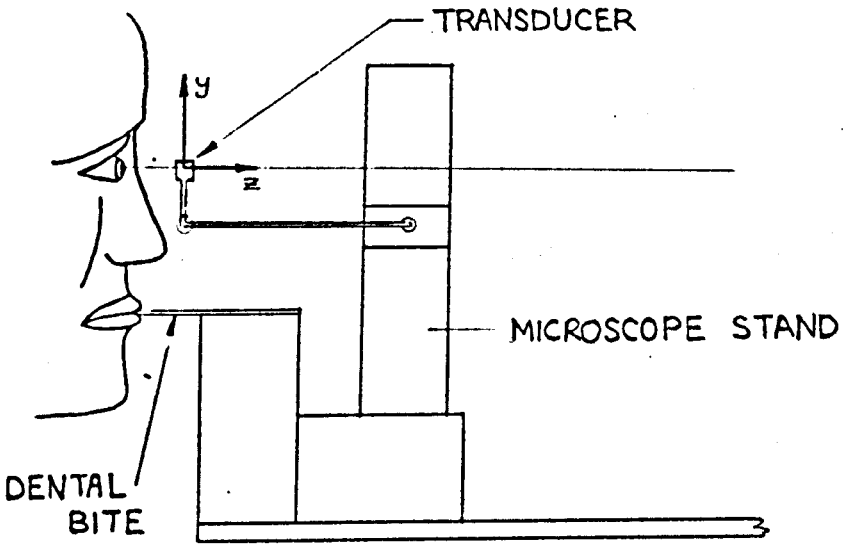

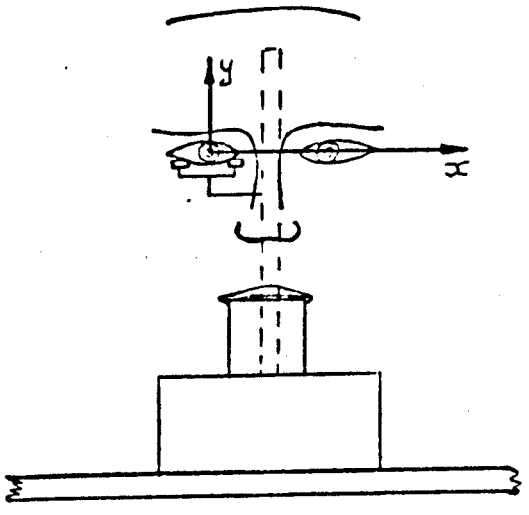

FIGURE 2.0.1

Some experiments carried out with an infra-red image converter suggested that

(5) When viewed in monochromatic light with wavelength 0.9μ, the eye appears to be a black hole in a white diffusive sphere.

The variation in performance with geometry is very serious. It means that gross errors can result from small distortions in the structure of the transducer, from small movements of the transducer relative to the subject's head, or from the translation of the eyeball in the z direction (see figure (2.0.1.) and chapter (1)). Also, the transducer requires a very lengthy setting-up procedure to achieve reasonable performance. This may take up to two hours, and is hampered by the movement of the eyeball into the head as described in chapter (1).

The problems associated with eyelids seems to limit users to those whose eyes are normally fairly wide open, as it is a considerable strain deliberately to hold the eyelids wider than normal.

From the initial testing phase, the project developed along two parallel paths; the design of the geometry, and the construction of a system which would allow the device to be used in any lighting conditions.

(2.1) Design of the geometry.

It was clear that eventually the transducer would be required to give measurements of rotation about both the vertical and horizontal axes of its scanning rotation. This influenced the design criteria which were chosen when a transducer was constructed which would measure only rotation about the vertical axis. The following quantities were chosen to be optimized in the design of the transducer geometry.

(1) linearity * (local and general)

(2) cross-talk

(3) range

(4) sensitivity

(5) immunity to small variations in geometry

Of these properties, the fifth is by far the most important. It is clearly intolerable to spend a large amount of time checking and setting up the transducer. General linearity, that is linearity of the device over its entire range, should be within ± 5% for most applications. (This linearity was obtainable for short periods with all versions). Local linearity is particularly important when the application requires a specified angular error, as apposed to a specified fractional error. Crosstalk (an indicated movement about one axis due to a movement about a perpendicular axis) would be undesirable for a single-dimension device, and a serious fault in the two-dimentional one.

Observations of the NPL subject's eyeballs, using an infra-red image converter and the gallium arsenide sources, supported the following design assumptions about the system, at the infra-red wavelength to be used.

---

* The term 'linearity' is used here to mean 'fractional linearity error'. It is defined fully in appendix (3). The linearity of the instrument is good if the figure quoted is small.

(1) The sclera behaves as a diffusive, spherical surface. The conjunctiva and cornea are perfectly transmissive.

(2) The iris and pupil have negligable reflectivity compared with that of the sclera.

(3) The limbus is circular.

(4) The infra-red sources provide uniform illumination over the areas 'seen' by the photo-transistors.

The model of the eyeball then, at the infra-red wavelength of interest, is like a table-tennis ball on which is painted a black patch with a circular boundary.

Two further assumptions were made in order to allow the design to proceed, they were

(5) the areas seen by the photo-transistors are circular

(6) the sensitivity of the photo-transistors to infra-red is uniform over these areas

Assumptions (2), (5) and (6) were later found to be false, and in some cases markedly so (see chapter (3)). If all six assumptions do hold, then the behaviour of the transducer is governed entirely by the geometry of intersecting circles. We will therefore investigate this subject now.

(Page 83)

Consider the figure (2.1.1), in which all dimensions are normalised with respect to the radius of the limbus.

The two circular areas, radius a, are the areas seen by the photo-transistors, and the outline of the pupil is shown dotted. The output of the transducer is the amplified difference in the outputs of the two photo-transistors.

Output α $A_2 - A_1$

$A_2 = \pi a^2 - A_2'$

$A_1 = \pi a^2 - A_1'$

Output α $A_1' - A_2'$

It is more convenient for us to calculate the areas A_1' and A_2' than A_1 and A_2 , and we see that this information is just as useful.

Let AREA (r_1, r_2, b) be the common area of two circles radii r_1 and r_2 and central seperation b. This function of (r_1, r_2, b) is found in Appendix (A.1.)

Hence we have a simple way of computing the response of the transducer as a function of x and y given c. In practice it is more efficient to form a look-up table of AREA (1, a, b) against b for each a, and to interpolate in b each time AREA is required.

Now consider figure (2.1.3). To a satisfactory approximation, we find that for a small change δz in z,

$$\frac{\delta c}{\delta z} = \tan \theta$$

$$\frac{\delta a}{\delta z'} = \tan \alpha$$

$$\frac{z}{z'} = \cos \theta$$

So, the resulting changes δa and δc in a and c are related approximately by

$$\frac{\delta a}{\delta c} = \frac{\tan \alpha}{\cos \theta . \tan \theta} = \frac{\tan \alpha}{\sin \theta}$$

We must choose θ such that $\frac{\delta a}{\delta c}$ is the best approximation to the ideal value.

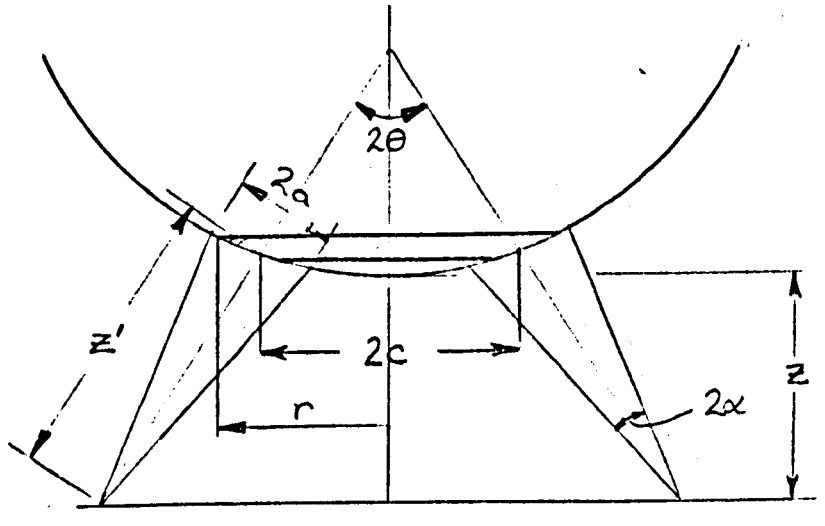

figure (2.1.3)

The design process now becomes (see figures 2.1.1, 2, 3)

Given α,

(1) Choose a and c such that

(i) there is a closely linear relationship between the output and x

(ii) the output has a small sensitivity to y

(iii) the output has the minimum variation with respect to a

(2) Choose a relationship between c and a so that as they vary, the performance remains most nearly constant. Choose θ such that

$$\frac{\delta \eta}{\delta c} = \frac{\tan \alpha}{\sin \theta}$$

most nearly satisfies this relationship.

This design is most conveniently carried out using the computer programme suggested earlier in this chapter. An Algol programme was written which, given a and c as data, computes OUTPUT (x_t, y_t) for an array of values of (x_t, y_t). Taking each value of x as the maximum range, it computes LINEARITY, and for each x_t as origin it computes CURVE (These terms are defined in Appendix (2)). The programme also finds the value of x, for each y_t, for which the LINEARITY reaches a prescribed limit TL, and the area (LINAREA) over which the linearity is within this limit.

There is no purpose in computing results for cases where the field of view of either of the transistors is entirely sclera or entirely iris. That is for:

$$c + |x| > 1 + a \qquad (1)$$

$$c - |x| < |1 - a| \qquad (2)$$

i.e. x should be not greater than the lesser of

$$1 - c + a$$

$$c - |1 - a|$$

These conditions also imply limits on c and a, and by substituting $|x| = 0$ in (1) and (2) we get

$$c > 1 + a$$

$$c < |1 - a|$$

These conditions are represented graphically in figure (2.1.4) Looking again at (1) and (2), we see that the maximum range of x is achieved for ($c = 1$) when ($a < 1$) and ($c = a$) when ($a > 1$). figure (2.1.4) shows this also, for the x range is the shorter vertical distance to the boundary of the useful region.

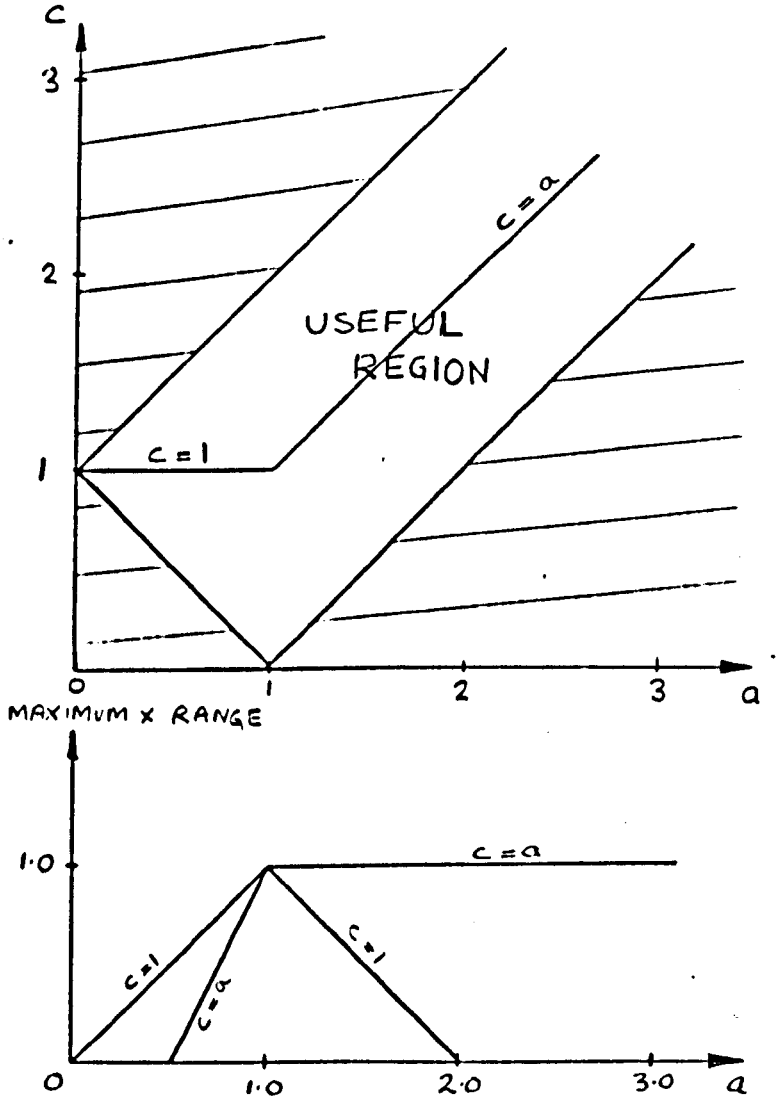

figure (2.1.4)

The observations with the NPL transducer showed that difficulties arise when the subject's eyelids are within the areas seen by the transistors. We would therefore like to keep these areas as small as possible, and to choose the data for the programme accordingly.

(2.2) Modification for use in any lighting conditions.

The system represented in figure (2.2.1) (which is believed novel) was constructed using simple transistorised amplifiers and transistor switches. In the dark, the performance of this system was the same as the previous version, but it was still of little use in daylight because the ambient illumination was sufficient to saturate the photo-transistors. Ordinary photographic infra-red filters were placed in front of the photo-transistors. Again the performance of the device was unchanged in the dark, but it could also be used in subdued daylight. In strong light there was sufficient infra-red to cause the saturation of the first stage of the amplifier. To overcome this difficulty, active d.c. negative feedback was applied to the amplifier and saturation did not occur except in full sunlight.

The resulting system was subject to serious drift due both to the changes in leakage of the photo-transistors, and to drift of the amplifiers.

The system was rebuilt using integrated circuit operational amplifiers, and a field effect device as a preamplifier. The new system was now much more stable, and less sensitive to variation in ambient illumination.

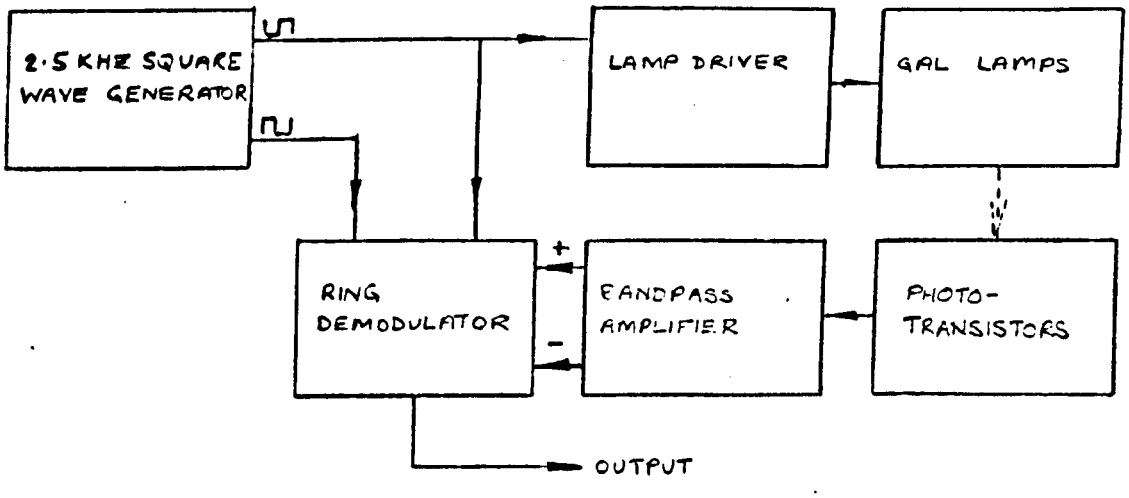

FIGURE 2·2·1

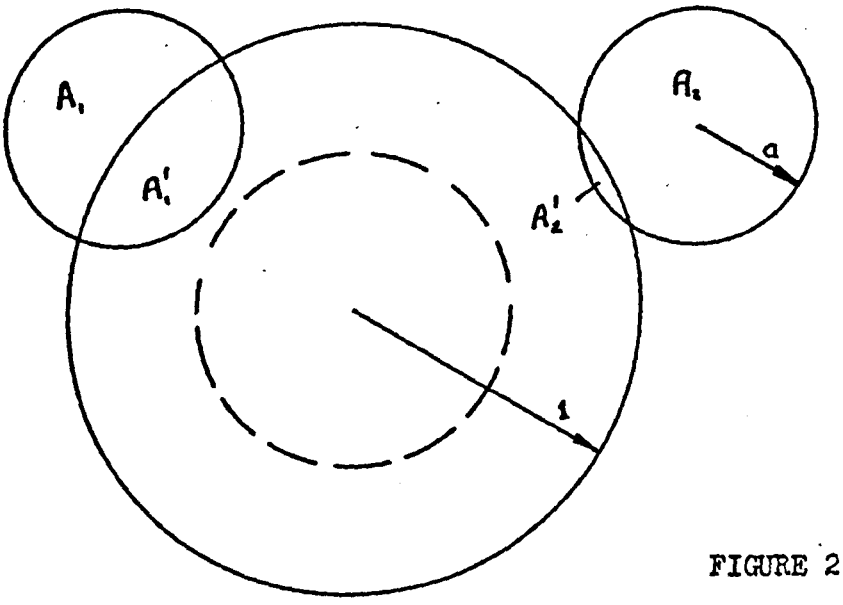

FIGURE 2.2.1

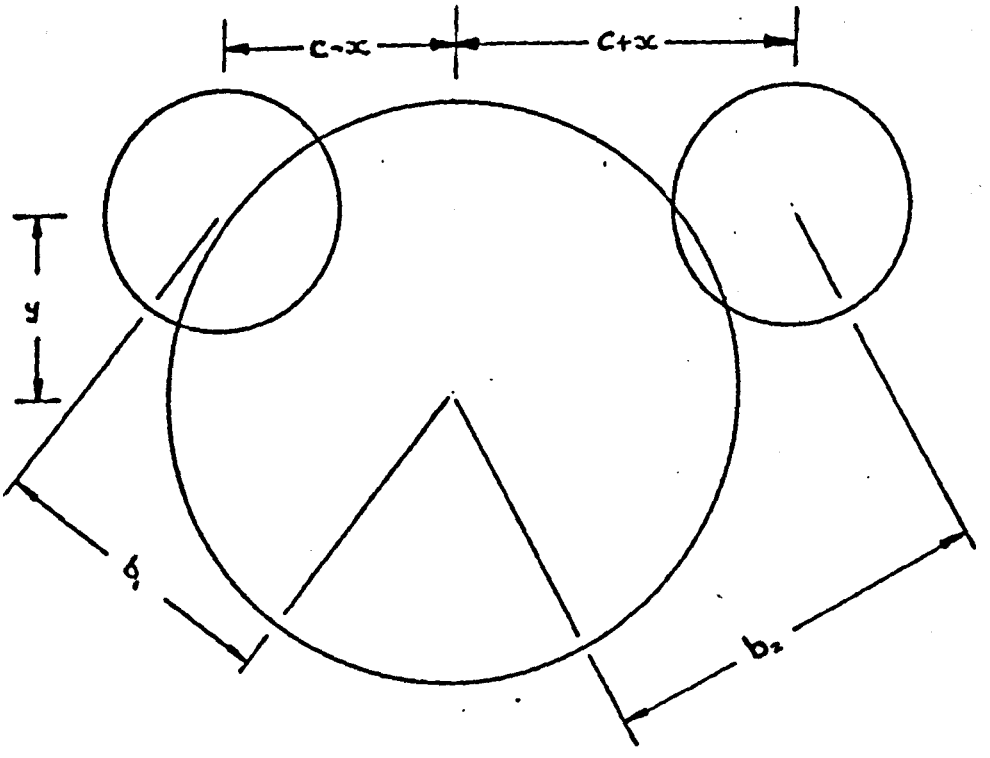

FIGURE 2.2.2

(2.3) Modification for use in two dimensions.

A transducer was constructed which had two receiving channels each identical to the single channel version. The new transducer used the same infra-red transmitting system, which served both channels.

There is insufficient space between the eyelids to construct a system that uses one channel for rotations about the horizontal axis and the other for rotations about the vertical axis. Instead, two axes were chosen inclined at equal angles to the vertical axis, and summing amplifiers were used to operate upon the outputs to produce a horizontal and a vertical signal.

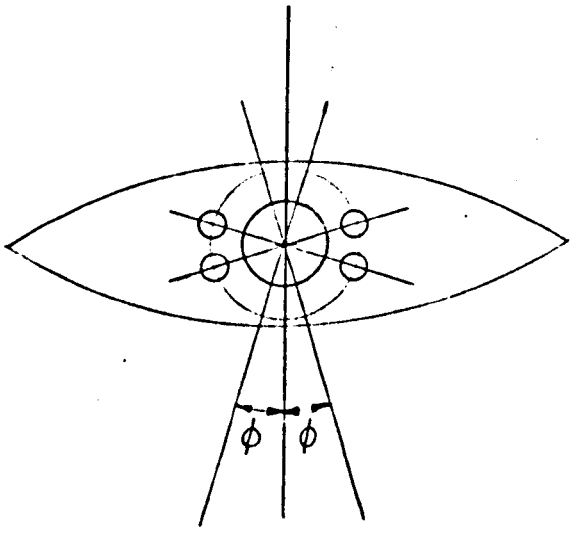

Clearly the horizontal resolution will be superior to the vertical, but in many applications this is acceptable.

Chapter (3). Observations with the eye position transducer, and with the infra-red image converter.

The experimental work fell into three distinct categories, testing of equipment, experiments to test design assumptions, and investigations into one particular application. The observations made as a result of experiments in the last two categories will now be recorded.

(3.1) Evidence in support of design assumptions.

Here again a natural division falls, in the experimental work, between work done with the eye position transducer itself and work done with other devices.

Two other means were employed to obtain evidence of the validity of the assumptions. At NPL an infra-red image converter was available which would convert an infra-red image into a visible image. Recently (1969) an infra-red film has become available (Kodak Infra-red 35 mm).. which is adequate for photography by illumination of the gallium arsenide lamps.

The assumptions are now considered one by one in the light of the evidence from all these experiments

(1) The sclera behaves as a diffusive spherical surface. The conjunctiva and cornea are perfectly transmissive.

Clearly the sclera is not perfectly spherical, and the conjunctiva and the fluid film carried by it will be reflective in some degree, but experiments with just one photo-transistor showed that variations in the output, due to all effects, were very small when the area seen by the transistor lay outside the limbus, compared with the signal in normal operation.

Reflection from the cornea would cause errors because of the corneal bulge, but it was not possible to see any reflection with the image converter. Some reflection is apparent in photographs taken with the infra-red film.

(2) The iris and pupil have negligible reflectivity when compared with the sclera.

This assumption was supported well by the NPL subject. Measured responses corresponded closely to the calculated response, and observations with the image converter were very similar to the model of the eye. However, it would appear that it was by chance that he was such a good subject, having his iris pigmentation such that the assumption was supported. No work with other subjects has shown the same evidence. Figure (1) is an infra-red photograph of my own eye showing clearly that the assumption is invalid.

(3) The limbus is circular

This is very closely true for all subjects, as can be justified by inspection of photographs of their eyes.

(4) The infra-red sources provide uniform illumination over the areas seen by the photo-transistors.

This was justified by an experiment in which a table-tennis ball was placed in the position of the subject's eye, and viewed with the image converter. Additional support was given by changing the positions of the gallium arsenide lamps and observing that there was no consequent change in response for small changes.

(6) and (5) The areas seen by the photo-transistors are circular. The sensitivity of the photo-transistors is uniform over these circular areas.

This information was given by the manufacturer, but Texas Instruments stated later that the areas seen by the transistors are elliptical, and that the sensitivity varies considerably over these areas, and from one transistor to another. They now produce another photo-transistor which satisfies the assumption closely, and which does not show wide production spreads. Unfortunately this transistor is extremely small and difficult to mount. It has not yet been incorporated into the apparatus.

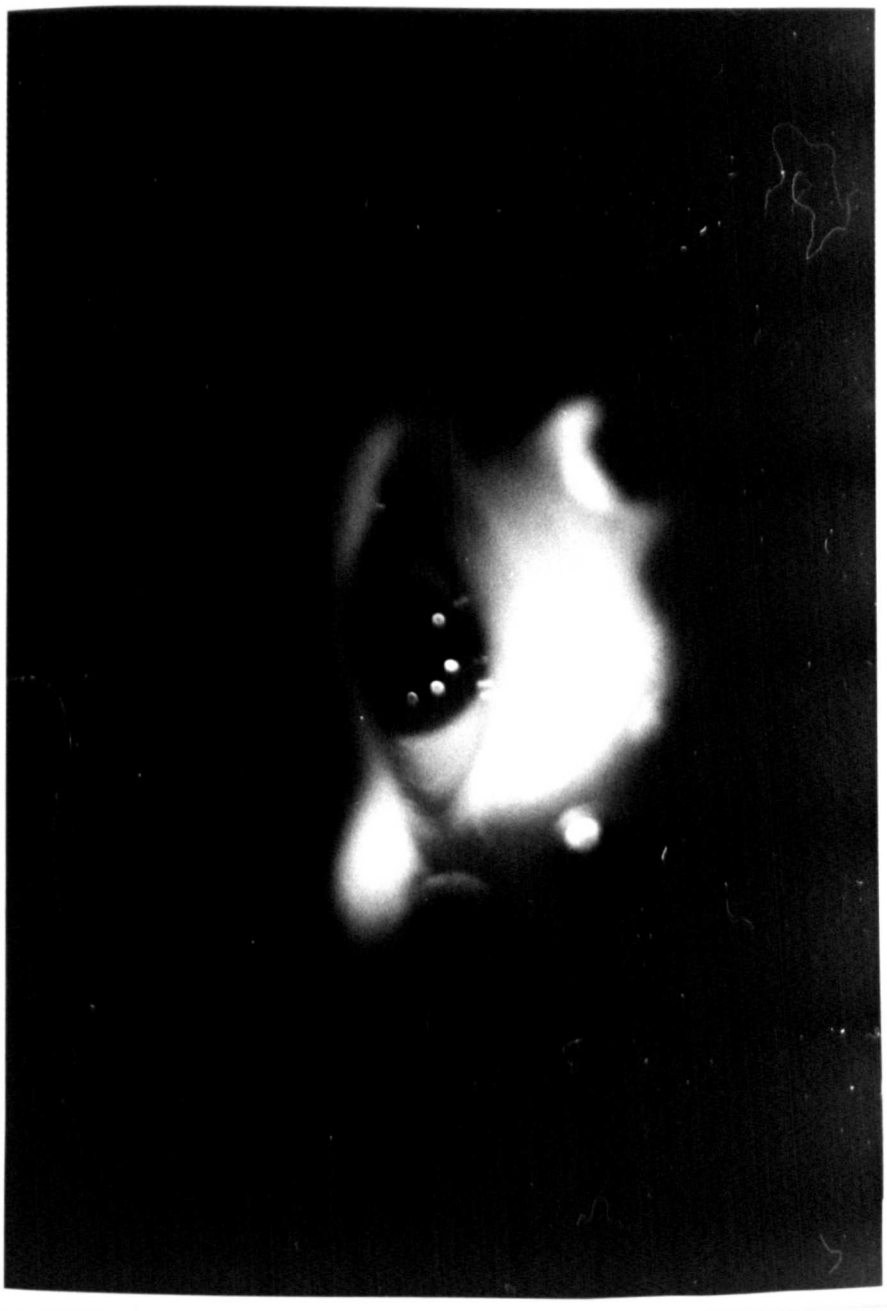

The author's eye photographed on infra-red film, with 0.9 mono-chromatic illumination

(3.2) Preliminary experiments in typewriter control.

While I was still at NPL I used the NPL transducer in the experimental set up shown in figure (1)

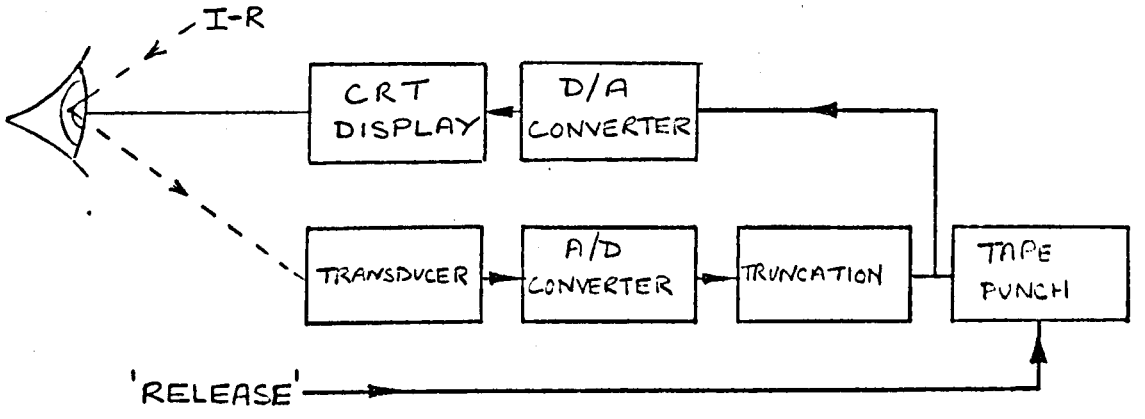

figure 3.2.1

A linear array of characters was displayed on the mask of a CRT. The subject viewed the CRT, with the transducer in position in front of his eye, and with his head secured with the dental bite. Various character arrays were used having 8, 16, 32 and 64 characters in a horizontal line subtending an angle of 12° at the subject's eye. A press-button switch was used to generate a 'release' signal for the paper tape punch, when the spot on the CRT display coincided with the required letter.

Four subjects were used in the experiment. The first was the subject with whom I did the majority of the experiments at NPL. He had by now become quite accustomed to the apparatus, after about three weeks experience as a subject in other experiments. After two 50 second trial runs he was able to use the device to punch about 70 characters per minute, with perhaps one or two errors, from an array of 64 characters. The three other subjects, all typists new to the equipment, were able to punch about 20 characters per minute, two from an array of 32 characters, and the third from an array of 8 characters. This subject was very nervous and had a 50% error rate when the display contained 16 characters.

The visual feedback was originally intended to allow the subject to dispense with the bite and use only a head-rest. Only the experienced subject tried this. He found that he was unable to type for as long as one minute because his neck became very tired from holding his head still.

(3.3) General experimental observations.

At no time did any subject become really comfortable when using either the NPL transducer, or the spectacle-borne Warwick device. All complained of sore, dry eyes after 60 to 90 seconds of use. This was not due to the infra-red illumination of their eyeballs, for they complained whether or not the lamps were on, and whether or not they knew they were on. In any case the infra-red flux reaching the eyeball is less than that from a 100 watt filament lamp at a distance of 3 feet from the eye.

It was very disturbing to the subject if the output of the transducer is displayed in front of him with no filtering, and this causes the amplitude of the high frequency components of his eyeball movements to increase. The subjects found that the feedback signal in the typewriter control experiment was satisfactory in that it removed all the jitter from the display, whilst responding promptly.

(4) Conclusion.

The eye position transducer described in this thesis is a relatively simple device which is able to measure eyeball rotations over a range $\pm 6^{o}$ to an accuracy of 0.2^{o} to 1.0^{o} depending upon the subject, and the conditions of use. It has the great advantages that the subject need not wear heavy equipment on his head, and that the associated electronics are simple and compact. When the device is used with visual feedback, the subject is able to locate points with an accuracy limited only by his eyeball tremor.

The transducer has been applied to a disabled person's typing machine by M.H.Birley[4] in his B.Sc. project. Starting from the work described in section 3.2 of this thesis, he constructed a typing system which uses a two-dimensional array of letters (see figure 4.0.1). The output of the transducer is coded into typewriter control signals using a small process control computer (see figure 4.0.2). Birley used this system to study the problems of visual feedback, and the requirements of the visual display. He concluded that the system was practical and that high typing speeds could be achieved after training.

Also at the University of Warwick, P.H. Landers is using the eye position transducer to study the relationship between optical and vestibular stimuli.

Dr. B..Craske, at the University of Southampton, is using a copy of the transducer to study the behaviour of subjects performing a sorting task.

Certain disadvantages of the transducer have become apparent, and these should form the basis of further work.

(1) The transducer characteristics are constant, under varying lighting conditions, only if the reflectivity of the iris is equal to the apparent reflectivity of the pupil, measured at 0.9μ. This is not always the case.

(2) A considerable amount of time is required for setting up the transducer and for subject acclimatization.

Consideration of further work must include a study of possible alternative methods of measuring eyeball position. Mr. R.L.Hyde of the British Aircraft Corporation suggested that better results might be achievable using a closed-circuit television technique. A small television camera would scan the eyeball, and the changes in signal level between sclera and pupil detected.

More complex television systems have been used, for example, the system described in reference (5). This gives very high accuracy at the expense of great complexity.

sp	sp	1	2	3	4	Ø	sp	sp
:	=	*	•	(	)	'	<	>
;	5	6	7	8	9	Y	Q	-
B	P	N	R	S	T	O	W	X
K	M	C	A	E	I	D	F	V
J	U	H	,	cr	L	G	Z	bs
sp	sp	sp	tab	tab	tab	sp	sp	sp

FIGURE 4·0·1

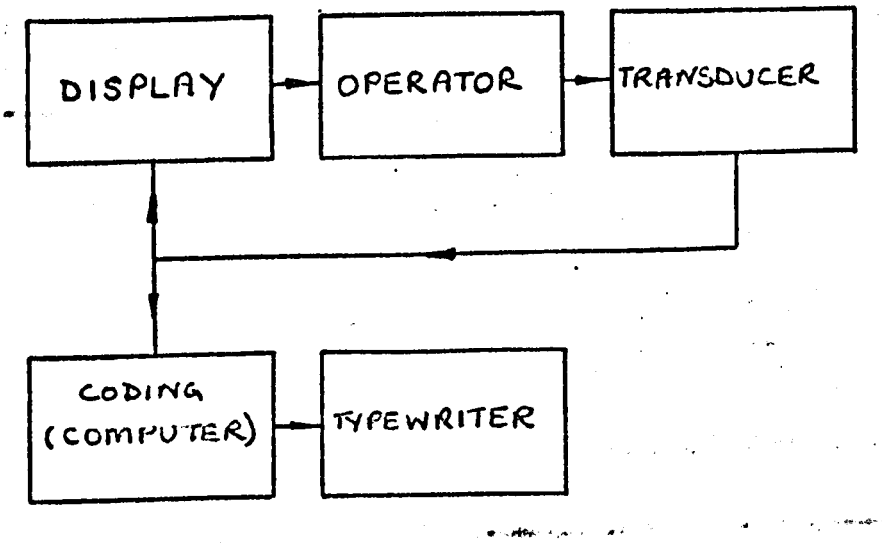

FIGURE 4·0·2

References

1. Young, L.R., Measuring Eye Movements. Am.J.Med. Electronics, Vol 2, No.4, 1963, pp.300 - 307.
2. Plumb, G.O., An Infra-red Instrument for Detecting Eye Movements. Instrument Review, Jan. 1967.
3. Hughes, M.A., An Investigation into Methods for Monitoring Eye Movement, B.A.C. Internal Tech. Note, ST.1815.
4. Birley, M.H., B.Sc. Dissertation, 1968. University of Warwick.
5. Kelly, D.H., and Crane, H.D., N.A.S.A. Report CR - 1121.

Appendix 1.

The common area of two circles.

The purpose of this appendix is to derive a relationship between centre separation and common area of two circles, which is suitable for mechanisation on a digital computer.

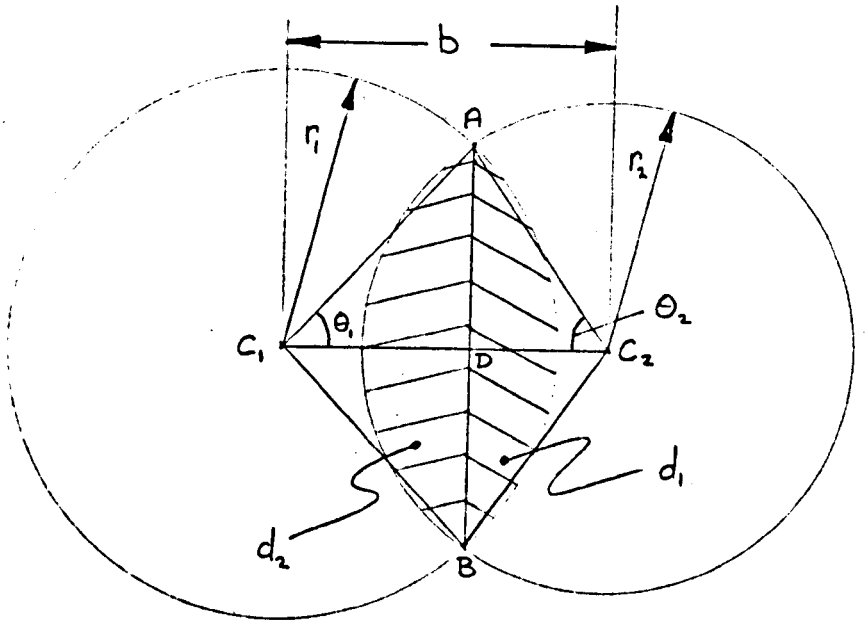

figure (A.1.1)

Consider two circles radii r_1 and r_2, with centre separation b (see figure (A.1.1)).

Case (1) $|b| > r_1 + r_2$ (see figure (A.1.2))

Clearly, if $|b| \geq r_1 + r_2$, then the circles do not intersect, and their common area is zero.

Case (2) $r_1 < r_2$, $|b| \leq (r_2 - r_1)$ (see figure A.1.2)

the circle of radius θ, is completely enclosed by the other so,

Common area = πr_1^2

Case (3) $r_2 < r_1$, $|b| \leq (r_1 - r_2)$ (see figure A.1.2)

the circle of radius r_2 is completely enclosed by the other, so their

Common area = πr_2^2

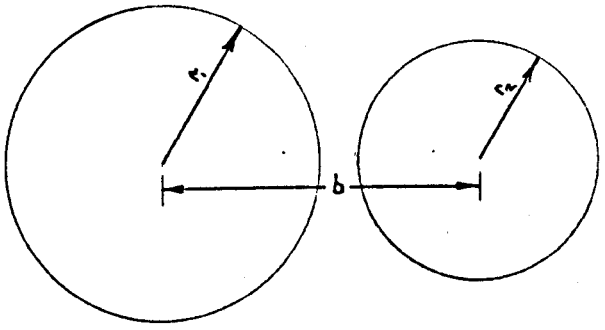

CASE 1

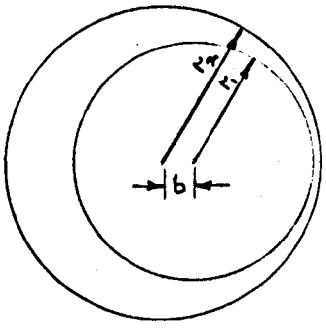

CASE 2

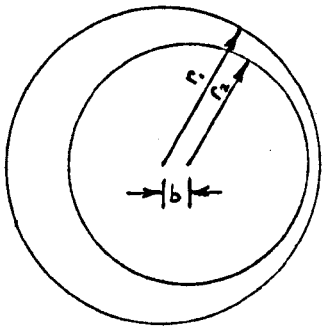

CASE 3

FIGURE A·1·2

Cases (2) and (3) reduce to the same condition

$$|b| \leq |(r_1 - r_2)|$$

then Common area = $\pi \times (\text{lesser}(r_1, r_2))^2$

Case (4) otherwise (figure (A.1.1), i.e. $|(r_1 - r_2)| < |b| < r_1 + r_2$

Common area = $d_1 + d_2$

$$= r_1^2(\theta_1 - \sin\theta_1 \cos\theta_1) + r_2^2(\theta_2 - \sin\theta_2 \cos\theta_2)$$

$$= r_1^2(\theta_1 - 0.5 \sin 2\theta_1) + r_2^2(\theta_2 - 0.5 \sin 2\theta_2)$$

$$|b| = r_1 \cos\theta_1 + r_2 \cos\theta_2$$

$$AD = r_1 \sin\theta_1 = r_2 \sin\theta_2$$

$$\therefore \quad \sin^2\theta_1 = \left(\frac{r_2}{r_1}\right)^2 \sin^2\theta_2$$

$$\therefore \quad \cos^2\theta_1 = 1 - \left(\frac{r_2}{r_1}\right)^2 \sin^2\theta_2$$

$$= 1 - \left(\frac{r_2}{r_1}\right)^2 (1 - \cos^2\theta_2)$$

$$= \left\{\frac{|b| - r_2 \cos\theta_2}{r_1}\right\}^2$$

Hence.

$$(b - r_2 \cos\theta_2)^2 = r_1^2 - r_2^2 (1 - \cos^2\theta_2)$$

$$b^2 - 2|b| r_2 \cos\theta_2 + r_2^2 \cos^2\theta_2 = r_1^2 - r_2^2 + r_2^2 \cos^2\theta_2$$

$$\therefore \quad \text{Cos}\,\theta_2 = \left\{\frac{b^2 + r_2^2 - r_1^2}{2|b| r_2}\right\}$$

Similarly

$$\text{Cos}\,\theta_1 = \left\{\frac{b^2 + r_1^2 - r_2^2}{2|b| r_1}\right\}$$

Hence, given b, r_1, and r_2, the common area is easily found by the following process.

if $|b| \leq |r_1 - r_2|$

then common area = $\pi \times \text{lesser}^2(r_1, r_2)$

if $|b| > r_1 + r_2$

then common area = 0

otherwise θ

$$\theta_1 = \text{Cos}^{-1}\left\{\frac{b^2 + r_1^2 - r_2^2}{2|b| r_1}\right\}$$

$$\theta_2 = \text{Cos}^{-1}\left\{ \frac{b^2 + r_2^2 - r_1^2}{2xr_2} \right\}$$

Common area = $r_1^2 \ (\theta_1 - 0.5 \sin 2\theta_1)$

$+ r_2^2 \ (\theta_2 - 0.5 \sin 2\theta_2)$

Appendix (2). Linearity.

The linearity of an instrument is usually quoted in one of two ways, each giving totally different information. This will be illustrated by reference to the hypothetical characteristic of figure (1). In both cases the figure quoted is an error in the linearity and so the figure quoted under the heading "linearity" should be small.

The first measure of linearity is the maximum fractional error in the indicated input, $\frac{CB}{BA}$. The second is the maximum error in the indicated value of the input, as a fraction of the instrument's full scale deflection $\frac{DE}{OF}$. Clearly the first figure may imply a poorer performance than the second. The choice between these two measures of linearity depends upon the nature of the instrument, and upon its application.

The eye position transducer tends to be

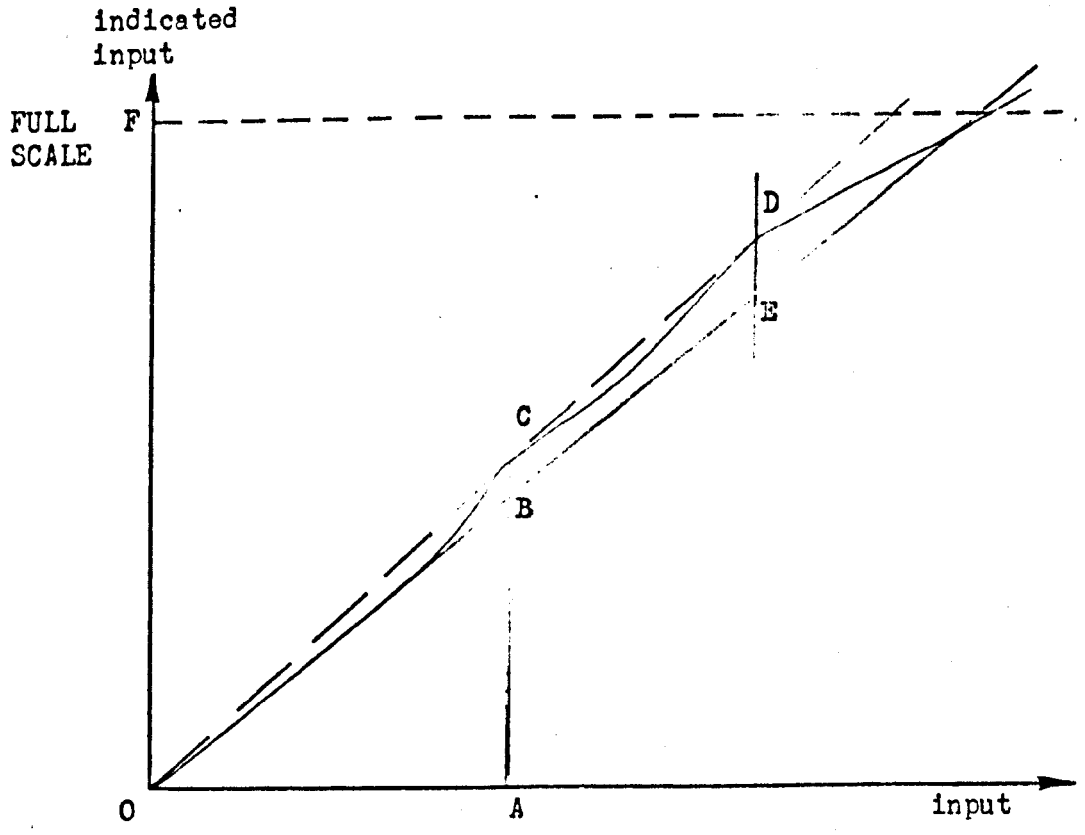

figure (A.2.1)

most linear near the origin. It would seem appropriate therefore to choose the fractional error definition of "linearity". This will not always be the best choice, for instance the other definition would be more appropriate for the typing application, but in order to avoid confusion only the first will be used.

The input to the transducer is eye position and the output is a voltage. The output is the indicated value of the input. We are at liberty to choose the scale factor that we assign to the output, so that the linearity error is minimized. To achieve this we must choose the gain such that the size of the maximum negative fractional error is equal to the maximum positive fractional error.

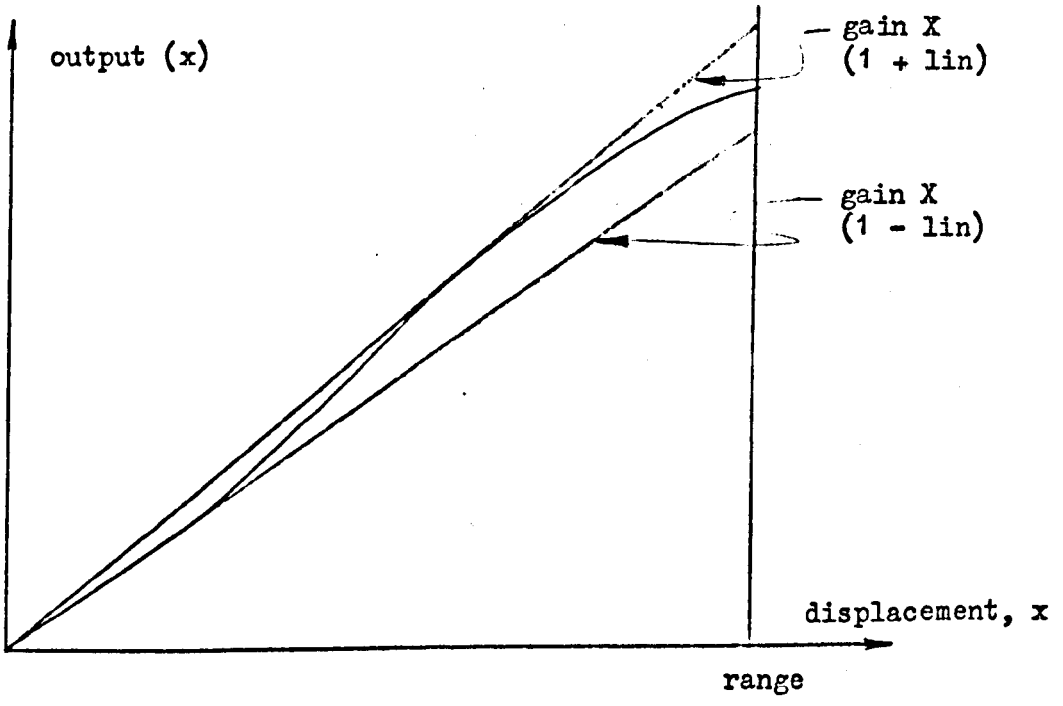

figure (A.2.2)

Consider an arbitrary point on the characteristic in figure (A.2.2). The fractional error is

$$\text{ferror} = \frac{\text{Output (x)} - \text{Gain X x}}{\text{Gain X x}}$$

We must choose the gain and linearity such that

$$\left.\begin{array}{l} f \text{ error} \geq -\text{linearity} \\ f \text{ error} \leq \text{linearity} \end{array}\right) \quad \text{for all } x^{\times}$$

Clearly the entire characteristic will be enclosed by the two straight lines with slope

gain X (1 + linearity)

gain X (1 - linearity)

The Algol programme finds the maximum range x for which a prescribed linearity tolerance, TL%, is not exceeded, and the corresponding gain. It then uses this value of gain to find the range, for each of a sequence of values of y, for which TL is not exceeded. This results in a boundary in the x - y plane of the region of operation with a linearity of TL%. An example is given in figure (A.2.3). The programme also evaluates the linearity when the current value of x, output (x) is taken as origin. This gives a crude measure of the curvature of the characteristic, and is quoted as a percentage as 'CURVE'.

FIG. A·2·3
BOUNDARIES OF 5% LINEARITY

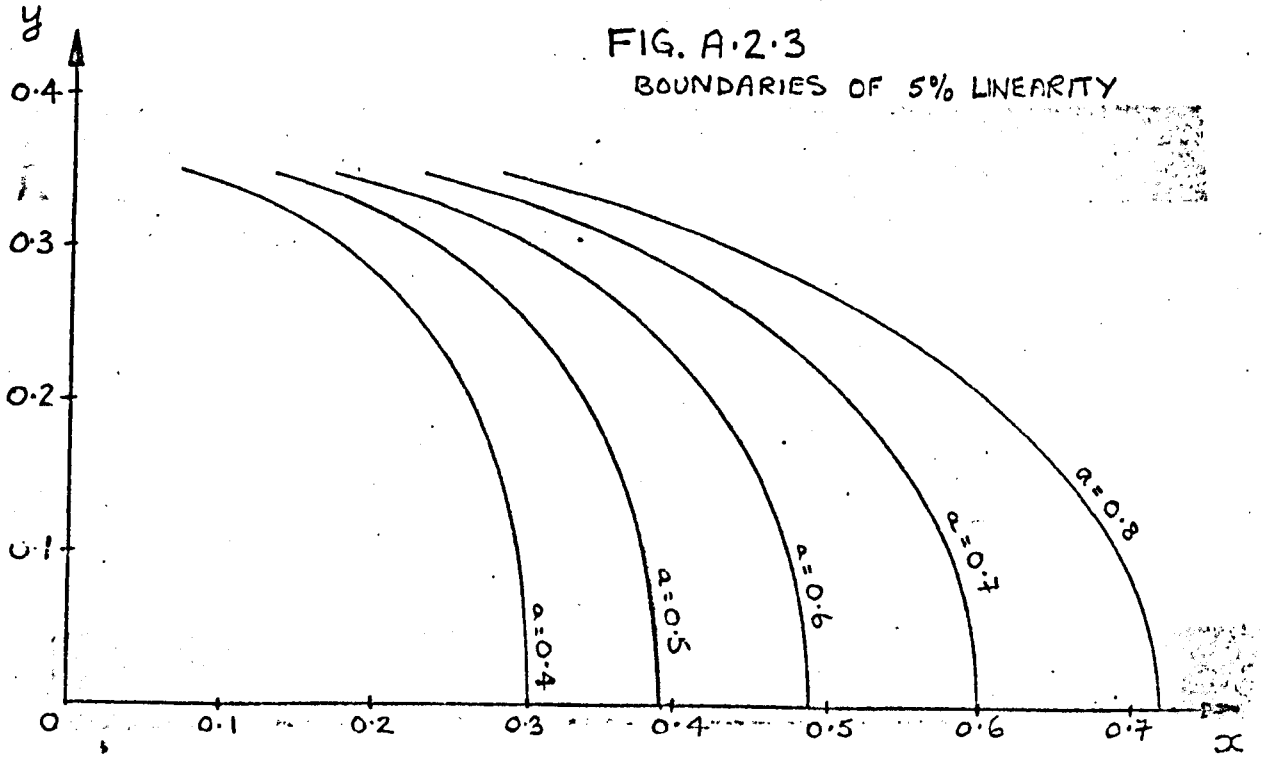

SECTION 3.

EXPERIMENTAL DETERMINATION OF THE REGION OF ASYMPTOTIC STABILITY BY REVERSE TIME SIMULATION

Electronics Letters, September 1967
Vol.3, No. 9, pp 431, 2.

EXPERIMENTAL DETERMINATION OF THE REGION OF ASYMPTOTIC STABILITY BY REVERSE-TIME SIMULATION

The experimental determination of the region of asymptotic stability of a second-order time-invariant system may be considerably simplified by taking advantage of the nature of the trajectories which form the boundary of the region. These trajectories are easily found by reverse-time simulation. Applications of the technique are presented.

Introduction: The state of a second-order time-invariant system is uniquely defined, at any instant, by the value of the output x, and of its derivative dx/dt. This leads to the use of the 'phase plane' (a plot of dx/dt against x) as a representation of the system state.

Consider the general second-order system

$$\frac{d^2x}{dt^2} + f\left(x, \frac{dx}{dt}\right) = 0 \quad . \quad . \quad . \quad . \quad . \quad . \quad . \quad . \quad . \quad (1)$$

and let

$$\frac{dx}{dt} = v \quad . \quad . \quad . \quad . \quad . \quad . \quad . \quad . \quad . \quad . \quad . \quad . \quad (2)$$

i.e.

$$\frac{dv}{dt} + f(x, v) = 0 \quad . \quad . \quad . \quad . \quad . \quad . \quad . \quad . \quad . \quad (3)$$

now

$$\frac{dv}{dt} = -f(x, v) = \frac{v dv}{dx} \quad . \quad . \quad . \quad . \quad . \quad . \quad . \quad . \quad (4)$$

hence

$$\frac{dv}{dx} = -\frac{1}{v} f(x, v) \quad . \quad . \quad . \quad . \quad . \quad . \quad . \quad . \quad . \quad (5)$$

But dv/dx is the gradient of the trajectory through the point (x, v) in the phase plane, and is uniquely defined for all cases except for $v = 0$, $f = 0$. It follows that there is only one trajectory through any point in the phase plane for which v and f are not simultaneously zero.

Consider the ensemble of trajectories shown in Fig. 1. If the system is released from an initial condition lying within the closed curve a, the response converges asymptotically to the stable focus at the origin. If it is released from without the curve a, the response is unstable and diverges continuously from the origin. The closed curve a is an unstable-limit cycle.[1] By eqn. 5, no trajectory can cross this curve, and since the curve represents an unstable régime, any trajectory starting near to the curve diverges from it as the motion progresses. Hence this curve defines the boundary between a stable and an unstable response. Much effort has been applied to the analytic determination of the curve a for classes of non-linear systems.

Time reversal: Consider the effect of running the system in reverse time, so that the trajectories are described in the reverse direction. The original unstable-limit cycle becomes a stable-limit cycle, to which trajectories approach from within and without. In general, reversing the direction of the independent variable has the following effects:

(*a*) a stable limit cycle becomes an unstable limit cycle and vice versa
(*b*) a stable focus becomes an unstable focus and vice versa
(*c*) a stable node becomes an unstable node and vice versa
(*d*) saddle points are unchanged apart from reversal of the direction along the trajectories.

Returning to eqn. 1, define a new independent variable $s = -t$

$$\frac{dx}{ds} = -\frac{dx}{dt}$$

$$\frac{d^2x}{ds^2} = \frac{d^2x}{dt^2}$$

so that the eqn. 1 becomes

$$\frac{d^2x}{ds^2} = f\left(x, -\frac{dx}{ds}\right) = 0$$

i.e. the effect of the change of variable is to reverse the sign of the first derivative term.

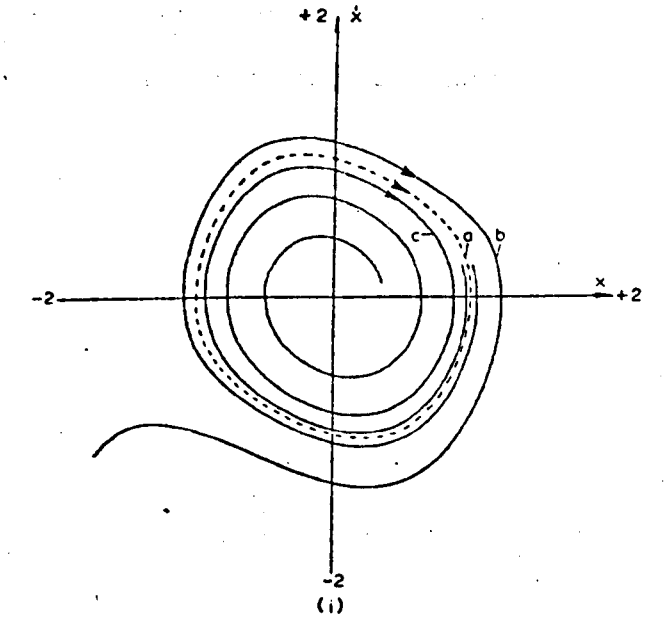

(i)

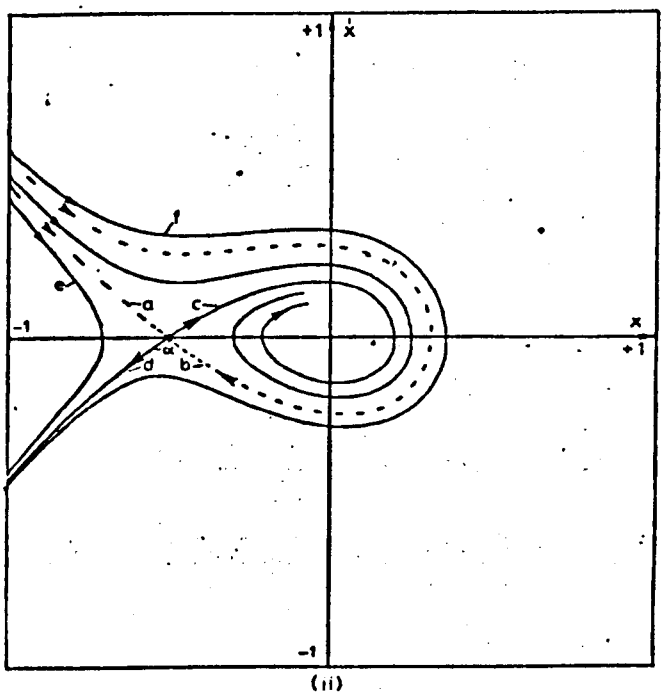

(ii)

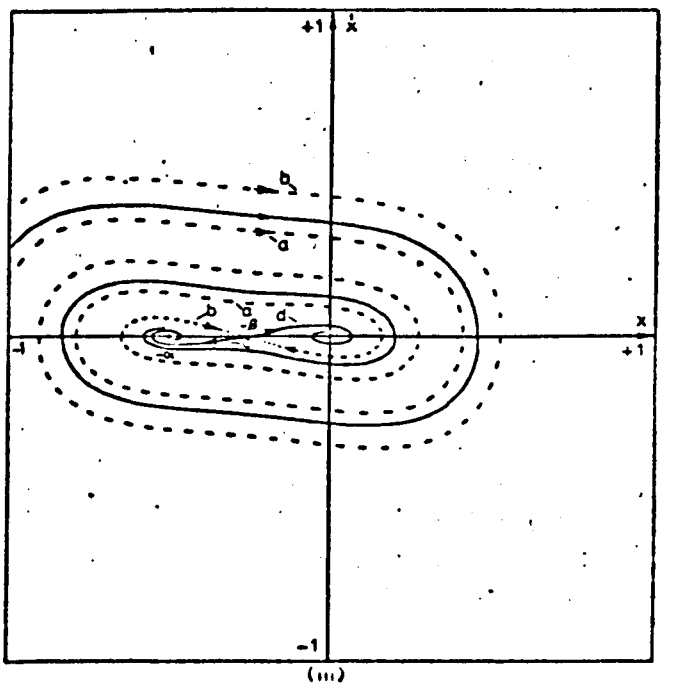

(iii)

Fig. 1 *Phase portraits*

(i) $\ddot{x} + 0{\cdot}25(1 - x^2)\dot{x} + x = 0$
(ii) $\ddot{x} + 0{\cdot}1\dot{x} + x(0{\cdot}5 + x) = 0$
(iii) $\ddot{x} + 0{\cdot}1\dot{x} + x(0{\cdot}5 + x)(0{\cdot}25 + x) = 0$

Consider, as an example, the system having Fig. 1(i) as phase portrait

$$\frac{d^2x}{dt^2} + \epsilon(1 - x^2)\frac{dx}{dt} + x = 0 \quad . \quad . \quad . \quad . \quad . \quad . \quad (6)$$

replacing t by $-s$ we get

$$\frac{d^2x}{ds^2} + \epsilon(1 - x^2)\left(-\frac{dx}{ds}\right) + x = 0. \quad . \quad . \quad . \quad . \quad (7)$$

Since the system of eqn. 7 is the same as that of eqn. 6 with the sign of the independent variable reversed, the response of eqn. 7 will be identical to a record of the response of eqn. 6 played in reverse. Thus, releasing the system from any initial condition will give a steady-state closed trajectory a which defines the region of asymptotic stability of the first system. Because of the reversal of the sign of the first derivative of the response, it is necessary to invert the vertical axis of the phase plane for the trajectories to be identical in this plot.

Open stability boundaries: When the region of asymptotic stability is open, the trajectories defining the stability region must meet at a saddle point. By simulating the system in reverse time, with initial conditions corresponding to the position of this saddle point (which always lies along the x axis), the stability region of the original system is readily determined.

Consider the system[2]

$$\frac{d^2x}{dt^2} + 2\xi\frac{dx}{dt} + (x + \alpha)x = 0$$

having the phase portrait of Fig. 1(ii).

Here, the boundary of stability is formed by the two trajectories a and b which tend, in the limit, to the saddle point s at $(-\alpha, 0)$. There is obviously considerable difficulty in finding these two trajectories experimentally by normal simulation. However, it is a simple task to release the system in reverse-time simulation from the points $(-\alpha \pm \delta, 0)$ where δ is small and the reversed trajectories a and b result. Releasing the system in normal simulation from the same points adds considerably to the comprehension of the phase portrait.

Practically, although δ must be small to give the trajectories a and b accurately, it must be sufficiently large to ensure that the simulation does not take a very long time.

Determination of a separatrix: This same technique may be applied to find the separatrix of a system such as

$$\ddot{x} + 2\xi x + (\alpha + x)(\beta + x)x = 0$$
$$0 < \alpha < \beta$$

which has the phase portrait of Fig. 1(iii).

Figs. 1(i), (ii) and (iii) were obtained directly by simulation, as follows

Forward time:	Fig. 1(i)	trajectories	*b, c*
	Fig. 1 (ii)	„	*c, d, e, f*
	Fig. 1(iii)	„	*c, d*
Reverse time	Fig. 1 (i)	trajectory	*a*
	Fig. 1 (ii)	„	*a, b*
	Fig. 1(iii)	„	*a, b*

J. L. DOUCE
T. M. W. WEEDON

School of Engineering Science
University of Warwick
Coventry, England

29th August 1967

References

1 MINORSKY, N.: 'Non linear mechanics' (Edwards, 1947), chap. 4
2 KERR, C. N., and MCLELLAN, G. D. S.: 'The control of two output-dependent processes', *in* 'Automatic and remote control', Proceedings of the 2nd Congress of the International Federation of Automatic Control held in Basle, Switzerland, 1963